FURFURYLAMINE-BASED POLYBENZOXAZINE ADSORBENT FOR CO₂ CAPTURE: EFFECT OF CARBONIZATION TEMPERATURE AND ACTIVATION METHODS

Thanabhumi Vongtiang

A Thesis Submitted in Partial Fulfillment of the Requirements

for the Degree of Master of Science

The Petroleum and Petrochemical College, Chulalongkorn University

in Academic Partnership with

The University of Michigan, The University of Oklahoma,

Case Western Reserve University, and Institut Français du Pétrole

2018

Thesis Title: Furfurylamine-based Polybenzoxazine Adsorbent for CO_2 Capture: Effect of Carbonization Temperature and Activation Methods

By: Thanabhumi Vongtiang

Program: Petroleum Technology

Thesis Advisors: Asst. Prof. Uthaiporn Suriyapraphadilok
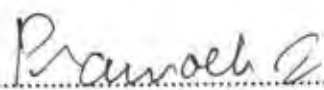
Assoc. Prof. Thanyalak Chaisuwan

Accepted by The Petroleum and Petrochemical College, Chulalongkorn University, in partial fulfilment of the requirements for the Degree of Master of Science.
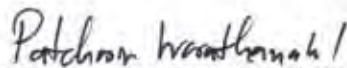
.... College Dean

(Prof. Suwabun Chirachanchai)

Thesis Committee:

....

(Asst. Prof. Uthaiporn Suriyapraphadilok)

....

(Assoc. Prof. Thanyalak Chaisuwan)

....

(Prof. Pramoch Rangsunvigit)

....

(Assoc. Prof. Patcharin Worathanakul)

ABSTRACT

5973015063:   Petroleum Technology Program
              Thanabhumi Vongtiang: Furfurylamine-based Polybenzoxazine
              Adsorbent for CO_2 Capture: Effect of Carbonization Temperature
              and Activation Methods
              Thesis Advisors: Asst. Prof. Uthaiporn Suriyapraphadilok and Assoc.
              Prof. Thanyalak Chaisuwan 99 pp.
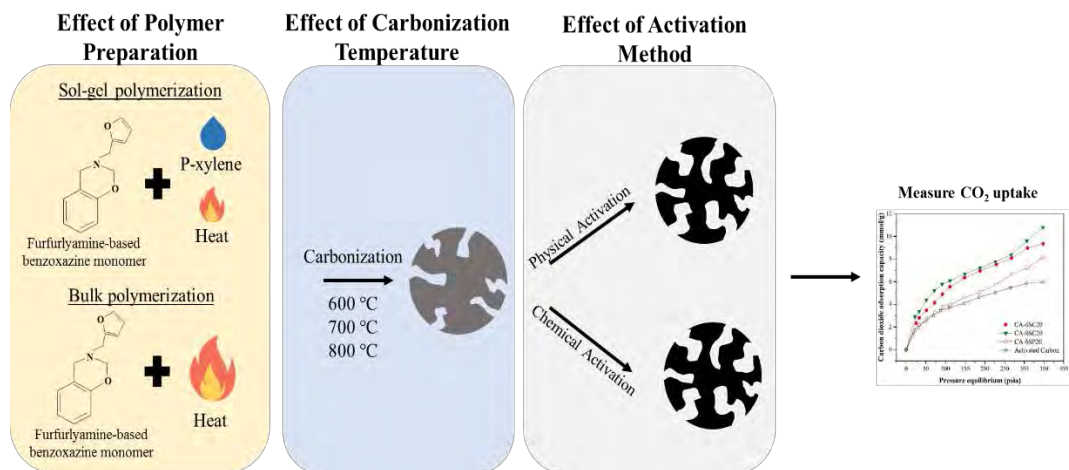Keywords: Carbon adsorbent/ CO_2 capture/ Furfurylamine/ Polybenzoxazine

        Carbon sorbents are of interest for post-combustion CO_2 capture. Polymers are one of the potential precursors to develop carbon adsorbent with suitable surface functionalities. In this research, furfurylamine-based polybezoxazine was used to produce the carbon adsorbent because of its superior properties such as high char yield, high thermal stability, and low water adsorption. To obtain the carbon adsorbent, benzoxazine monomer was prepared by using furfurylamine, paraformaldehyde, and phenol. Polymerization by a sol-gel technique using xylene as a solvent was employed. The obtained polymer was carbonized at various temperatures: 600, 700, and 800 °C. Physical and chemical activation were then conducted at 900 °C by using CO_2 and KOH as an activating agent, respectively. The CO_2 adsorption performance was conducted using a volumetric method at 40, 70, and 110 °C. The results show that both surface morphology and functionalities play a key role in CO_2 adsorption performance. Chemical activation gave the carbon adsorbent with higher surface area and pore volume than the physical activated adsorbents. The conversion of pyridinic functionalities to pyrrolic and pyridonic functionalities was revealed in the XPS analysis in both adsorbents activated by chemical and physical methods. The adsorbent carbonized at 800 °C and activated and chemical activated gave the highest CO_2 adsorption capacity at all adsorption temperatures as a result of its high surface area (1,273 m^2/g), high pore volume (0.537 cm^3/g micropore volume and 0.7891 cm^3/g total pore volume) and suitable surface functionalities.

บทคัดย่อ

ธนภูมิ วงศ์เที่ยง : ตัวดูดซับจากพอลิเบนซอกซาซีนที่มีองค์ประกอบของเฟอร์ฟิวริลามีนเพื่อการดูดซับก๊าซคาร์บอนไดออกไซด์: อิทธิพลของอุณหภูมิที่ใช้ในการคาร์บอไนซ์และการกระตุ้นด้วยวิธีที่หลากหลาย (Furfurylamine-based Polybenzoxazine Adsorbent for CO_2 Capture: Effect of Carbonization Temperature and Activation Methods) อ. ที่ปรึกษา : ผศ. ดร. อุทัยพร สุริยประภาดิลก และ รองศาสตราจารย์ ดร. ธัญญลักษณ์ ฉายสุวรรณ 99 หน้า

ตัวดูดซับประเภทคาร์บอนเป็นตัวดูดซับที่น่าสนใจสำหรับการดูดซับก๊าซคาร์บอนไดออกไซด์ที่เกิดขึ้นจากกระบวนการเผาไหม้ในอุตสาหกรรม พอลิเมอร์เป็นสารตั้งต้นที่มีศักยภาพในการพัฒนาตัวดูดซับประเภทคาร์บอนให้มีหมู่ฟังก์ชันบนพื้นผิวที่เหมาะสม งานวิจัยนี้ได้นำพอลิเบนซอกซาซีนที่มีองค์ประกอบของเฟอร์ฟิวริลามีนมาใช้เป็นสารตั้งต้นในการผลิตตัวดูดซับประเภทคาร์บอนเพราะคุณสมบัติที่ดีเยี่ยมของพอลิเมอร์ชนิดนี้ ได้แก่ การให้ปริมาณถ่านที่สูง มีเสถียรภาพทางความร้อนที่สูง และการดูดซับความชื้นที่ต่ำ ในการสังเคราะห์พอลิเมอร์เพื่อใช้ในการสร้างตัวดูดซับ สารมอนอเมอร์ถูกเตรียมจากเฟอร์ฟิวริลามีน พาราฟอร์มัลดีไฮด์ และฟีนอล ตัวทำละลายไซลีนถูกใช้ในขั้นตอนพอลิเมอไรเซชั่นด้วยวิธีการแบบโซล-เจล พอลิเมอร์ที่เตรียมได้จะถูกนำไปคาร์บอไนซ์ที่อุณหภูมิที่ต่างกัน คือ ที่ 600 700 และ 800 องศาเซลเซียส แล้วถูกนำไปกระตุ้นด้วยวิธีการทางกายภาพโดยใช้ก๊าซคาร์บอนไดออกไซด์และทางเคมีโดยใช้โพแทสเซียมไฮดรอกไซด์ที่อุณหภูมิ 900 องศาเซลเซียส ตัวดูดซับที่ได้ถูกนำไปทดสอบกับเครื่องดูดซับก๊าซคาร์บอไดออกไซด์ด้วยวิธีการทางปริมาตร โดยทำการดูดซับที่อุณหภูมิ 40 70 และ 110 องศาเซลเซียส จากผลการทดลองที่เกิดขึ้น ลักษณะสัณฐานวิทยาและหมู่ฟังก์ชันบนพื้นผิวของตัวดูดซับเป็นปัจจัยที่สำคัญสำหรับการดูดซับก๊าซคาร์บอนไดออกไซด์ การกระตุ้นทางเคมีสามารถสร้างตัวดูดซับที่มีพื้นที่ผิวสัมผัสและปริมาตรของรูพรุนที่สูงกว่าตัวดูดซับที่ผลิตจากการกระตุ้นทางกายภาพ จากการวิเคราะห์ด้วย XPS พบว่าตัวดูดซับที่ถูกกระตุ้นทางเคมีและกายภาพมีการเปลี่ยนแปลงของหมู่ฟังก์ชันไพริดินิกไปเป็นหมู่ฟังก์ชันไพโรลิกและไพริโดนิก ตัวดูดซับที่ผ่านการคาร์บอไนเซชั่นที่อุณหภูมิ 800 องศาเซลเซียส และถูกกระตุ้นด้วยวิธีการทางเคมีสามารถดูดซับก๊าซคาร์บอไดออกไซด์ได้ในปริมาณที่มากที่สุดในทุกอุณหภูมิที่ทำการดูดซับ เนื่องจากการมีพื้นที่ผิวสัมผัสที่สูง (1,273 ม^2/กรัม) ปริมาตรของรูพรุนที่สูง (รูพรุนขนาดไมโคร 0.537 ซม^3/กรัม และ รูพรุนทั้งหมด 0.7891 ซม^3/กรัม) และมีหมู่ฟังก์ชันบนพื้นผิวของตัวดูดซับที่เหมาะสม

GRAPHICAL ABSTRACT

Effect of Polymer Preparation

Sol-gel polymerization

Furfurlyamine-based benzoxazine monomer + P-xylene + Heat

Bulk polymerization

Furfurlyamine-based benzoxazine monomer + Heat

Effect of Carbonization Temperature

Carbonization → 600 °C 700 °C 800 °C

Effect of Activation Method

Physical Activation

Chemical Activation

Measure CO$_2$ uptake

ACKNOWLEDGEMENTS

TABLE OF CONTENTS

LIST OF TABLES

LIST OF FIGURES

FIGURE   **PAGE**

CHAPTER I

INTRODUCTION

The demand of energy used for anthropogenic activities has highly increased from the past, meaning that today more greenhouse gases is emitted to the atmosphere. Carbon dioxide (CO_2) is one of the greenhouse gases emitted from many processes such as combustion of fossil fuels (petroleum, natural gas, and coal) of power plants, deforestation, and chemical processes. The total CO_2 emitted to atmosphere is around 33 Gt per year in 2014 (Sethia *et al.*, 2014) and the CO_2 concentration in the atmosphere has increased rapidly from preindustrial period of 280 ppm (Leung *et al.*, 2014) to 406.67 ppm in April 2017 (ESRL, 2017). Therefore, the increase of CO_2 emission is an important problem creating global warming.

To solve this problem, carbon capture and storage technology (CCS) is a technology developed in term of economic and effective separation process to reduce the amount of CO_2 emission from power plants and industries. Nowadays, chemical absorption is generally used to capture CO_2 with using aqueous alkanolamine solutions such as monoethanolamine, or diethanolamine as absorbent to capture CO_2, but it has many problems including degradation of amine, corrosion problem, and also high energy requirement to regenerate solvent. Therefore, the alternative technologies are considered for CO_2 capture. Adsorption process is one of the alternative technologies using adsorbent as the key factor to capture CO_2. Adsorbent can be developed into many forms such as clays, carbon molecular sieves (CMSs), zeolite, polymers, and metal organic frame works (MOFs) to capture CO_2. Furthermore, adsorption process can solve the corrosion problems and high energy consumption in chemical absorption (Sethia *et al.*, 2014).

Carbon adsorbent synthesized from polymers is an interesting material for CO_2 adsorption application since the different polymers can give various structures of the carbon adsorbent with excellent properties (e.g. high strength, high surface area, high total pore volume, and high micropore volume, low water absorption) to capture CO_2. Furthermore, the adsorbent from polymer can be engineered to contain suitable surface functionality to adsorb CO_2. Xu *et al.* (2018) used various polybenzoxazines to synthesize the carbon adsorbent suitable to adsorb CO_2.

To improve the CO_2 adsorption performance of the carbon adsorbent, this research prepared the carbon adsorbent from the furfurylamine-based polybenzoxazine. Bulk and sol-gel polymerization were used to synthesize the polymer. Various conditions for carbonization temperatures and activation techniques (chemical and physical activation) were employed to obtain carbon adsorbents. Their morphology, chemical properties and CO_2 adsorption capacity were analyzed and discusse

CHAPTER II
THEORETICAL BACKGROUND AND LITERATURE REVIEW

2.1 Global Warming

The continuous growth of industry affects the increase of energy demand, so many energy resources such as petroleum, coal, and natural gas are highly consumed to produce more electricity. When the industries consume more energy, they will create more greenhouse gas to the atmosphere. It is a main cause creating a global warming. These greenhouse gasses consist of methane, nitrous oxide, carbon dioxide, hydrofluorocarbons, and chlorofluorocarbons but the main gas is carbon dioxide. Carbon dioxide emission is found that there has been increased more than 48% in the past twenty years, and it has become the main greenhouse gas having to be reduced (Leung *et al.*, 2014). The average greenhouse gas emission in each year is shown in Figure 2.1.
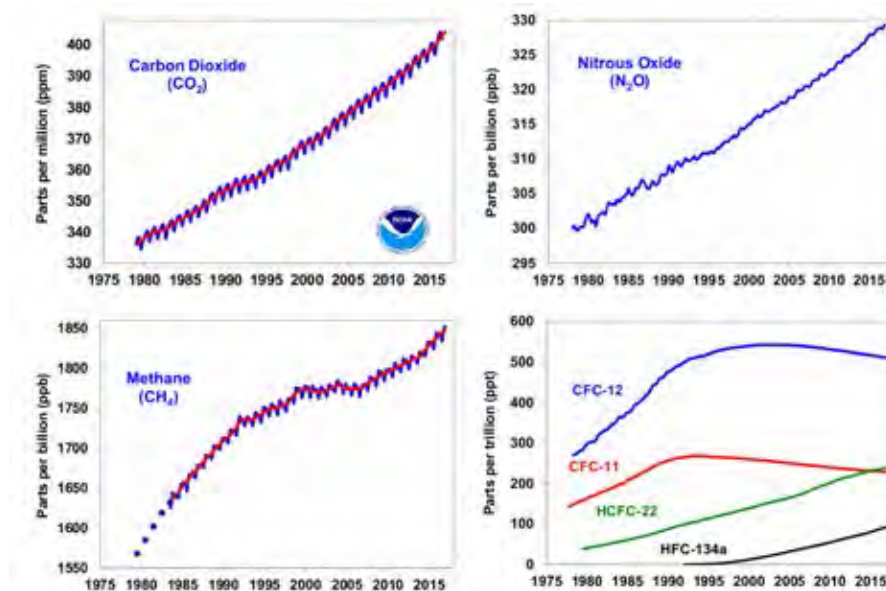
Figure 2.1 Average of greenhouse gasses emission in each year (ESRL, 2017).

2.2 Carbon Dioxide Capture and Separation Technology (CCS)

Carbon dioxide capture and separation technology (CCS) is a comprehensive system that can reduce typically 85 to 90 % of CO_2 emission from various emission sources such as large-scale power plants and industrial processes. The system includes capture, separation, transportation, utilization, and storage. CCS consists of three main technologies such as post combustion, pre combustion, and oxy-fuel combustion as shown in Figure 2.2 (Leung *et al.*, 2014).
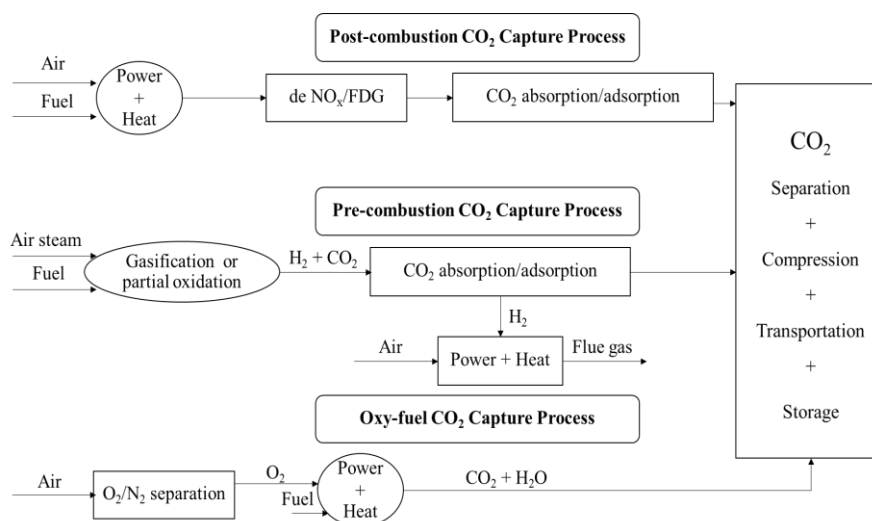
Figure 2.2 Carbon dioxide capture and separation technologies (Leung *et al.*, 2014)**.**

2.2.1 Post-combustion Capture

Post-combustion CO_2 capture is a technology used to capture CO_2 from the combustion flue gas containing CO_2 around $4 - 14$ % at ambient pressure before CO_2 is released to atmosphere. Furthermore, this technology is potentially installed in gas-fired and coal-fired power plants (Leung *et al.*, 2014).

2.2.2 Pre-combustion Capture

For pre-combustion, fossil fuels are pre-treated before they are gasified under low oxygen concentration to obtain syngas (CO and H_2). After obtaining syngas, the water gas shift reactions are occurred by steam reforming, generate high amount of H_2, and covert CO into CO_2. The gas mixture after steam reforming contains

CO_2 at a concentration of more than 20% which is preferred by the pre-combustion CO_2 capture because this technology gives higher efficiency at higher CO_2 concentration in the feed (Leung *et al.*, 2014).

2.2.3 Oxy-fuel Combustion Capture

The oxy-fuel combustion technology uses oxygen in place of air to combust fuels. It can reduce highly reduce N_2 in flue gas after combustion. When the amount of N_2 in flue gas is decreased, it also can greatly reduce NO_x released to atmosphere. Furthermore, this technology uses high amount of oxygen to combust fuels and causes much higher CO_2 concentration in the flue gas. The CO_2 concentration is in a high level around 80-98% depending on fuel; therefore, oxy-fuel combustion CO_2 capture is needed to be installed to efficiently capture high amount of CO_2 before being released to the atmosphere. Table 2.1 shows a comparison of different technologies for CO_2 capture (Leung *et al.*, 2014).

Table 2.1 Comparison of different technologies for CO_2 capture (Leung *et al.*, 2014)

Capture technology	Advantages	Disadvantages
Post-combustion	Easily installed or retrofitted the existing plant.	The efficiency depends on the CO_2 concentration
Pre-combustion	High potential with increasing amount of CO_2 capture.	Problem with heat transfer High costs for installation and operating
Oxy-fuel combustion	Very high concentration of CO_2 can be captured; More efficient than the other technologies.	Corrosion problem Efficiency rapidly drop from contaminants

2.3 Adsorption

Adsorption is a technology using adsorbent material to capture CO_2. There are many types of adsorbents such as zeolites, polymers, carbon molecular sieves (CMS), activated carbons, amine-containing porous materials, and metal organic frameworks (MOFs). The adsorbents can be developed to increase the efficiency of CO_2 capture. Furthermore, this technology uses less energy for adsorbent regeneration and has no corrosion problems, so it is suitable for use in the power plants (Sethia *et al.*, 2014). Besides, Types of adsorption are considered from the regeneration process of adsorbent, for instance, pressure swing adsorption (PSA), vacuum swing adsorption (VSA), Thermal swing adsorption (TSA), and electrical swing adsorption (ESA).

2.3.1 Pressure Swing Adsorption (PSA)

Pressure swing adsorption (PSA) is used to separate some gas species from a mixture of gases under pressure. It operates at near-ambient temperatures. Specific adsorbents (zeolites, activated carbon, molecular sieves, etc.) are used as a trap, preferentially adsorbing the target gas species at high pressure. The process will swing to low pressure for desorbing the adsorbed material (Chai *et al.*, 2011).

2.3.2 Vacuum Swing Adsorption (VSA)

Vacuum swing adsorption (VSA) operates near room temperature at atmospheric pressure and swings pressure to vacuum for desorbing the adsorbed material (Yu *et al.*, 2012).

2.3.3 Thermal Swing Adsorption (TSA)

Thermal swing adsorption (TSA) is a simple process and more economic when it is compared with other processes. TSA uses hot air or steam in a regeneration process, but the regeneration time is longer than that of PSA. Furthermore, it has been widely used in industry for removal and recovery of hydrocarbon and solvent vapor (Ghoshal *et al.*, 2002).

2.3.4 Electric Swing Adsorption (ESA)

Electric swing adsorption (ESA) is a technique similar to temperature swing adsorption (TSA) in term of heating process. After adsorption on solid surface, the fixed bed is heated by electricity for the desorption process (Grande *et al.*, 2009).

2.4 Physical and Chemical Adsorptions

2.4.1 Physical Adsorption or Physisorption

Physical adsorption is a general phenomenon which normally occurs as a multiple layer at high relative pressure. The physisorbed molecules can be desorbed and returned to the original form of fluid phase. This phenomenon is an exothermic process, but the energy that is involved with physisorption is not much more than the condensation energy of the adsorptive. Furthermore, physical adsorption process reaches equilibrium fairly rapidly (Rouquerol *et al.*, 2014).

2.4.2 Chemical Adsorption or Chemisorption

Chemical adsorption is occurred by reaction of the adsorbed molecule linking with surface and the adsorption is specifically limited to a mono layer. For the chemisorbed molecule, it loses its original form or identity and cannot be recovered by desorption. At low temperature, this system may not have sufficient thermal energy to reach the equilibrium; therefore, an activation energy is involved in the chemical adsorption (Rouquerol *et al.*, 2014).

2.5 Types of Adsorption Isotherms

2.5.1 Classification of Gas Physical Adsorption Isotherms

The Isotherms of the adsorbed gas molecule with the physisorption can be classified into nine groups from an extended IUPAC classification as shown in the Figure 2.3. Type I(a) and I(b) isotherms are indicated the microporous adsorbent, but Type I(a) classifies the adsorbent containing the narrow micropores whereas Types I(b) indicates the existing of wider micropores. Because the narrow range of relative pressure necessary to attain the plateau is an indication of a limited range of pore size and the appearance of a nearly horizontal plateau indicates a very small external surface area. Type II isotherms can be obtained with a non-porous or a macroporous adsorbent since the unrestricted multimolecular adsorption is appeared at the high relative pressure. The Type II(a) completely reverses between adsorption and desorption which can be explained by monolayer-mutilayer adsorption on a stable and open adsorbent's surface, but Type II(b) exhibits the hysteresis loop which results the

inter-particle capillary condensation. In case of Type III, this shape is convex to the relative pressure axis and it can indicate the macroporous or non-porous adsorbent that give the weak interaction between adsorbate and adsorbent. For the Type IV, it is a characteristic of mesoporous adsorbents. Type IV is classified into two types. Type IV(a) is a common type when compared with Type IV(b), which consider by using hysteresis loop. The hysteresis loop is related to the filling and withdrawal of the mesopores. Type IV(a) is composed of hysteresis loop, but IV(b) is completely reversible; therefore, The hysteresis loop is not appeared on the Type IV(b). Type V isotherm is similar with Type III which is associated with the weak adsorbate-adsorbent interactions, but this shape exhibits the hysteresis loop which explains about the pore filling and emptying; therefore, Type V can indicate a mesoporous or microporous adsorbents. The last Type is Type VI isotherm indicating the layer-by-layer adsorption on a uniform surface. This shape is a characteristic of graphitised carbon (Rouquerol *et al.*, 2014).
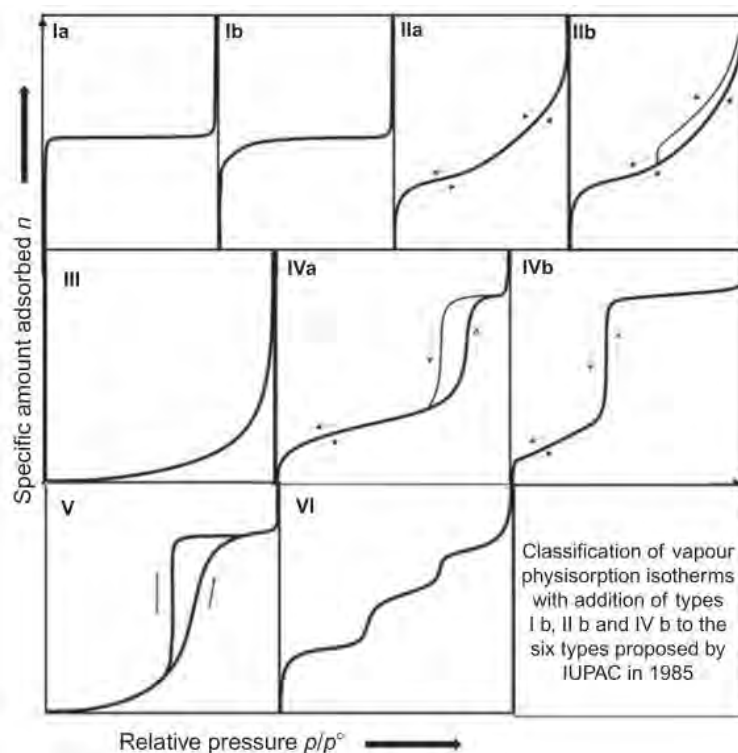
Figure 2.3 Classification of physical adsorption isotherms combining proposals from IUPAC (Rouquerol *et al.*, 2014)

2.5.2 Chemical adsorption of Gasses

This system gives a simple type of isotherm similar to the Type I(a) of physical adsorption isotherms since chemical adsorption is occurred in a monolayer. However, the chemisorption is difficult to obtain the equilibrium data and the reaction may be undetected at low temperature or pressure; therefore, the experimental condition is important to detect the chemisorption reaction (Rouquerol *et al.*, 2014).

2.6 Theories of Surface Area Analysis

2.6.1 The Langmuir Theory

Langmuir gave various mechanisms of adsorption based on the ideal of a limited number of adsorption sites. There are six mechanisms where (i) the only one kind of adsorbing site is occurred, (ii) there is more than one kind of adsorbing sites, (iii) the adsorbing surface is amorphous and presents a continuum of adsorbing sites, (iv) more than one molecule can be accommodated in each site, (v) There is not relating to the adsorption, and (vi) multilayer adsorption is occurred. However, Langmuir model provided that the adsorption on a plane surface was found only one kind of elementary space and in which each space can adsorb one molecule. Therefore, the Langmuir model could not apply for either porosity or physical adsorption. The Langmuir model is appropriate for an ideal form of chemisorption. Nevertheless, there are a few exceptional physisorption systems which can be applied to monolayer completion. The Langmuir equation might be used to identify the Type I of physisorption isotherm, but it is not suitable for the multilayer adsorption. The Langmuir equation is shown in the equation 2.1.

$$\frac{n}{n_l} = \frac{bp}{1+bp} \tag{2.1}$$

Where the parameters n is the specific amount of gas adsorbed at the equilibrium pressure, n_l and b are to be regarded as empirical constants within stated ranges of p and T (Sing *et al.*, 2014).

2.6.2 The Brunauer-Emmett-Teller Theory (BET)

There is the evidence that the physical adsorption of gas is not limited to monolayer adsorption if the relative pressure increased above a certain level. The

BET theory can conclude that the beginning of the middle almost linear section of a Type II isotherm was the point most likely to correspond to monolayer. The BET equation is most widely used of all adsorption isotherm equations which can determine the surface area of porous and non-porous adsorbents. The BET equation is shown in the equation 2.2.

$$\frac{p/p^{\circ}}{n(1-p/p^{\circ})} = \frac{1}{n_m C} + \frac{C-1}{n_m C}\left(\frac{p}{p^{\circ}}\right) \tag{2.2}$$

Where n($=n^a/m^s$) is the amount adsorbed at relative pressure p/p° and n_m (= n_m^a /m^s) is the monolayer capacity. In the BET theory, the parameter C is exponentially related to E1 (the first-layer adsorption energy) (Sing *et al.*, 2014).

2.7 Adsorbents

Adsorbents include zeolite, carbon materials, metal oxide (CaO), metal organic frameworks (MOFs, amine-modified materials (AMMs), and Layered double hydroxides (LDH). Each adsorbent performs their good properties and performances in the suitable conditions, those are adsorption temperature.

Shen *et al.* (2010) prepared activated carbon beads by using coal tar pitch blended with naphthalene. The mixture was stirred and heated under N_2 atmosphere. Then, it was crushed into particles and emulsion method was conducted to obtain pitch spheres. After that, they were stabilized, carbonized, and activated. From the results, activated carbon beads contained macropores, mesopores, and micropores which the amount of micropores is very high as a result from the high BET specific surface area of 845.87 m²/g. Furthermore, this adsorbent obtained the CO_2 adsorption capacity around 1.918 mol/kg at 30 °C and 1 bar (Shen *et al.*, 2010).

Regufe *et al.* (2018) produced honeycomb monolith composed of humic acid (5% w/w), activated carbon (28% w/w), and 13X zeolite (67% w/w) for CO_2 adsorption. Materials were blended by a ball mill to make a uniform distribution. Then, water was slowly dropped into the solid mixture until it contained 80% by weight of solid mixture. The slurry was extruded with 15 ton pressure and dried at ambient temperature for 1 day. The honeycomb monolith was obtained. After that, calcination was employed at 600 °C for 24 h. The results show that honeycomb monolith

contained micropores, mesopores, and macropores which it had a large amount of micropores and mesopores. The pores size distribution was indicated in a range of diameters between 50 and 150 Å. For CO_2 adsorption performance, the CO_2 adsorption capacity of this adsorbent is 1.56 mol/kg at 298 K and 1 bar (Regufe *et al.*, 2018).

Bolotov *et al.* (2018) synthesized the MOF adsorbent: $Zn_2(tdc)_2dabco$. Thiophene-2,5-dicarboxylic acid was mixed with $Zn(NO_3)_2.6H_2O$. Then, the dabco was added into the mixture. It was stirred and heated at 100 °C for 20 h. After that, DMF was employed to wash the adsorbent. Finally, it was heated at 90 °C in vacuo for 10 h and the MOF adsorbent was obtained. From the results, $Zn_2(tdc)_2dabco$ adsorbent gave the BET surface area and pore volume around 1,553 m^2/g and 0.68 cm^3/g, respectively. Besides, this adsorbent could adsorb CO_2 at 25 °C and 1 bar around 1.932 mol/kg (Bolotov *et al.*, 2018).

Huang *et al.* (2003) prepared MCM-48 modified by amine functional groups. To produce surface-modified MCM-48, cetyltrimethyl ammonia bromide, water, abosolute ethanol, and aqueous ammonia were mixed and stirred at ambient temperature for 10 h. Then, it was filtrated and washed until the MCM-48 was obtained. This adsorbent had the BET surface area around 1,389 m^2/g and amine groups on the adsorbent's surface increase the affinity between adsorbent and CO_2 since the amine groups is the basic component. Therefore, this adsorbent obtained high CO_2 adsorption capacity around 2.25 mol/kg at 25 °C and 1 bar (Huang *et al.*, 2003).

Fayemiwo *et al.* (2018) synthesized the nitrogen-rich polymer for CO_2 adsorption. This polymer was prepared by using different methacrylamide (MAAM) contents mixed with ethylene glycol dimethacrylate and azobisisobutyronitrile. Then, the mixture was dissolved in acetronitrile and polymerized at 60 °C for 24 h. After that, it was crushed and sieved with size around 90-212 μm. For the characterization, the increase of MAAM content affect the adsorbent to contain high amount of nitrogen element, but the BET surface of the adsorbent was decreased. Furthermore, the increase of nitrogen functionality could not increase the CO_2 adsorption capacity because the nitrogen functionality did not stay on the surface of the adsorbent. Therefore, the polymer could obtain CO_2 adsorption capacity of 0.79 mol/kg at 25 °C and 1 bar (Fayemiwo *et al.*, 2018).

From many adsorbents used for CO_2 adsorption, they can be classified into two types by different adsorption temperature. One is the adsorbents exhibiting good performances at low temperature (below 200 °C) such as zeolite, carbon materials, metal organic frameworks (MOFs), and amine-based materials (AMMs). The other one is adsorbents exhibiting good performances at high temperature (above 200 °C). The two types of adsorbents are compared in the Table 2.2 in terms of adsorption temperature, performance, and cost (Chen *et al.*, 2013).

Table 2.2 Comparing various adsorbents (Chen *et al.*, 2013)

| Type of adsorbent | Adsorbent | Adsorption condition | | CO₂ capture capacity (mmol/g) | Adsorbent cost |
		Pressure (bar)	Temperature (°C)		
Low temperature adsorbents	Activated carbon	1	0	2.8-8.6	Low
		1	25	1.5-4.8	
	Zeolite	1	25	0.75-4.66	Low
		0.15	0	2.5-5.2	
	MOFs	0.1	25	0.1-5.95	High
		0.5	25	0.6-7.2	
		≥ 14	25	6.8-54.5	
	AMMs	1	75	2.0-4.95	Medium
		0.1-0.15	25	0.79-14.0	
		4×10^{-4}	25	1.05-1.77	
High temperature adsorbents	LDH	0.15	200-400	< 1	Low
	CaO	0.15	650-800	8.0-11.0	Low

2.7.1 Carbon Molecular Sieve (CMS)

Carbon molecular sieve (CMS) is a porous carbon material containing pores of the size closed to the molecular dimensions of the gas molecules. For

separation, the energy of interaction between the diffusing molecules and the carbon atoms consists of two interactions such as dispersive and repulsive. When the pores become suitable for the size of the diffusing molecules, the repulsive force will be the dominating force. It affects the diffusing molecules to require the activation energy for passing through the obstacle. Furthermore, different molecule size effectively helps gas molecules to separate from carbon molecular sieve. Besides, CMS can be obtained from the pyrolysis of polymeric or biomass materials (Jones *et al.*, 1994).

2.7.1.1 *Pyrolysis Technology*

Pyrolysis technology or thermal decomposition process, this process is operated without oxygen in a system with high temperature (e.g. 300-500 °C) to convert lignocellulosic biomass, polymeric materials and others into carbon materials in solid or liquid phase. Pyrolysis technology has another name called carbonization (Roy *et al.*, 2017).

2.7.1.2 *Biomass Precursors*

Many biomass materials can be used as precursor for preparation of low-cost carbon molecular sieve. Bello *et al.* (2002) produced CMS from oil palm shell to separate air. Oil palm shells were crushed in type of particle around 1-3 cm in diameter. The particle of oil palm shells (100g) were dried in an oven at 120 °C for 24 hours. After drying, the crushed palm shells were carbonized in a reactor with flowing N_2. The final carbonization temperature is around 600 to 1000 °C with a constant heating rate, and it was held for 1 hour at the final temperature. After cooling to room temperature, the samples were sieved into powder. The result showed the micropore, surface area and micropore volume decreased with increasing carbonization temperature. The O_2/N_2 selectivity of the CMS samples increased with increasing carbonization temperature. Therefore, the final temperature in carbonization is the key parameter to control micropore surface area, micropore volumes and selectivity of CMS. Furthermore, CMSs obtained from oil palm shell are highly desirable to air separation (Bello *et al.*, 2002).

Tan *et al.* (2004) prepared CMS from eucalyptus globulus charcoal by pyrolyzing under partial combustion condition in poor oxygen atmosphere. The precursors were carbonized around 830 or 870 °C by using a heating

rate around 4 °C/min for 2 hours with N_2 flow. The obtained samples were mixed with mineral tar and dried at 110 °C. After that, this sample was compressed to a pellet form. Eventually, they were activated with heat treatment in flowing carbon dioxide under different conditions. From the results, CMS from eucalyptus globulus obtained high selectivity for the CO_2/CH_4 separation. An increasing in carbonization temperature caused small amount of oxygen surface groups and distribution of narrow micropore size. Furthermore, the different activated conditions showed that short carbonization time and high heating rate were factors to obtain better results (Tan *et al.*, 2004).

Banisheykholeslami *et al.* (2015) studied the preparation of carbon molecular sieve by using broom corn stalk as a precursor and methane deposition method for selective CO_2/CH_4 separation. Broom corn stalks were dried and crushed, then they were treated with heat treatment at 30 °C for 20 min with flowing N_2. After carbonization, the obtained sample was cooled with flowing N_2 before it was soaked in a $ZnCl_2$ solution. It was then heated and stirred at 75 °C for 8 hours to activate with chemical. The solution was dried at 110 °C in an oven for 48 hours. After drying, the samples were manipulated at different temperatures of heat treatment such as 800 (AC800) and 950 °C (AC950) with rate of heating at 20 °C/min under N_2 atmosphere and held for 1 hour at final temperature, then the samples were cooled to room temperature. When temperature approached to the room temperature, the samples were washed with 0.05 M HCl to eliminate excess activating agent until pH was neutral and dried at 110 °C for 24 hours. After that, the activated carbons would be modified the pore by chemical vapor deposition (CVD). They were heated up to 800 °C (deposition temperature) with heating rate of 20 °C/min under N_2 atmosphere and exposed to a mixed gas including with N_2 and CH_4 for 2 hours. They were then cooled down with flowing N_2 until the carbon molecular sieve (CMS) was obtained. The result showed that AC800, AC900 and CMS obtained average pore diameter of 2.0219, 2.1946 and 1.4717 nm, respectively. Surface area was 1121.3, 1048 and 815.6 m^2/g, respectively. Total pore volume was 0.5668, 0.5750 and 0.3001 m^2/g, respectively, and micro pore volume per total pore volume was 39.71, 30.82 and 60.53 %, respectively. From CO_2/CH_4 separation, the CMS can separate better than the activated carbon. Furthermore, the CMS was prepared from broom corn stalk that

derived higher selectivity when compared to CMS prepared from other biomass materials (Banisheykholeslami *et al.*, 2015).

2.7.1.3 *Polymer Precursors*

Jones *et al.* (1994) studied about carbon molecular sieve from polyimide precursors for gas separation. In this study, an asymmetric hollow fiber polyimide was pyrolyzed to prepare carbon molecular sieve. Pyrolysis condition was operated at 500 and 550 °C, under vacuum (< 1 torr) with a heating rate of 13.3 °C/min. When temperature approached to the final pyrolysis temperature, the heating rate was retarded to 0.25 °C/min. At the final pyrolysis temperature, the sample was held for 2 hours, then it was cooled to room temperature. The results obtained from a thermal conductivity detector (TCD) in gas chromatography analyzer. The individual species was calculated in term of flux and reported in gas permeation units (GPU). In O_2/N_2 separation, the selectivity of the 500 °C and 550 °C pyrolysis protocol was in a range of 8.5 - 11.5 with fluxes of O_2 around 20 to 50 GPU and in a range of 11.0 - 14.0 with fluxes of O_2 around 15 to 40 GPU. The selectivity of other mixed gas separations such as H_2/CH_4, CO_2/CH_4, and CO_2/N_2 from carbon molecular sieve derived from polyimide precursor was higher than other conventional polymeric material precursors (Jones *et al.*, 1994).

Steel *et al.* (2005) investigated the pyrolysis parameters which affected to carbon molecular sieve in term of gas separation properties. In this study, using structures and polyimide precursors were 6FDA/BPDA-DAM and Matrimid®. The polyimide precursors were carbonized at 550 °C and 800 °C. The carbonization process was operated with a constant heating rate of 4 °C/min under vacuum pressure at <<0.03 mmHg, then it was held for either 2 or 8 hours at the final pyrolysis temperature. From results, pore size distribution analysis used a Micromeritics ASAP 20210 and porosimetry instrument to analyze. The micropore from analysis was around 4-11 Å, micropore volume of Matrimid-derived carbon (550 °C) was 0.113 cm^3/g, 6FDA/BPDA-DAM-derived carbon (550 °C) was around 0.157 cm^3/g, Matrimid derived carbon (800 °C) was 0.138 cm^3/g, and 6FDA/BPDA-DAM-derived carbon (550 °C) was 0.179 cm^3/g. Therefore, the increase of final pyrolysis temperature and thermal soaking time increased the micropore volume. Furthermore,

this modification gave higher selectivity and lower permeability material for both O_2/N_2 separation and CO_2/CH_4 separation; however, lower selectivity and lower permeability were obtained for the separation of C_3H_6 and C_3H_8 (Steel *et al.*, 2005).

Rungta *et al.* (2015) used Matrimid® as a precursor to produce carbon molecular sieve. Matrimid was pyrolyzed at a final pyrolysis temperature of 500 °C, 550 °C, 675 °C, and 800 °C under vacuum and inert argon. The heating protocol was started with a heating rate of 13.3 °C/min at 50 °C to 250 °C, followed by a heating rate of 3.85 °C/min at 250 °C to (T_{max} − 15 °C) and the final heating rate of 0.25 °C/min at (T_{max} − 15 °C) to T_{max} °C, where T_{max} is the final pyrolysis temperature. After temperature approached the final pyrolysis temperature, the sample was held for 2 hours and cooled down to room temperature to obtain carbon molecular sieve. The results showed that the total pore volume (<< 10.8 Å) of CMS-500, CMS-550 and CMS-675 was 0.0560 cm^3/g, 0.1041 cm^3/g and 0.1136 cm^3/g, respectively. Pore volume (< 4.2 Å) of CMS-500, CMS-550 and CMS-675 was found around 0.0008 cm^3/g, 0.0018 cm^3/g and 0.0081 cm^3/g, respectively. Total surface area of CMS-500, CMS-550 and CMS-675 was found around 191.2 m^2/g, 478.1 m^2/g and 466.8 m^2/g, respectively. It means that the final pyrolysis temperature affects the morphology of carbon molecular sieve (Rungta *et al.*, 2015).

2.8 Polybenzoxazine (PBZ)

Polybenzoxazine (PBZ) is a thermoset polymer which is classified as a new type of phenolic resin. It has been recently studied because of its superior characteristics to other conventional phenolic resins, such as high thermal stability, good mechanical properties, low water absorption, near zero shrinkage upon curing, flame retardance and easy processibility, etc. (Chaisuwan *et al.*, 2010). To obtain polybenzoxazine, benzoxazine monomers are thermally ring-opening polymerized. The benzoxazine monomers are heated at temperatures in the range of 160 to 250 °C for the ring-opening polymerization. Benzoxazine is a molecule in which a heterocyclic six-membered ring containing nitrogen and oxygen atom (an oxazine ring) attached to a benzene ring. Differences of benzoxazine structures depend on the position of the heteroatoms as shown in Figure 2.4 (Ishida, 2011).

(a) 1, 3-Benzoxazine   (b) 3, 1-Benzoxazine   (c) 1, 4-Benzoxazine   (d) 1, 3-Benzoxazine
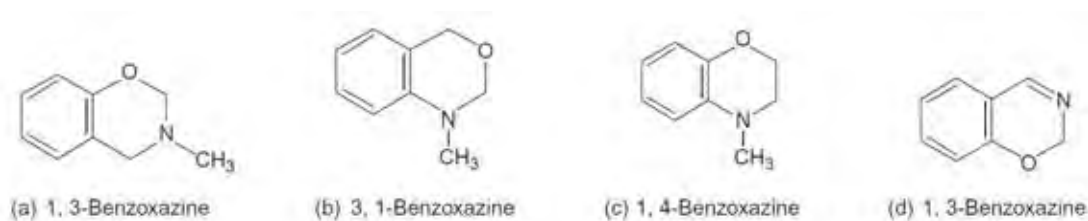
Figure 2.4 Different structures of benzoxazine molecules.

2.8.1 Benzoxazine Monomer

Benzoxazine monomers are synthesized from raw materials including aldehyde, phenol derivatives and primary or secondary amines. Various raw materials can be used to design a functionalized benzoxazine monomer for the unique properties (Liu *et al.*, 2005). Benzoxazine monomers can be classified in two types in terms of phenol derivatives such as monofunctional benzoxazine and difunctional benzoxazine. Monofunctional benzoxazine is prepared by using precursors based on phenol reacted with primary amine. The reaction is shown in Figure 2.5. Nevertheless, polymerization of monofunctional benzoxazine obtains small oligomers and produces low cross-linked polymer, resulting in less strong structure. Therefore, it is mixed with the groups that polymerize in non-benzoxazine chemistry. For difunctional benzoxazine monomer, it can be divided in two main classes: the combination of bisphenol with primary amine as shown in Figure 2.6 and the combination of secondary amine with monophenolic derivative is shown in Figure 2.7 (Alhassan *et al.*, 2011).
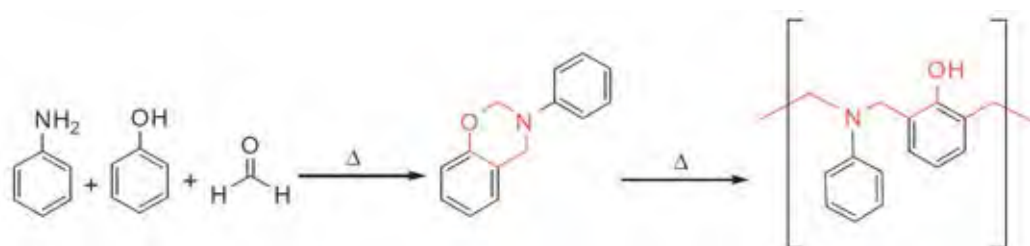
Figure 2.5 Monofunctional benzoxazine monomer and polybenzoxazine from the combination of aniline and phenol (P-a).
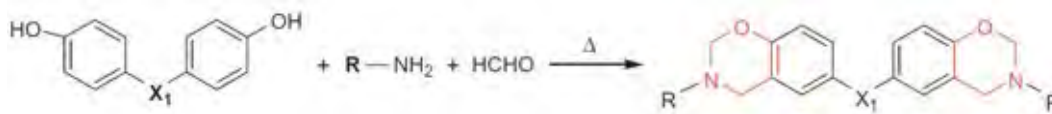
Figure 2.6 Difunctional benzoxazine monomer from the combination of bisphenol and primary amine.
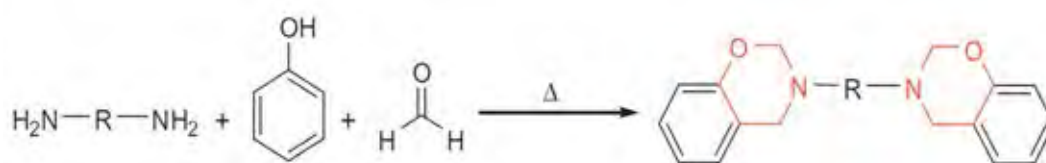
Figure 2.7 Difunctional benzoxazine monomer from the combination of secondary amine and monophenolic derivative.

There are various methods to synthesize benzoxazine monomers and polybenzoxazine. Liu *et al.* (2005) studied the performance of benzoxazine monomers containing furan group. In their study, there were two benzoxazine monomer preparations. Starting from P-FBz or 3-furfuryl-3,4-dihydro-2H-1,3-benzoxazine was prepared by using formaldehyde (37% by weight in water, 1.62 g, 20 mmol), furfurylamine (0.97 g, 10 mmol), and phenol (0.94 g, 10 mmol) as precursors. These substances were dissolved in 10, 4, and 1 ml dioxane, respectively. The formaldehyde solution was charged with ice bath, then the furfurylamine solution was slowly added to keep the temperature of reaction below 10 °C, the solution was stirred for 30 min. After stirring, phenol was added in the mixture, and the temperature went to 85 °C due to the exothermic reaction. The reaction was kept for 24 hours. The dioxane solvent was eliminated by using a rotary evaporator. The solution was then dissolved in 50 ml diethyl ether and washed by distilled water before 3 N NaOH$_{(aq)}$. Another monomer was BPA-FBz or bis(3-fufuryl-3,4-dihydro-2H-1,3-benzoxazinyl)isopropane preparation. The monomer preparation was similar to the P-FBz preparation but phenol component was replaced by bisphenol-A component. The preparation of two benzoxazine monomers is shown in Figure 2.8. The benzoxazine monomers were

polymerized following by a step-curing at 160 °C (1 hour), 200 °C (2 hours) and 240 °C (2 hours) in an air circulating oven. The reaction mechanism to obtain polybenzoxazine is shown in Figure 2.9. The result showed that polybenzoxazine containing furan group exhibited excellent properties such as good thermal stability, high glass transition temperatures over 300 °C, high cross-linking density and high char yields (Liu *et al.*, 2005)
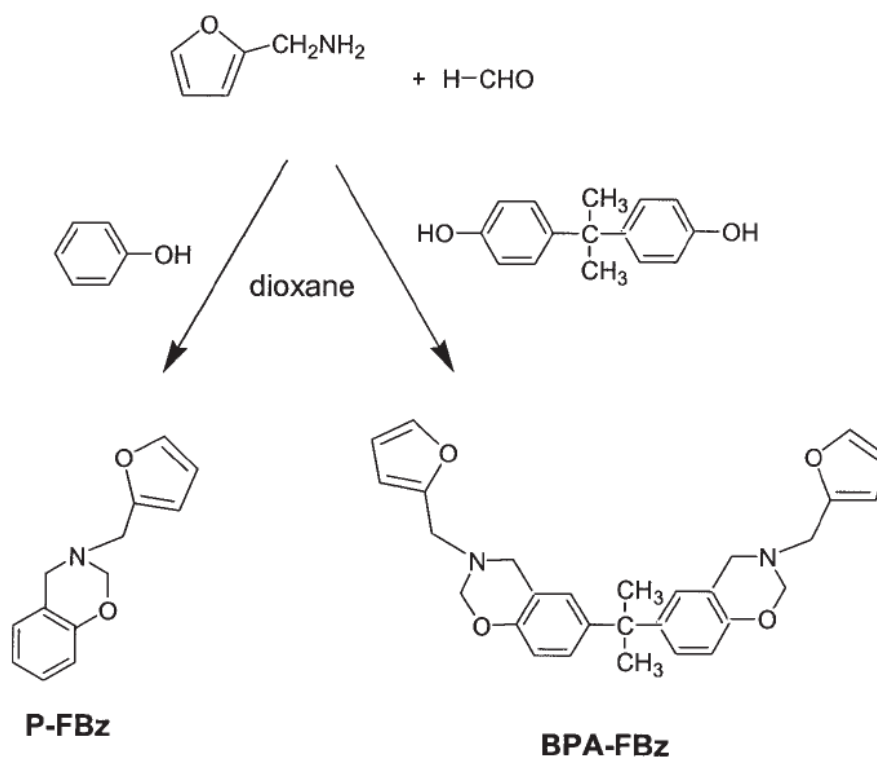
Figure 2.8 Benzoxazine monomer preparations (P-FBz and BPA-FBz).
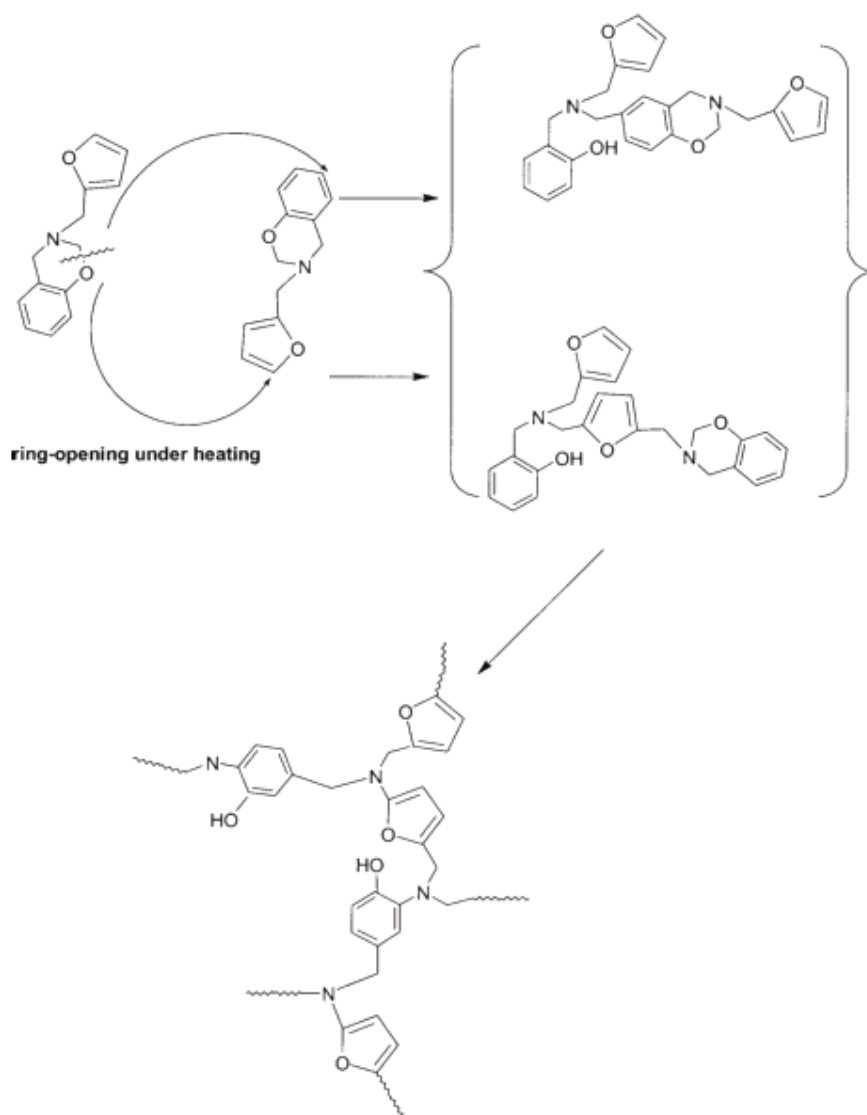
Figure 2.9 P-FBz polymerization.

Wang *et al.* (2013) prepared bio-based polybenzoxazine by using a curing agent and studied its thermal properties. The materials used in this experiment included furfurylamine, methanesulfonic, paraformaldehyde, methyl p-toluenesulfonate or PTSM, p-toluaic acid (PTS), guiacol, dimethyl sulfoxide and anhydrous ethanol. To prepare Bzf or 3-Furfury-8-methoxy-3,4-dihydro-2H-1,3-benzoxazine monomer, the Bzf monomer was prepared by two methods: with solvent and without solvent. For solvent method preparation, 7.5 ml solution of

paraformaldehyde with water (37% w/w), 4.9 g furfurylamine in 100 ml ethanol and 6.2 g guiacol were mixed. Then the solution was heated for 48 hours at 50 °C. After that, it was dried under vacuum, and a white solid of Bzf monomer was obtained. The yield of this method was 68%. For a solvent-less preparation, 4.4 ml furfurylamine, 3.3 g paraformaldehyde and 6.2 g guaiacol were mixed until the solids disappeared at room temperature. After mixing, the solution was heated for 1 hour at 70 °C, then it was cooled down from 70 °C to room temperature. To obtain a white solid of Bzf monomer, ethanol was added in the solution to crystallize Bzf monomer. Then it was dried and filtered, and Bzf monomer was obtained. This method gave 92% yield (Wang *et al.*, 2012). The monomer synthesis reaction is shown in Figure 2.10. To polymerize the monomer, 4.9 g Bzf monomer and 5.0 ml PTSM in acetone solution were mixed homogeneously. Acetone was removed from a solution by drying in an oven. After that, a solution was polymerized with various heating temperature such as 140 °C, 160 °C, 180 °C, and 200 °C for 4 hours. The result showed that the obtained polybenzoxazine exhibited good thermal stability and high char yield (Wang *et al.*, 2013).
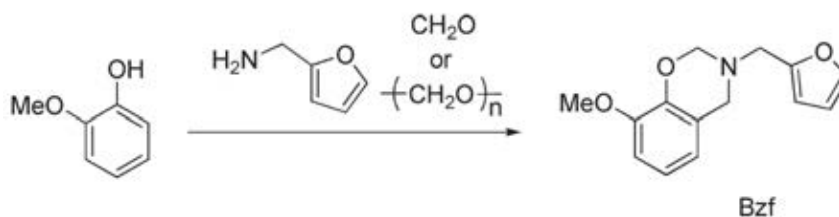
Figure 2.10 Preparation of Bzf monomer.

2.8.2 Sol-gel Polymerization

A sol-gel polymerization is used to generate micro and mesoporous structure in the polymer. This technique employs solvent to penetrate in the monomer content before it is partially polymerized. After partially polymerization, the solvent is eliminated from the solution. Finally, the polymer is fully polymerized and the porous structure is obtained in the polymer.

Lorjai *et al.* (2009) prepared porous structure of organic aerogel polybenzoxazine from a sol-gel preparation. In their study, benzoxazine monomer was prepared using a solventless method. The precursors used in the benzoxazine monomer preparation were paraformaldehyde, bisphenol A, and aniline with a 4:1:2 molar ratio. All precursors were mixed at 110 °C for 60 min until a solution became a clearly yellow solution. Then the monomer was obtained. To obtain the aerogel polybenzoxazine from a sol-gel preparation, xylene was used as a solvent to prepare benzoxazine solution. The solutions with 20 and 40 wt% bezoxazine were added into vials, sealed, and placed into an oven. They were then slowly heated until the temperature approached 130 °C for 96 hours for partially curing benzoxazine. After that, the partially cured benzoxazine hydrogels were dried at room temperature and atmospheric pressure for 48 hours to eliminate xylene, and organic aerogels were obtained. The organic aerogels were cured following a step-curing procedure: at 160, 180 °C for 1 hour, at each temperature and 200 °C for 2 hours. Finally, the obtained organic aerogels were cooled down to room temperature. After the curing process, they were carbonized following carbonization procedure to obtain the carbon aerogels. The results showed that the pore structure of carbon aerogels was a microporous structure, with pore diameters of less than 2 nm. The surface area were around 384 m^2/g for 20 wt% benzoxzine and 391 m^2/g for 40 wt% benzoxzine (Lorjai *et al.*, 2009).

Liu *et al.* (2010) prepared benzoxazine containing fluorine to characterize the properties. For this research, FDP-FBz was a benzoxazine monomer. It was prepared from the precursors including FDP, furfurylamine and formaldehyde. 1.66 g furfurylamine, 2.78 g formaldehyde and 3.0 g FDP were added into 5, 10 and 30 ml dioxane. The solution of furfurylamine was slowly poured to the solution of formaldehyde. Then a mixed solution was stirred for 30 min. After that, the solution of FDP was poured to a mixed solution, it was heated at 105 °C for 36 hours. The solvent was eliminated by an evaporator. The pH of the solution was adjusted until neutral. The solution was then recrystallized with ethanol to obtain high purity FDP-FBz. To polymerize FDP-FBz, 5 wt% FDP-FBz was dissolved in THF before adding p-toluenesulfonic (curing promoter). The mixed solution was polymerized following a procedure in an oven, at 160 °C for 3 hours, 200 °C for 2 hours, and 240 °C for 2 hours. Finally, the mixed solution became FDP-FBz polymer.

2.9 Methods of Adsorption Measurement

Typical methods to measure the adsorption isotherm of the adsorbents are volumetric, gravimetric and temperature programmed desorption (TPD) method.

2.9.1 Volumetric Method

Volumetric method is the basic method for the adsorption equilibrium measurement. The main concept is to measure the pressure drop after the adsorbents adsorb CO_2 molecules at a constant volume. This apparatus mainly consists of a reservoir and a sample cell. First, the sample is placed into a sample cell. Then, the reservoir and sample cell are all degassed. After that, the reservoir is filled with CO_2 molecules and CO_2 molecules are expanded to a sample cell. Finally, the adsorption capacity is calculated with the ideal gas equation by subtracting the number of molecules at the final equilibrium from the number of initial molecules (Blackman *et al.*, 2006).

2.9.2 Gravimetric Method

Thermal gravimetric analyzer is generally used in the gravimetric measurement. This method is very sensitive for all gas that was adsorbed. Very small amounts of sample (1-10 mg) was used to measure the adsorption capacity. Only 0.01 or 1 wt% of impurities can cause an inaccuracy. Therefore, this method is suitable for an adsorbent with high adsorption capacity (Blackman *et al.*, 2006).

2.9.3 Temperature Programmed Desorption (TPD)

Similar to the gravimetric method, a sample of 1-10 mg was used in the TPD technique for measuring the adsorption capacity. The temperature is controlled between 90 and 970 K under vacuum. To measure the amount of adsorbed molecules, the mass spectrometry is employed by calculating the amount of molecules from the desorption process (Blackman *et al.*, 2006)

CHAPTER III
EXPERIMENTAL

3.1 Motivation

In these days, the growth of population increases continuously, causing an increase in the demand of energy. Huge amount of energy resources is extremely consumed to produce more electricity and other goods and facilities. As a result, abundant CO_2 emission is emitted to the atmosphere and creates the global warming.

To handle the CO_2 emission problem, there are many techniques employed to reduce CO_2 emission. This research has focused on the adsorption technique. There are several porous materials used for adsorbents such as carbon molecular sieve (CMS), zeolites, polymers, and metal organic frame works (MOFs). These adsorbents are more advantages over the currently used amine absorption in terms of less energy consumption during regeneration, lower number of equipment count, and lower capital cost.

One of the attractive adsorbents is the carbon adsorbent derived from polymers. It can give various structures from different polymer precursors and suitable surface functionality can be designed. These effects make the carbon adsorbent derived from polymers a potential adsorbent to capture the CO_2

The aim of this research was to prepare the adsorbent from polybenzoxazine and develop the structure by using the different synthesis methods, various carbonization temperatures, and different activations to obtain high CO_2 adsorption capacity.

3.2 Hypothesis

3.2.1 The furfurylamine-based polybenzoxazine adsorbent activated with chemical activation will give higher CO_2 capacity than activated with physical activation. Because chemical activation can generate more micropore and mesopore than physical activation.

3.2.2 The adsorbent synthesized by sol-gel polymerization will give higher porosity than the adsorbent synthesized by bulk polymerization because the solvent can diffuse and stay in the polymer layer until it is partially cured. After the solvent will be removed and interconnected pores will be created. Therefore, the obtained adsorbent will contain high porosity and give high CO_2 adsorption capacity.

3.2.3 In sol-gel polymerization, the lowest monomer component in adsorbent will give higher porous structure than other weight percentages since the high amount of solvent can create more porous structure to the polymer skeleton. The adsorbent will be obtained in a fine particle size. Therefore, it will increase the CO_2 adsorption capacity.

3.2.4 The increase of carbonization temperature will generate more micropores, but it has the limit to increase the temperature for generating micropores because the high carbonization temperature may break the microporous structure and cause pore collapse. Therefore, the adsorbent will be carbonized at the appropriate temperature.

3.3 Objectives

3.3.1 <u>To study the effect of polymer preparations between bulk and sol-gel techniques on the porosity of furfurylamine-based polybenzoxazine adsorbent.</u>

3.3.2 <u>To investigate the effect of physical activation and chemical activation on the porosity of furfurylamine-based polybenzoxazine adsorbent.</u>

3.3.3 <u>To study the effect monomer content in the sol-gel adsorbent on the porous structure and CO_2 adsorption performance.</u>

3.3.4 <u>To investigate the effect of carbonization conditions on CO_2 adsorption capacity.</u>

3.4 Scope of Research

The scope of this research cover is as follows

3.4.1 <u>Benzoxazine monomer was prepared from furfurylamine, paraformaldehyde, and phenol.</u>

3.4.2 <u>P-xylene was used as the solvent in the sol-gel technique.</u>

3.4.3 <u>Various ratio of monomer to solvent in the sol-gel technique were studied and morphology of the obtained adsorbent was compared.</u>

3.4.4 <u>Polybenzoxazine was synthesized by the sol-gel polymerization approach.</u>

3.4.5 <u>Polybenzoxazine was carbonized at 600-800 °C under N_2 atmosphere following by activation using two different techniques: physical activation and chemical activation.</u>

3.4.6 <u>CO_2 was used in physical activation, while KOH was used as the activating agent in the chemical activation.</u>

3.4.7 <u>The CO_2 adsorption isotherm was studied at 40 °C, 70 °C, and 110 °C.</u>

3.5 Materials

3.5.1 Chemicals:

    3.5.1.1 *Paraformaldehyde, 95%, AR (Sigma Aldrich)*

    3.5.1.2 *Phenol, 99%, AR (Fisher Bioreagents)*

    3.5.1.3 *Furfurylamine, 99%, AR (Sigma Aldrich)*

    3.5.1.4 *p-Xylene, 99%, AR, 2.5 L (Sigma Aldrich)*

    3.5.1.5 *Acetone, 99.5%, AR, 20 L (RCI Labscan)*

    3.5.1.6 *Potassium hydroxide, 85%, AR, (Sigma Aldrich)*

    3.5.1.7 *Hydrochloric acid, 37%, AR, (Sigma Aldrich)*

3.5.2 Gasses

    3.5.2.1 *High purity (HP) carbon dioxide, 99.9 %*

    3.5.2.2 *High purity (HP) nitrogen, 99.99 %*

    3.5.2.3 *High purity (HP) helium, 99.995 %*

3.6 Equipment

3.6.1 CHN analyzer (LECO) (TruSpec Micro CHN/S)

3.6.2 Differential Scanning Calorimeter (Mettler Toledo) (DSC 204 F1)

3.6.3 Fourier Transform Infrared Spectrometer (FTIR) (Thermo Nicolet iS 5, Nexus 670)

3.6.4 Surface Area Analyzer (Quantachrome) (Autosorb-1MP)

3.6.5 Thermogravimetric Analyzer (Perkin-Elmer) (Pyris Diamond)

3.6.6 X-ray Photoelectron Spectroscopy (Kratos) (Axis Ultra DLD)

3.7 Experimental Procedures:

    3.7.1 <u>Benzoxazine Monomer Preparation</u>

        Benzoxazine monomer was prepared from furfurylamine, paraformaldehyde (95% purity) and phenol with a molar ratio of 1:2:1. Paraformaldehyde (95% purity) and phenol were weighted in a foil cup with a molar ratio of 2:1. After weighting, the mixture was heated at 80 °C until it melted, then 1 mol of furfurylamine was slowly added into the mixture and stirred at 110 °C for 40 min until it became a clearly yellow and homogeneous solution.

    3.7.2 <u>Polymerization of Benzoxazine Monomer</u>

        Bulk polymerization, Benzoxazine monomer was cured using a solventless method in an oven. It was heated by following the procedure: heating from room temperature to 100 °C for 14 min, 100 to 150 °C for 17 min, holding at 150 °C for 30 min, heating from 150 to 200 °C for 17 min, and holding at 200 °C for 60 min.

        Sol-gel polymerization, Benzoxazine monomer was mixed in xylene as a sol-gel solvent to obtain benzoxazine solution with various monomer contents (20, 30, 40 wt% of benzoxazine monomer). The solution was stirred until a homogenous solution was obtained. Then the solution was poured into a vial and sealed. After that, the vial was placed into an oil bath at suggested temperatures from Differential Scanning Calorimeter (DSC) test for partially curing. Finally, the partially cured benzoxazine polymer was cooled down to room temperature, and the sol-gel solvent was removed by a solvent exchange technique using acetone. Acetone was changed daily for five consecutive day and the polymer was dried at room temperature.

    3.7.3 <u>Carbonization of Polybenzoxazine</u>

        Polybenzoxazine was carbonized at various temperatures (600, 700, and 800 °C) for 2 hours under N_2 atmosphere.

    3.7.4 <u>Activation</u>

        Carbonized polybenzoxazine was activated with chemical activation and physical activation. The porous structure of the obtained adsorbent was analyzed with a Surface Area Analyzer (AS-1MP). In the chemical activation, carbonized polybenozaxine was activated by KOH in the weight ratio of 4:1 (KOH:carbonized

polybenzoxazine) under N2 atmosphere at 900 °C for 2 hours. For physical activation, it was activated by CO_2 at 900 °C for 2 hours.

3.7.5 Adsorption Measurement

The pressure decay adsorption approach was used to calculate the CO_2 adsorption capacity of the absorbent. All tubings and fittings have been made of high quality stainless steel to avoid corrosion along the process. The sizes of a reservoir and adsorber column are 50 and 10 cm^3, respectively. The volume of the adsorber column was measured using helium expansion and calculated from the ideal gas law (shown in Equation 1). The temperature was controlled at the same value throughout the reservoir and the adsorber column. First, the adsorbent was placed into the adsorber column and was then heated up to the desired temperature. Both reservoir and adsorber columns were degassed. After that, the lower needle valve was closed to isolate the adsorber column. The reservoir was pressurized with CO_2 to a desired pressure and the top needle valve (NV-1) was then closed. After the pressure and temperature were stable, the lower needle valve was opened and then the adsorption was started until reaching an equilibrium. The CO_2 adsorption capacity was determined by measuring the beginning pressure and equilibrium pressure. Equation 2 is used to determine the amount of CO_2 adsorption capacity. The schematic of the adsorption system is shown in Figure 3.1

$$\frac{P_1 V_1}{T_1} = \frac{P_2 V_2}{T_2} \tag{1}$$

Where P_1 = Pressure of helium before expansion

V_1 = Volume of the system excluding the adsorber column

T_1 = Temperature before helium expansion

P_2 = Pressure of helium after expansion

V_2 = Total Volume, V_1 + $V_{adsorber\ column}$

T_2 = Temperature after helium expansion

$$n_{ad} = \frac{P_i V_1}{ZRT_i} - \frac{P_f(V_1 + V_{ads\ column} + V_{adsorbent})}{ZRT_f} \tag{2}$$

Where n_{ad} = Amount of CO_2 adsorbed in the adsorbent

P_i = Initial CO_2 pressure, before experiment

P_f = Final CO_2 pressure, at equilibrium

V_1 = Volume of the system excluding adsorber column

$V_{ads\ column}$ = Volume of the adsorber column

$V_{adsorbent}$ = Volume of the solid adsorbent

Z = Compressibility factor
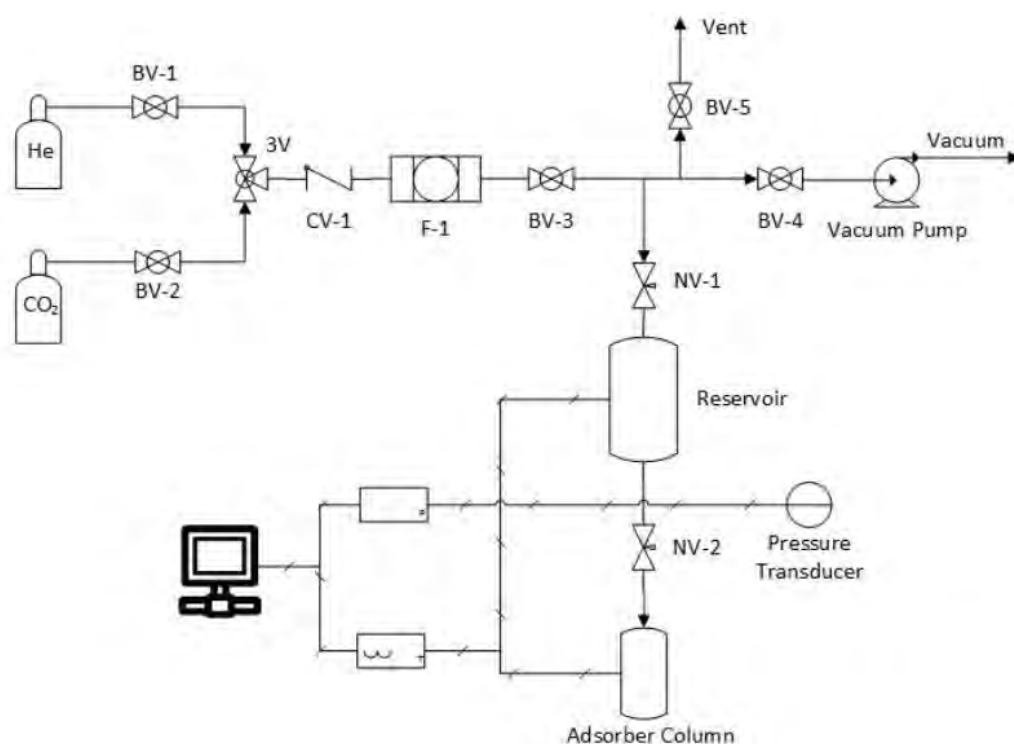
Figure 3.1 Schematic of the adsorption system.

3.7.6 Characterizations

3.7.6.1 Fourier Transform Infrared Spectrometer (FTIR)

FTIR was used to investigate the functional group related to the structure of benzoxazine monomer and polybenzoxazine by using Nicolet iS5 FT-IR spectrometer in the wave number range 400-4000 cm^{-1}.

3.7.6.2 Differential Scanning Calorimeter (DSC)

DSC was used to study the curing behavior of benzoxazine. 4-8 mg of benzoxazine sample was added into an aluminum pan, sealed, and analyzed with a heating rate of 10 °C/min from 30 °C to 300 °C under N_2 atmosphere.

3.7.6.3 Thermogravimetric Analyzer (TGA)

TGA was used to observe the thermal degradation behavior of benzoxazine sample. The sample was heated from 30 °C to 900 °C with a heating rate of 10 °C/min under N_2 atmosphere.

3.7.6.4 Surface Area Analyzer (AS-1MP)

A surface area analyzer was used to calculate the BET surface area based on the Brunauer-Emmett and Teller (BET) theory and pore size distribution with Barret-Joyner-Halenda (BJH) equation. The sample was degassed at 250 °C for 20 hours under vacuum to eliminate entire volatile adsorbed gases existing on an adsorbent surface. The surface area of the adsorbent was analyzed by using 17 adsorption points and 16 desorption points under the temperature of -196 °C with liquid N_2.

3.7.6.5 CHN analyzer

CHN analyzer was used to measure the composition of three elementals including carbon (C), hydrogen (H), and nitrogen (N). 0.1 g of sample was wrapped with a tin foil and put into the sample cell to analyze at 950 °C

3.7.6.6 Field Emission Scanning Electron Microscope (FE-SEM)

FE-SEM was used to observe the surface morphology of carbon adsorbent. The sample was placed on a carbon sticky tape, then it was coated with platinum. After coating, the images of sample were captured with a magnification from 20,000 to 100,000 times.

3.7.6.7 X-ray photoelectron spectroscopy (XPS)

XPS was used to determine the number of functional groups existing on the surface of carbon adsorbent. The sample was scanned using a wide scan by resolution pass energy of 160 eV following by a narrow scan by resolution pass energy of 20-40 eV.

CHAPTHER IV
RESULTS AND DISCUSSION

The modification of textural properties of polybenzoxazine has become the focus to improve the surface area, total pore volume, micropore volume, and average pore diameter properties to be appropriate for carbon dioxide adsorption. From the result, all properties can be improved. A sol-gel technique was used to synthesize the furfurylamine-based polybenzoxazine to help enhance porosity in the polymer skeleton. Carbonization temperatures were varied at 600, 700, and 800 °C under N_2 atmosphere to obtain high porous carbon material with appropriate nitrogen functionalities for CO2 adsorption. Two activation techniques were used including physical activation by CO_2 and chemical activation by potassium hydroxide (KOH).

4.1 Characterization of The Materials

4.1.1 Benzoxazine Monomer Characterization

To investigate the functional groups of benzoxazine monomer, Fourier Transform Infrared Spectrometer (FTIR) was employed to obtain the infrared spectrum of the absorption bands. To interpret the FTIR spectra, the characteristic of benzoxazine ring was absorbed at 1228-1230 cm^{-1} (C-O-C asymmetric stretching), 1017-1018 cm^{-1} (C-O-C symmetric stretching), and 1327-1333 cm^{-1} (CH$_2$ wagging). The benzene groups (disubstituted benzene) were absorbed at 1486 and 1498 cm^{-1}. The furan groups were displayed on absorption peaks at 1571, 976, and 763 cm^{-1}. Another absorption peak of the furan ring was shown at 925 cm^{-1} (Liu *et al.*, 2005). Figure 4.1 shows FTIR spectra of furfurylamine-derived benzoxazine monomer. The benzoxazine ring peaks were shown at 1220, 1011, and 1342 cm^{-1}. The benzene groups appeared at 1455 and 1488 cm^{-1}. Furthermore, the furan groups were absorbed at 1583, 985, and 731 cm^{-1} and another furan ring was absorbed at 927 cm^{-1}.
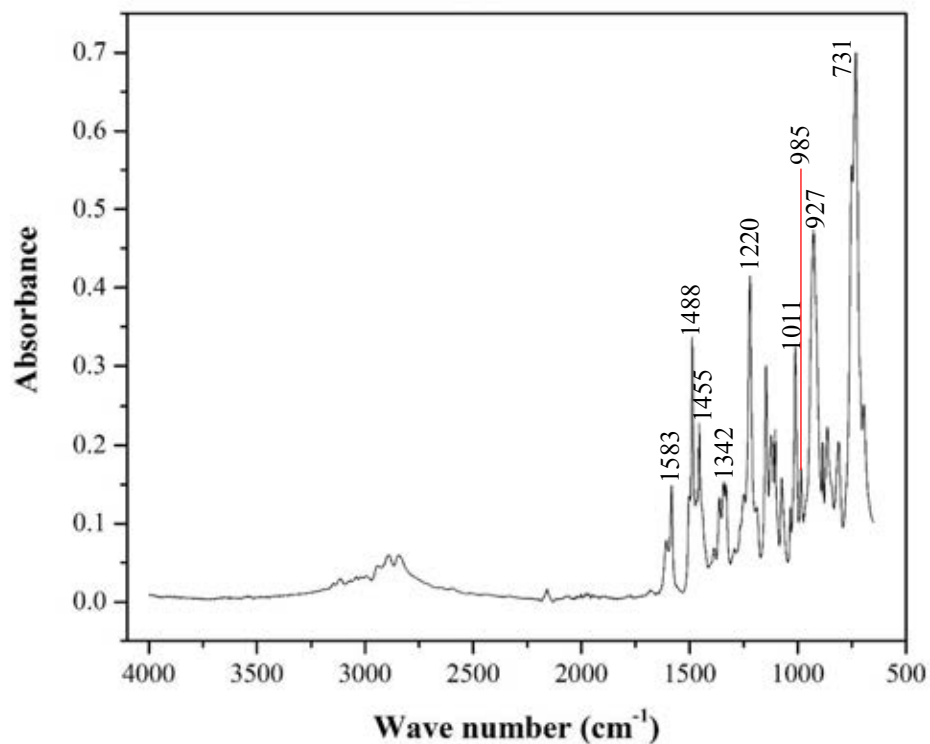
Figure 4.1 FT-IR spectra of furfurylamine-derived benzoxazine monomer.

Differential Scanning Calorimeter (DSC) was conducted to study the curing behavior of furfurylamine-derived benzoxazine monomer. The monomer was heated from 30 to 300 °C with a heating rate of 10 °C/min under nitrogen atmosphere. Figure 4.2 shows the curing behavior of benzoxazine monomer. From the results, it can be indicated that the ring opening polymerization temperature occurred around 130 and 220-260 °C, which suggested the temperature ranges during the gel formation of benzoxazine monomer.
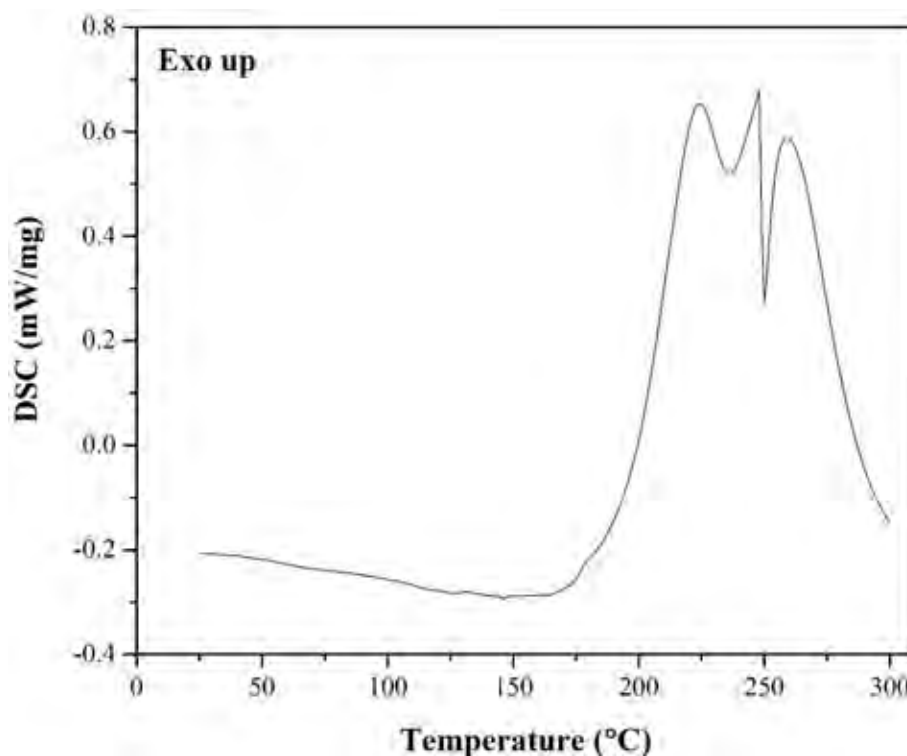
Figure 4.2 DSC thermograms of benzoxazine monomer with furfurylamine as an amine reactant.

4.1.2 Polybenzoxazine Characterization

Polybenzoxazine was cured by bulk and sol-gel polymerization. To probe the occurrence of ring opening polymerization, the FT-IR spectra of polybenzoxazine derived from furfurylamine as amine precursor was used to investigate the ring opening polymerization of benzoxazine monomer. The intensity of absorption peak at 1488 cm^{-1} (benzene groups) was clearly decreased, suggesting the occurrence of ring opening polymerization of benzoxazine monomer as shown in Figure 4.3. Furthermore, the intensity of absorption peak at 1583 cm^{-1} was reduced meaning that the furan groups involved in the polymerization reaction (Liu *et al.*, 2005).

Figure 4.3 FT-IR spectra of the furfurylamine-derived polybenzoxazine.

Figure 4.4 TGA thermograms of the furfurylamine-derived polybenzoxazine.

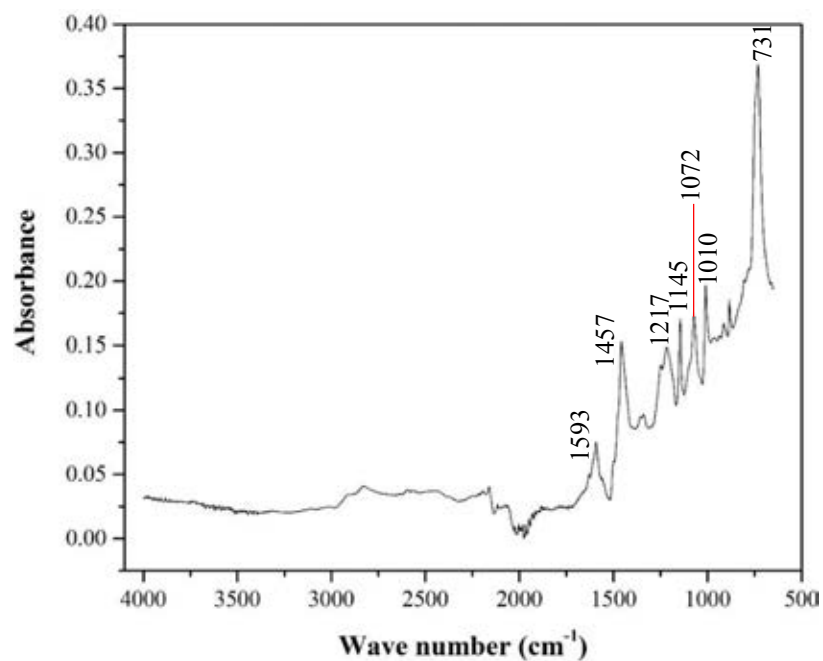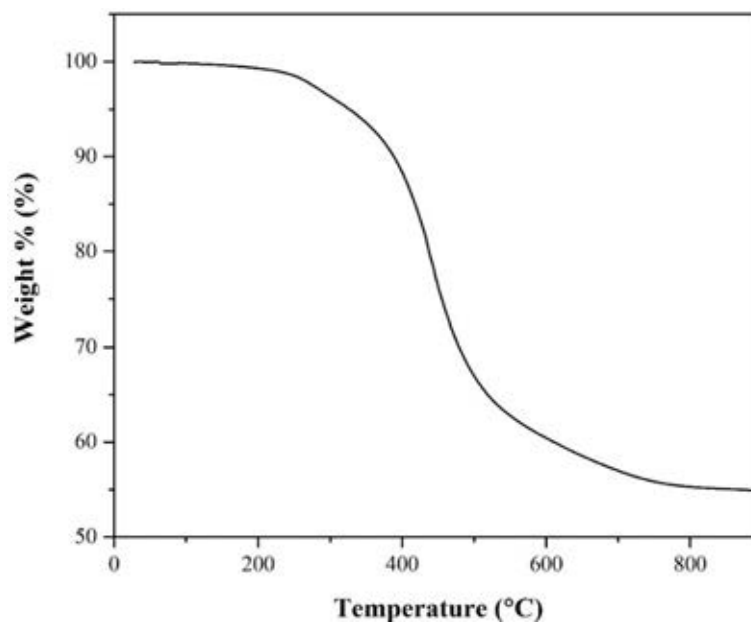Figure 4.4 shows the TGA thermograms of furfurylamine-based polybenzoxazine. The polybenzoxazine began to lose weight at 200 °C and the maximum weight loss was resulted in the temperature range of 400 °C – 500 °C from the thermal degradation of volatile materials. The char yield of polybenzoxazine derived from furfurylamine was 55.324 % which was very high since the polymer structure had high amount of crosslinking density that made the polymer structure be very dense.

4.1.3 Characterization of Carbon Adsorbents

Table 4.1 shows the element compositions of carbon adsorbents including carbon (C), hydrogen (H), nitrogen (N), and oxygen (O, by difference). It was observed that all polymer with different monomer ratio (i.e. denoted as PO-Sxx in Table 4.1) during the sol-gel polymerization gave similar elemental content. After carbonization under nitrogen atmosphere at 600, 700 and 800 °C (i.e. denoted as CA-xNxx in Table 4.1), the carbon content increased, while hydrogen and nitrogen contents decreased. All carbonized samples gave similar carbon content. The carbon content increased from *ca.* 68 wt% as a monomer to *ca.* 86 wt% after a carbonization process. It is noted that the nitrogen content was slightly decreased as the carbonization temperature increased. Two activation processes were performed on the carbonized samples: physical activation using carbon dioxide and chemical activation by KOH. The physical activation (i.e. denoted as CA-xSPxx in Table 4.1) gave similar carbon content while hydrogen and nitrogen contents decreased. In chemical activated samples (i.e. denoted as CA-xSCxx in Table 4.1), all carbon, hydrogen and nitrogen contents decreased and significantly increased in oxygen content was revealed. Since KOH was used in the chemical activation process, the samples were severely oxidized, giving high amount of oxygen functionalities in the samples. A smaller drop in the carbon content was observed in sample experienced higher carbonization temperature, i.e. carbon content of *ca.* 60 wt.% in CA-6SC20 v.s. carbon content of *ca.* 80 wt.% in CA-8SC20. Nevertheless, the nitrogen content decreased as the carbonization temperature increased in the chemical activated samples. To study the effect of nitrogen content on the CO_2 adsorption performance, the high amount of nitrogen

might affect the CO_2 adsorption capacity, which was further described in the next section.

Table 4.1 Element content of carbon adsorbents

Sample	% C	% H	% N	% O (by difference)
Activated carbon	88.98 ± 0.05	1.18 ± 0.13	0.26 ± 0.04	9.58
PO-S20	68.87 ± 0.42	5.11 ± 0.01	5.17 ± 0.06	20.85
PO-S30	67.86 ± 0.16	5.00 ± 0.05	5.16 ± 0.04	21.98
PO-S40	68.03 ± 1.34	4.94 ± 0.11	5.21 ± 0.05	21.82
CA-6N20	87.60 ± 4.96	2.27 ± 0.14	3.96 ± 0.06	6.17
CA-6N40	86.02 ± 4.80	2.16 ± 0.41	4.77 ± 0.65	7.05
CA-7N20	85.57 ± 0.47	1.42 ± 0.09	3.52 ± 0.04	9.49
CA-8N20	87.75 ± 1.01	1.01 ± 0.01	3.28 ± 0.07	7.96
CA-6SP20	81.24 ± 3.44	1.48 ± 0.30	2.34 ± 0.12	14.94
CA-6SP30	85.30 ± 2.69	0.99 ± 0.20	2.22 ± 0.12	11.49
CA-6SP40	86.66 ± 0.94	0.80 ± 0.02	2.41 ± 0.00	10.13
CA-6SC20	60.25 ± 6.87	1.32 ± 0.18	1.42 ± 0.42	37.01
CA-6SC40	64.96 ± 6.48	1.10 ± 0.52	1.70 ± 0.84	32.24
CA-7SC20	65.08 ± 1.48	1.80 ± 0.04	1.28 ± 0.28	31.84
CA-8SC20	78.72 ± 0.71	1.24 ± 0.24	0.37 ± 0.03	19.67

Note: CA is carbon adsorbent; numbers 6, 7, and 8 are the carbonization temperature at 600, 700, and 800 °C, respectively; B is bulk polymerization; S means the sol-gel polymerization; P stands for physical activation; C is chemical activation; N means sample without activation; and PO stands for polymer.

Figure 4.5 FE-SEM images of carbon adsorbents at magnification of 20,000x: (a) PO-S20, (b) PO-S30, (c) PO-S40, (d) CA-6N20, (e) CA-7N20, (f) CA-8N20, (g) CA-6SP20, and (h) CA-6SC20.
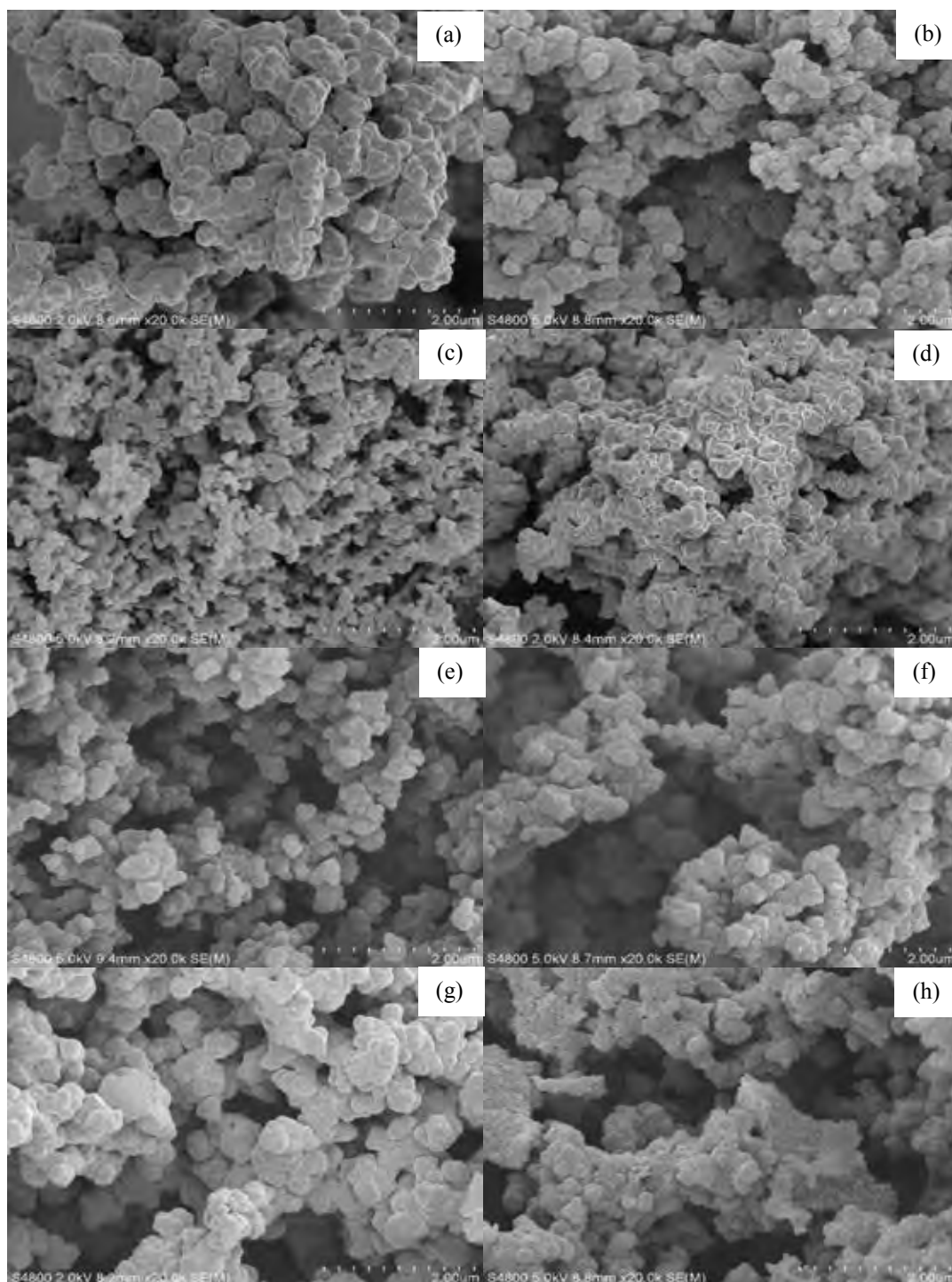
Figure 4.6 FE-SEM images of carbon adsorbents at magnification of 50,000x: (a) PO-S20, (b) PO-S30, (c) PO-S40, (d) CA-6N20, (e) CA-7N20, (f) CA-8N20, (g) CA-6SP20, and (h) CA-6SC20.
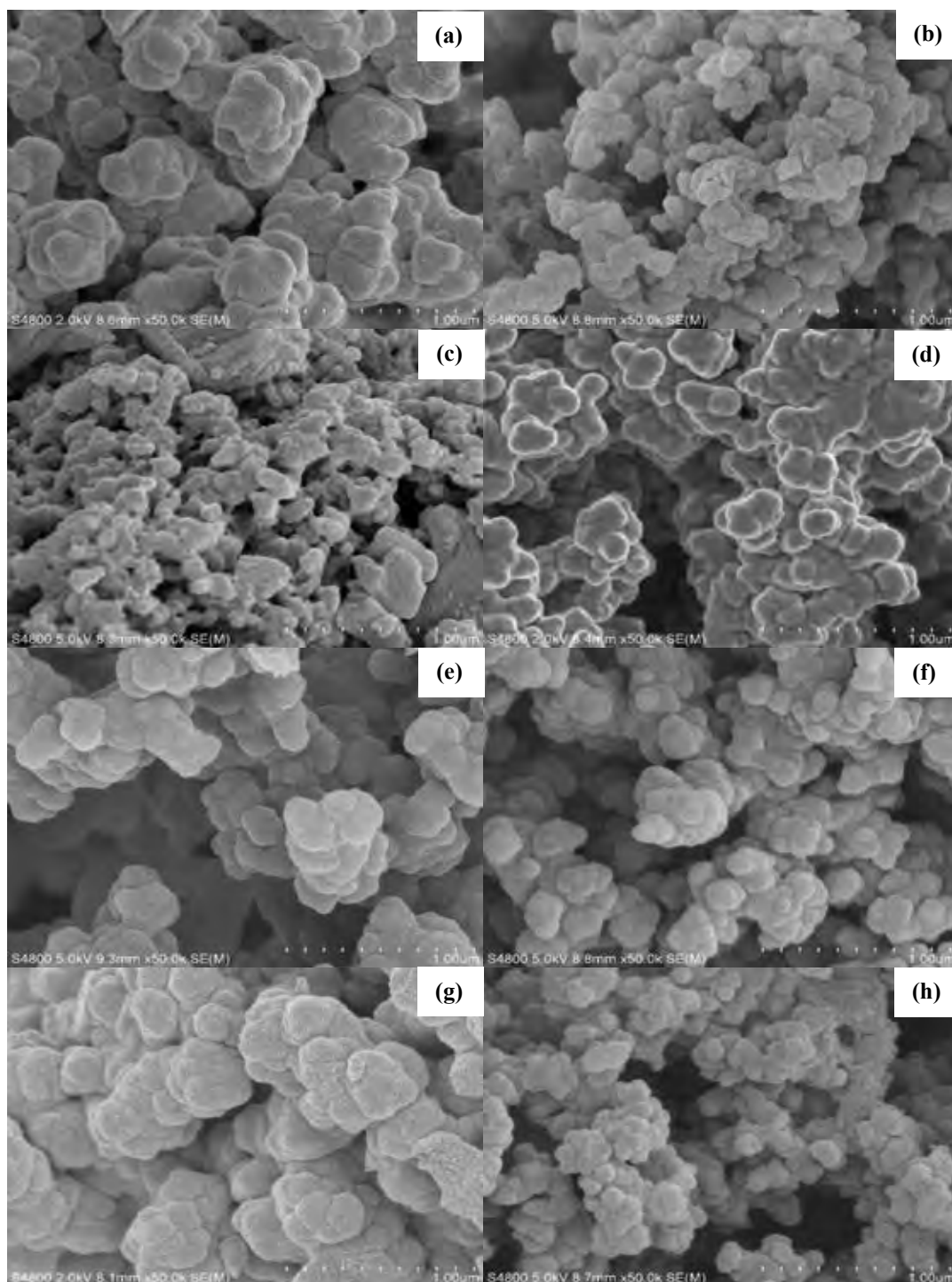
Figures 4.5 and 4.6 show the morphology of carbon adsorbents derived from furfurylamine-based polybenzoxazine with magnifications of 20,000x and 50,000x, respectively. Polymers were agglomerated by microgel particles with size around 1μm scale similar to the work of (Xu *et al.*, 2018). Figure 4.5(a), 4.5(b), and 4.5(c) display the polybenxozazine polymers synthesized by the sol-gel process with benzoxazine monomer of 20 wt%, 30 wt%, and 40 wt%, respectively. The polymer containing 20 wt% monomer were agglomerated with the biggest size of microgel particles when comparing with the polymer containing 30 and 40 wt% monomer. Three dimensional structure of porous carbon network with interconnected pores were obviously observed. Figure 4.5(d), 4.5(e), and 4.5(f) show the morphology of carbon adsorbents after carbonization at 600, 700, and 800 °C, respectively. As the carbonization temperature was higher, the size of the globules were smaller since microgel particles were partially removed and N_2 molecules can expand the structure of adsorbent. The adsorbent carbonized at 800 °C gave the highest porosity because the higher temperature could remove high amount of microgel particles according to the textural properties in the Table 4.2. However, carbonizing at 700 °C gave the similar porosity to at 600 °C; therefore, it might assume that increasing carbonization temperature could help the adsorbent to generate higher porosity. Figure 4.5(g) and 4.5(h) show the adsorbent activated with physical and chemical activation, respectively. Physical activation by CO_2 as an activating agent did not change the size of the globules as compared between Figure 4.6(a) and 4.6(g) for the micrographs of polymer and carbonized adsorbent with the same monomer content, respectively. On the other hand, the chemical activation enhanced porosity by using KOH to penetrate and generate high amount of pores as evidenced by the BET results explained in the next section.

To investigate the surface composition including carbon, oxygen, and nitrogen of carbon adsorbents obtained from furfurylamine-based polybenzoxazine, adsorbents were characterized by X-ray Photoelectron Spectroscopy (XPS) with the wide and narrow scanning modes. Figures 4.7 to 4.9 show the deconvoluted C 1s, O 1s, and N 1s XPS spectra of carbon adsorbents, respectively. For the C 1s envelope, it can be deconvoluted into six main binding energies as follows: 283.5 ± 0.10 (Carbide), 284.4 ± 0.06 (Graphite), 285.0 ± 0.10 (Aliphatic), 285.4 ± 0.11 (Carbon with nitrogen), 285.9 ± 0.07 (Hydroxyl, Ether), and 286.5 ± 0.23 (Carbonyl) as suggested by Burg *et*

al. (2002); Plaza *et al.* (2013); Thongwichit *et al.* (2015). Considering O 1s spectra, six deconvoluted envelope appeared at the binding energies of 530.1 ± 0.29, 531.3 ± 0.20, 532.0 ± 0.16, 532.8 ± 0.08, 533.6 ± 0.17, and 534.9 ± 0.10 correspond to oxides, carbonyl or carboxyl, ketones or lactones or acids or esters, hydroxyl or ether, hydroxyl attached to aromatic ring, and absorbed water, respectively (Burg *et al.*, 2002); (Plaza *et al.*, 2013); (Thongwichit *et al.*, 2015). The N 1s envelope were divided into six peaks with binding energies centered at 398.1 ± 0.24, 398.9 ± 0.24, 399.8 ± 0.20, 400.6 ± 0.18, 401.6 ± 0.31, and 402.6 ± 0.37 which indicated pyridinic, imine, amide or amine, pyrrolic or pyridonic, quaternary-N, and Oxided-N groups, respectively, as suggested by Liu *et al.* (2015); Thongwichit *et al.* (2015), and Pietrzak (2009). Tables 4.2 to 4.4 show the assigned binding energy and percent content of each surface functional groups obtained from the deconvoluted XPS spectra of carbon adsorbents.

Considering the carbonized adsorbents before activation, the carbon functional groups on the surface were mainly assigned to graphite, carbon with nitrogen, and carbonyl. The oxygen functionalities were mainly carbonyl, hydroxyl or ether, and hydroxyl attracted to aromatic ring, but another component that still remained was oxide. For the nitrogen functionalities, the adsorbents contained mainly pyridinic, amine, and pyrrolic or pyridonic.

After activation with physical and chemical activation at 900 °C under N_2 atmosphere, the physical activation affected oxygen and nitrogen functionalities on the surface of adsorbents to be changed. The oxide and carbonyl groups were transformed to ketones and hydroxyl was changed to hydroxyl attached to aromatic ring. For nitrogen functionalities, the pyridnic functional groups of adsorbents were transformed to the pyrrolic or pyridonic (45-53%). Howerver, other nitrogen functional groups were found as amine (7-27%), quaternary-N (16-35%), and oxided-N (3-12%) functionalities as shown in the Table 4.4. Considering chemical activation, the oxygen and nitrogen functional groups were changed the composition. The oxide and carbonyl groups were transformed to ketones. The pyridinic functional group in the nitrogen functionalities was changed to the pyrrolic or pyridonic group (25-44 %). However, the pyridinic functional group was not completely transformed and it still remained around 2-14 %. Furthermore, these two functional groups were the groups responsible for the strong basic character that adsorbed the acidic CO_2 (Nanthiya *et*

al., 2016). Besides, the other nitrogen functionalities found on the adsorbent's surface were imine (10-33 %), amine (9-35 %), and quaternary-N (2-35 %) as shown in the table 4.3.
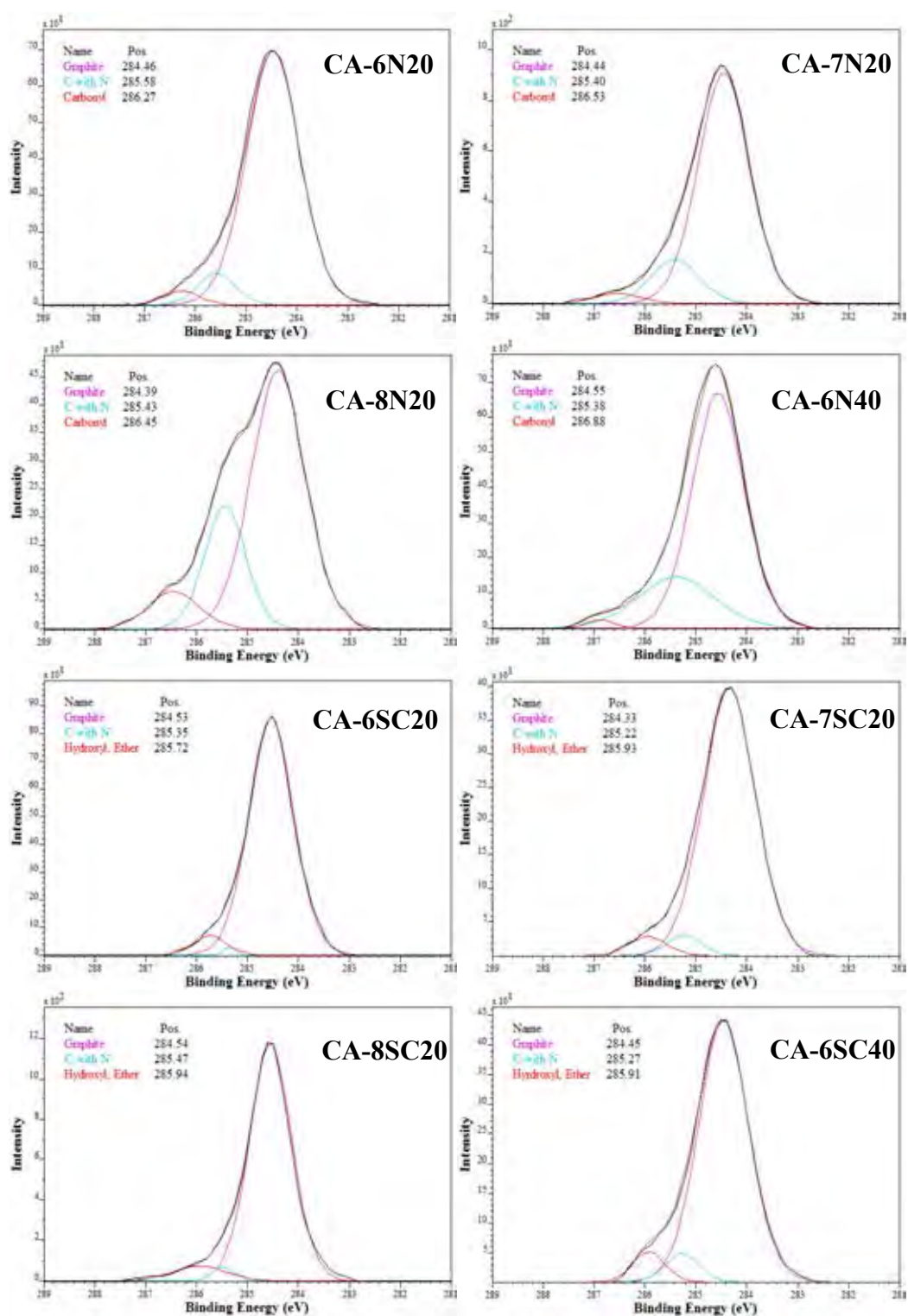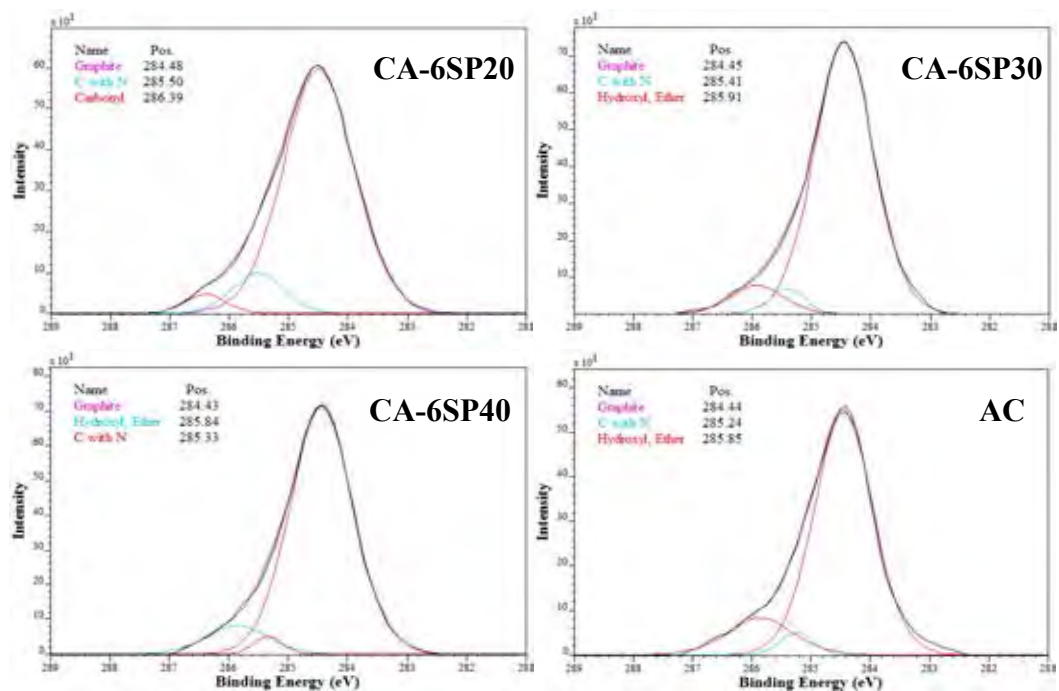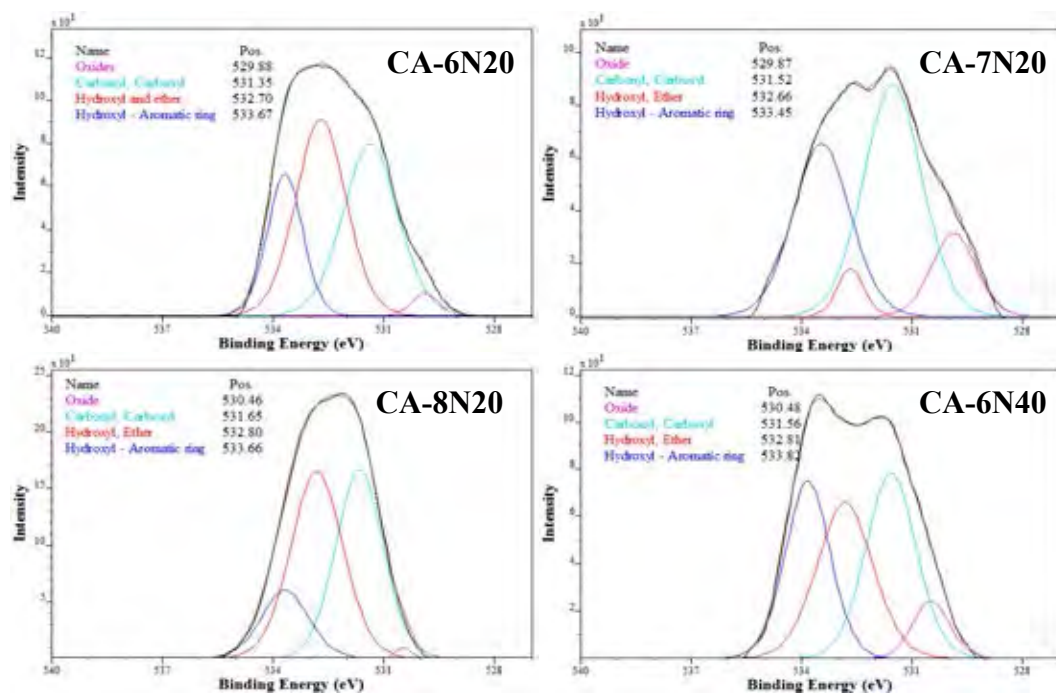
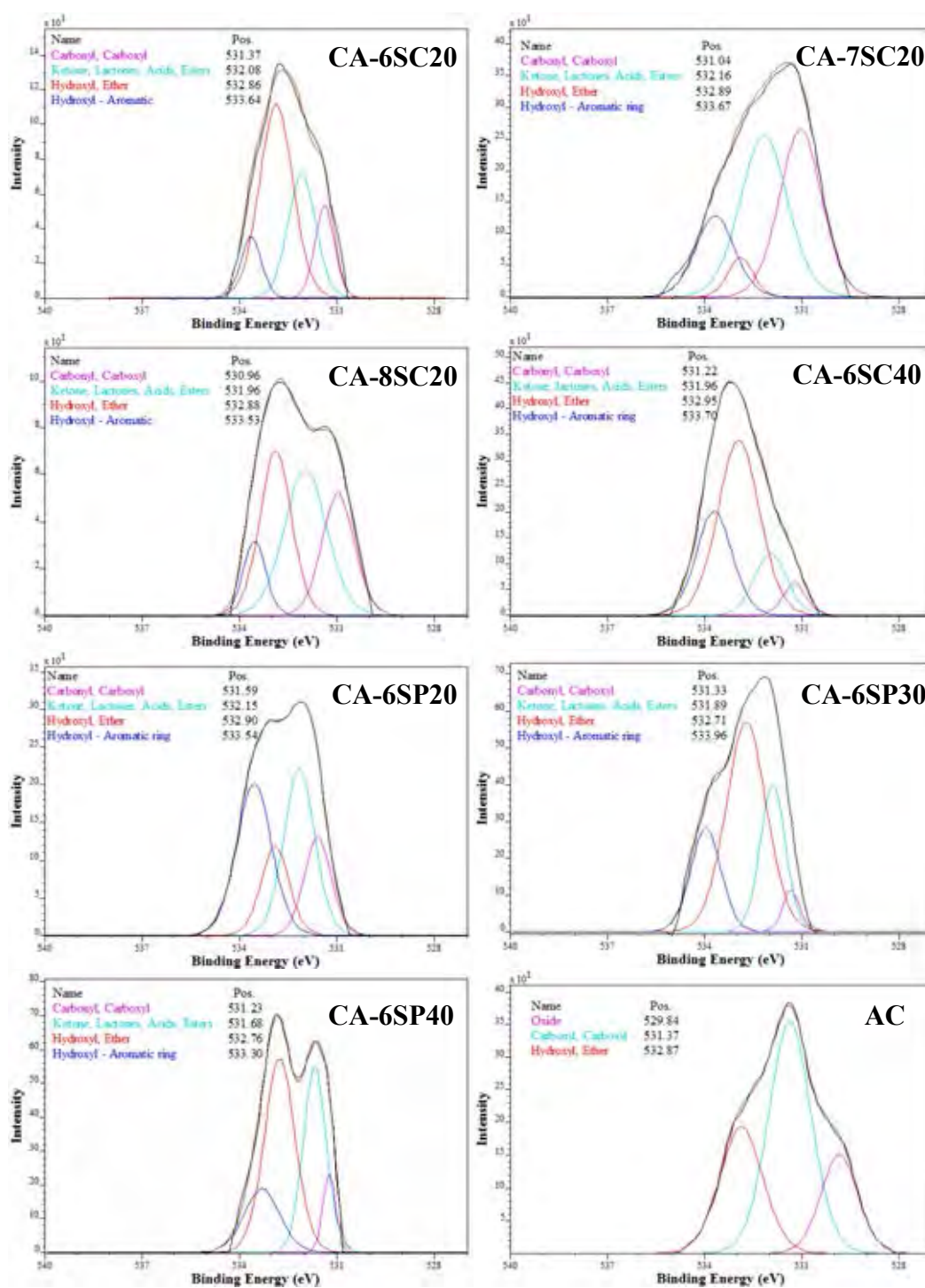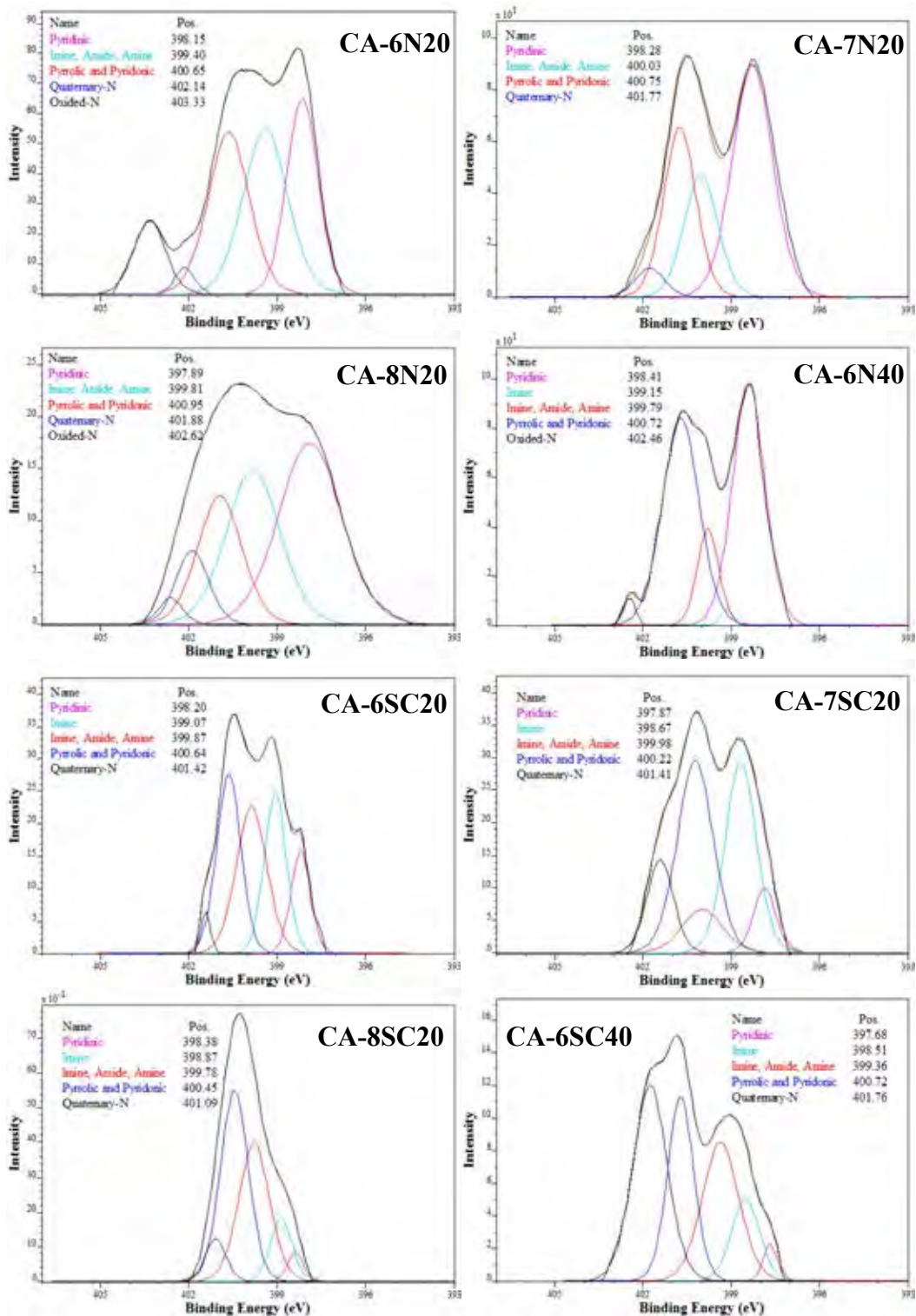**Figure 4.7** C 1s XPS spectra of carbon adsorbents

Figure 4.8 O 1s XPS spectra of carbon adsorbents

CA-6N20

Name	Pos.
Pyridinic	398.15
Imine, Amide, Amine	399.40
Pyrrolic and Pyridonic	400.65
Quaternary-N	402.14
Oxided-N	403.33

CA-7N20

Name	Pos.
Pyridinic	398.28
Imine, Amide, Amine	400.03
Pyrrolic and Pyridonic	400.75
Quaternary-N	401.77

CA-8N20

Name	Pos.
Pyridinic	397.89
Imine, Amide, Amine	399.81
Pyrrolic and Pyridonic	400.95
Quaternary-N	401.88
Oxided-N	402.62

CA-6N40

Name	Pos.
Pyridinic	398.41
Imine	399.15
Imine, Amide, Amine	399.79
Pyrrolic and Pyridonic	400.72
Oxided-N	402.46

CA-6SC20

Name	Pos.
Pyridinic	398.20
Imine	399.07
Imine, Amide, Amine	399.87
Pyrrolic and Pyridonic	400.64
Quaternary-N	401.42

CA-7SC20

Name	Pos.
Pyridinic	397.87
Imine	398.67
Imine, Amide, Amine	399.98
Pyrrolic and Pyridonic	400.22
Quaternary-N	401.41

CA-8SC20

Name	Pos.
Pyridinic	398.38
Imine	398.87
Imine, Amide, Amine	399.78
Pyrrolic and Pyridonic	400.45
Quaternary-N	401.09

CA-6SC40

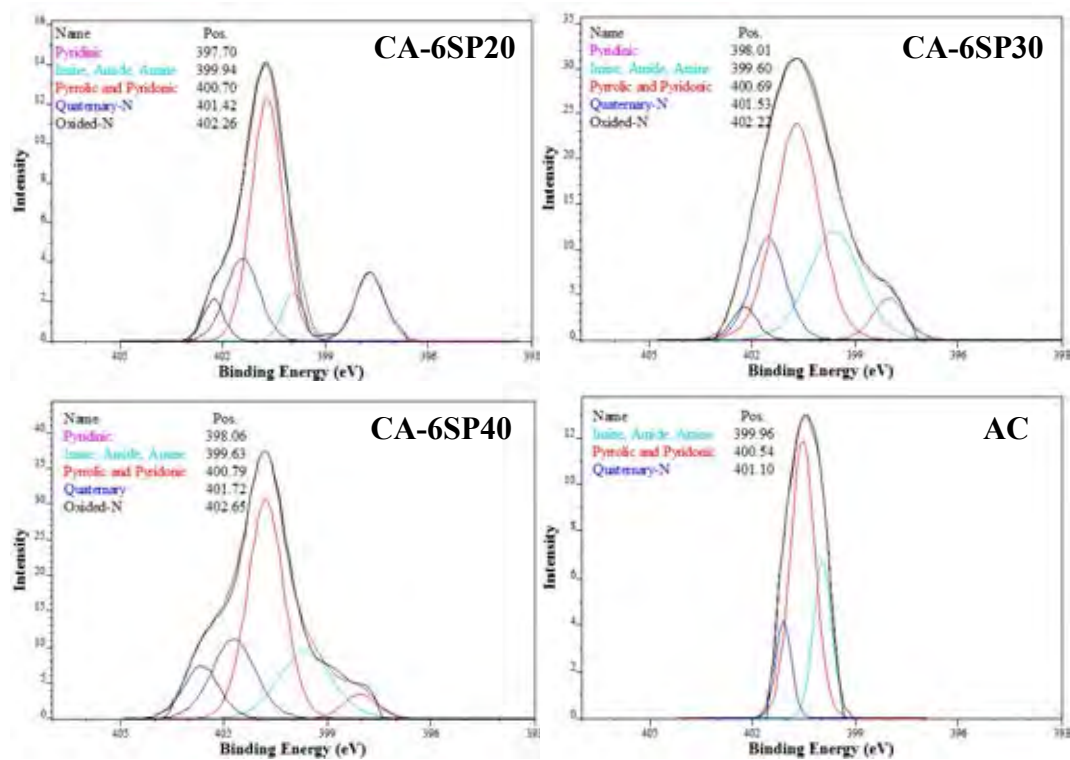| Name	Pos.
Pyridinic	397.68
Imine	398.51
Imine, Amide, Amine	399.36
Pyrrolic and Pyridonic	400.72
Quaternary-N	401.76

Figure 4.9 N 1s XPS spectra of carbon adsorbents

Table 4.2 XPS assignment of carbon adsorbents with no activation.

Region	Position (eV) (Reference)	Position (eV) (In this study)	Intensity (%)				Assignment
			CA-6N20	CA-7N20	CA-8N20	CA-6N40	
	283.5 ± 0.1	-	-	-	-	-	Carbide
	284.3 ± 0.1	284.4 ± 0.06	88.87	82.16	66.80	74.78	Graphite
C 1s	285.0 ± 0.1	-	-	-	-	-	Aliphatic
	285.4 ± 0.2	285.4 ± 0.11	7.85	14.70	24.17	23.81	C with N
	285.8 ± 0.1	285.9 ± 0.07	-	-	-	-	Hydroxyl, Ether
	286.6 ± 0.1	286.5 ± 0.23	3.28	3.14	9.03	1.41	Carbonyl
	530.3	530.1 ± 0.29	2.36	13.04	0.70	7.48	Oxide
	531.3 ± 0.1	531.3 ± 0.20	37.89	47.64	40.46	33.09	Carbonyl, Carboxyl
O 1s	532.1 ± 0.1	532.0 ± 0.16	-	-	-	-	Ketone, Lactones, Acids, Esters
	532.8	532.8 ± 0.08	39.66	4.52	44.18	31.14	Hydroxyl, Ether
	533.6 ± 0.1	533.6 ± 0.17	20.09	34.80	14.67	28.28	Hydroxyl – Aromatic ring
	534.9 ± 0.1	-	-	-	-	-	Absorbed water
	398.1 ± 0.1	398.1 ± 0.24	26.69	47.17	40.07	43.22	Pyridinic (N-6)
	398.9 ± 0.1	398.9 ± 0.24	-	-	-	1.06	Imine
N 1s	399.8 ± 0.2	399.8 ± 0.20	31.88	20.96	29.26	11.63	Imine, Amide, Amine
	400.7 ± 0.2	400.6 ± 0.18	29.01	27.71	19.99	42.31	Pyrrolic and Pyridonic (N-5)
	401.4 ± 0.3	401.6 ± 0.31	2.24	4.16	8.48	-	Quaternary-N
	402.8 ± 0.2	402.6 ± 0.37	10.18	-	2.19	1.78	Oxided-N

Table 4.3 XPS assignment of carbon adsorbents carbonized at 600, 700, and 800 °C and activated with chemical activation.

Region	Position (eV) (Reference)	Position (eV) (In this study)	Intensity (%)				Assignment
			CA-6SC20	CA-7SC20	CA-8SC20	CA-6SC40	
C 1s	283.5 ± 0.1	-	-	-	-	-	Carbide
	284.3 ± 0.1	284.4 ± 0.06	93.49	90.49	89.89	87.02	Graphite
	285.0 ± 0.1	-	-	-	-	-	Aliphatic
	285.4 ± 0.2	285.4 ± 0.11	0.81	4.73	2.76	6.45	C with N
	285.8 ± 0.1	285.9 ± 0.07	5.70	4.79	7.35	6.53	Hydroxyl, Ether
	286.6 ± 0.1	286.5 ± 0.23	-	-	-	-	Carbonyl
O 1s	530.3	530.1 ± 0.29	-	-	-	-	Oxide
	531.3 ± 0.1	531.3 ± 0.20	13.89	37.40	23.18	5.31	Carbonyl, Carboxyl
	532.1 ± 0.1	532.0 ± 0.16	26.66	40.42	36.39	14.77	Ketone, Lactones, Acids, Esters
	532.8	532.8 ± 0.08	49.60	5.35	30.51	52.86	Hydroxyl, Ether
	533.6 ± 0.1	533.6 ± 0.17	9.85	16.83	9.91	27.06	Hydroxyl – Aromatic ring
	534.9 ± 0.1	-	-	-	-	-	Absorbed water
N 1s	398.1 ± 0.1	398.1 ± 0.24	13.66	7.78	3.63	2.67	Pyridinic (N-6)
	398.9 ± 0.1	398.9 ± 0.24	23.79	32.15	10.99	11.90	Imine
	399.8 ± 0.2	399.8 ± 0.20	30.51	9.38	35.00	26.26	Imine, Amide, Amine
	400.7 ± 0.2	400.6 ± 0.18	29.40	37.46	43.22	25.72	Pyrrolic and Pyridonic (N-5)
	401.4 ± 0.3	401.6 ± 0.31	2.64	13.23	7.16	34.45	Quaternary-N
	402.8 ± 0.2	402.6 ± 0.37	-	-	-	-	Oxided-N

Table 4.4 XPS assignment of activated carbon and carbon adsorbents carbonized at 600 and activated with physical activation.

Region	Position (eV) (Reference)	Position (eV) (In this study)	Intensity (%)				Assignment
			CA-6SP20	CA-6SP30	CA-6SP40	Activated carbon	
C 1s	283.5 ± 0.1	-	-	-	-	-	Carbide
	284.3 ± 0.1	284.4 ± 0.06	85.84	87.04	87.18	82.01	Graphite
	285.0 ± 0.1	-	-	-	-	-	Aliphatic
	285.4 ± 0.2	285.4 ± 0.11	10.33	4.80	9.95	4.03	C with N
	285.8 ± 0.1	285.9 ± 0.07	3.84	8.16	2.87	13.96	Hydroxyl, Ether
	286.6 ± 0.1	286.5 ± 0.23	-	-	-	-	Carbonyl
O 1s	530.3	530.1 ± 0.29	-	-	-	19.26	Oxide
	531.3 ± 0.1	531.3 ± 0.20	17.04	4.49	7.34	51.93	Carbonyl, Carboxyl
	532.1 ± 0.1	532.0 ± 0.16	32.80	23.12	31.72	-	Ketone, Lactones, Acids, Esters
	532.8	532.8 ± 0.08	16.10	52.86	43.86	28.81	Hydroxyl, Ether
	533.6 ± 0.1	533.6 ± 0.17	34.07	19.52	17.08	-	Hydroxyl – Aromatic ring
	534.9 ± 0.1	-	-	-	-	-	Absorbed water
N 1s	398.1 ± 0.1	398.1 ± 0.24	14.26	6.22	4.46	-	Pyridinic (N-6)
	398.9 ± 0.1	398.9 ± 0.24	-	-	-	-	Imine
	399.8 ± 0.2	399.8 ± 0.20	7.39	26.93	20.10	25.88	Imine, Amide, Amine
	400.7 ± 0.2	400.6 ± 0.18	53.10	46.37	45.14	60.73	Pyrrolic and Pyridonic (N-5)
	401.4 ± 0.3	401.6 ± 0.31	19.19	16.67	19.65	13.39	Quaternary-N
	402.8 ± 0.2	402.6 ± 0.37	6.06	3.80	10.65	-	Oxided-N

4.2   Effect of Different Polymerizations Process on the Structure of Polybenzoxazine.

After polymerization process, polybenzoxazine samples were carbonized at 600, 700 and 800 °C and activated with physical or chemical activation to enhance the porosity in the adsorbent structure. Table 4.2 shows textural properties of different adsorbents synthesized with different techniques by using the Brunauer-Emmett Teller equation, Barret-Joyner-Halenda equation, and t-plot method to calculate BET surface area, pore size distribution, and micropore volume, respectively. The sol-gel polymerization gave significantly better textural properties of polybenzoxazine than the bulk polymerization in terms of BET surface area, total pore volume, and micropore volume. This result affected the polybenzoxazine synthesized with sol-gel technique to be more porous structure than polybenzoxazine prepared by bulk polymerization.

Table 4.5 BET surface area, total pore volume, micropore volume, and average pore diameter of all adsorbents

Sample	S_{BET} (m^2/g)	V_{Total} (cm^3/g)	V_{Micro} (cm^3/g)	D_{Avg} (nm)
Bulk polymerization				
• Physical activation (CA-6BP)	49.40	0.0434	0.022063	3.51979
• Chemical activation (CA-6BC)	10.83	0.0059	0.000830	2.20043
Sol-gel polymerization				
• No carbonization				
- PO-S20	3.671	0.2046	0.000	222.9
- PO-S30	8.195	0.3594	0.000	175.4
- PO-S40	12.883	0.4141	0.000	128.6
• No activation				
- CA-6N20	326.712	0.2413	0.145	2.954
- CA-6N40	437.754	0.5291	0.183	4.834
- CA-7N20	325.344	0.2303	0.143	2.832
- CA-8N20	393.420	0.2677	0.165	2.712
• Physical activation				
- CA-6SP20	621.033	0.3552	0.291	2.288
- CA-6SP30	499.808	0.4211	0.228	3.370
- CA-6SP40	516.248	0.7207	0.243	5.584

Table 4.5 BET surface area, total pore volume, micropore volume, and average pore diameter of all adsorbents (continuous)

Sample	S_{BET} (m²/g)	V_{Total} (cm³/g)	V_{Micro} (cm³/g)	D_{Avg} (nm)
Sol-gel polymerization				
• Chemical activation				
- CA-6SC20	1237.144	0.7609	0.499	2.460
- CA-6SC40	812.228	0.7387	0.312	3.638
- CA-7SC20	979.131	0.6761	0.270	2.762
- CA-8SC20	1273.321	0.7891	0.537	2.479
Activated Carbon	892.967	0.4920	0.379	2.204

Note: CA is carbon adsorbent**,** 6, 7, and 8 is the carbonization temperature (600, 700, and 800 °C), B is bulk polymerization, S is sol-gel polymerization, P is physical activation, C chemical activation, N is no activation, PO is polymer. S_{BET} : specific surface area calculated using Brunauer–Emmett Teller equation, V_{total} : total pore volume, V_{micro} : micropore volume determined from the t-plot method, D_p : average pore diameter.

4.3 Effect of Monomer Content on The Structure of Adsorbents

In term of monomer content, the carbonized polybenzoxazine with 40 wt.% monomer content during the sol-gel process (CA-6N40 in Table 4.2) gave higher BET surface area and total pore volume than the sample with 20 wt.% monomer (CA-6N20 in Table 4.2); however, this high monomer content sample gave higher average pore diameter (4.834 nm in CA-6N40) than the sample with lower monomer content (2.954 nm in CA-6N20). The adsorbent containing 40 wt% monomer may contain too high monomer content; hence, the polymer structure was dense. The dense polymer then obstructed the path way for gas to evolve during carbonization, resulting in widening of the pores as evidenced from the high meso and macro pore volume (difference of total pore volume and micro pore volume) and the higher average pore size of the

adsorbent contained 40 wt% monomer (CA-6N40) as compared to the adsorbent contained 20 wt%. (CA-6N20).

After activation both physical and chemical activation, the activated adsorbents generally gave higher BET surface area, higher pore volume both micro- and mesopores and smaller average pore size. Comparing between physical and chemical activation, the chemical activation could generate a significant higher micropores as seen by the significant improvement in micropore volume. Hence, the chemical activation gives adsorbents with a well-developed porosity with higher surface area, higher microporosity and narrower average pore size than those obtained by physical adsorption. Figures 4.5(a), 4.5(b), 4.5(c), 4.5(d), 4.5(e), 4.5(f), and 4.5(g) show the nitrogen adsorption isotherms of CA-6SP20, CA-6SP30, CA-6SP40, CA-6SC20, CA-6SC40, CA-7SC20, and CA-8SC20, respectively.
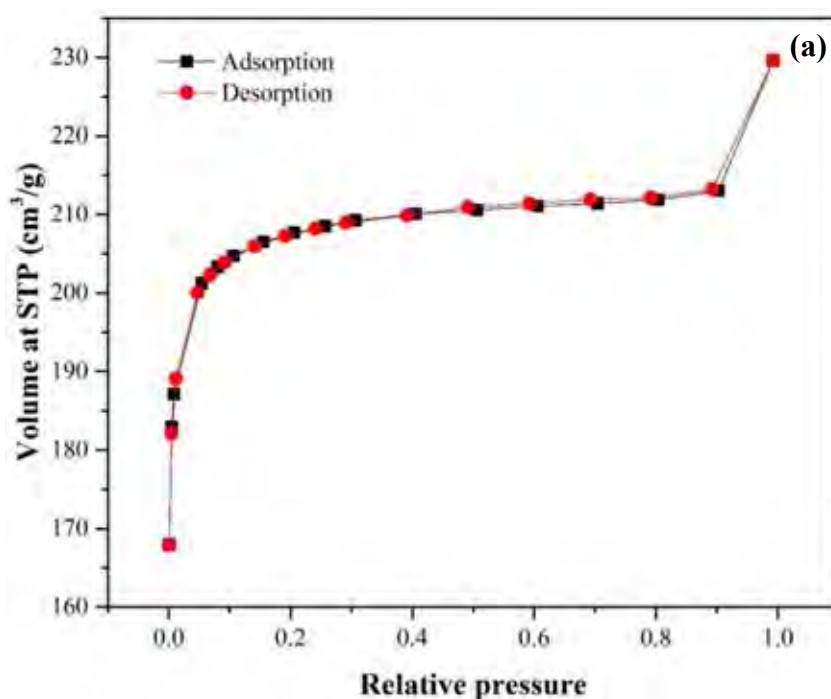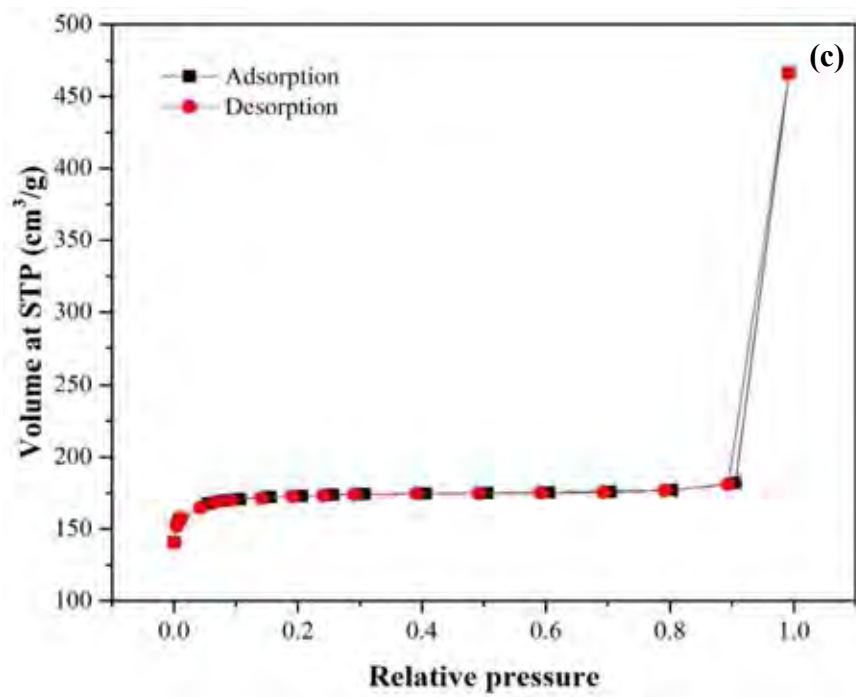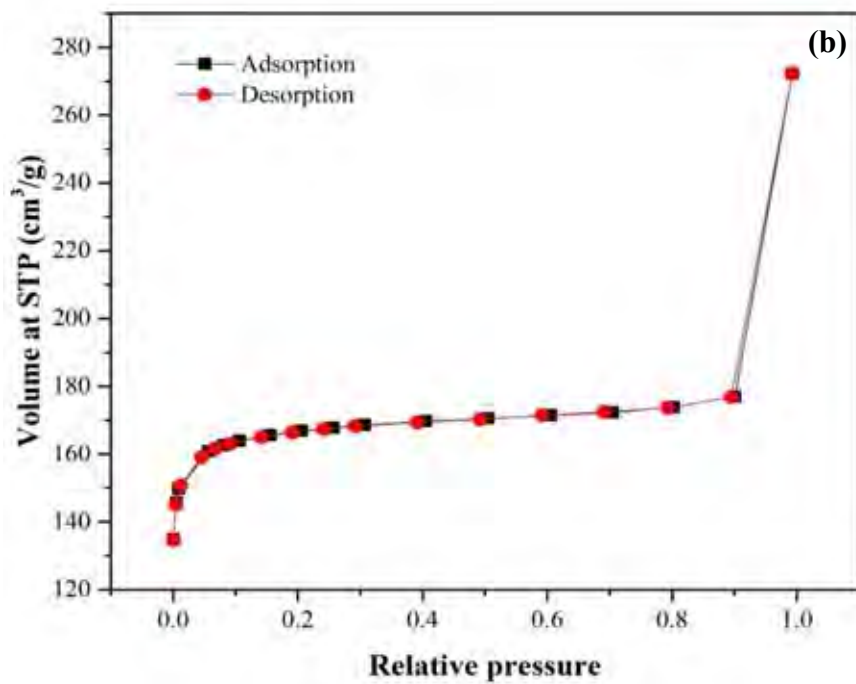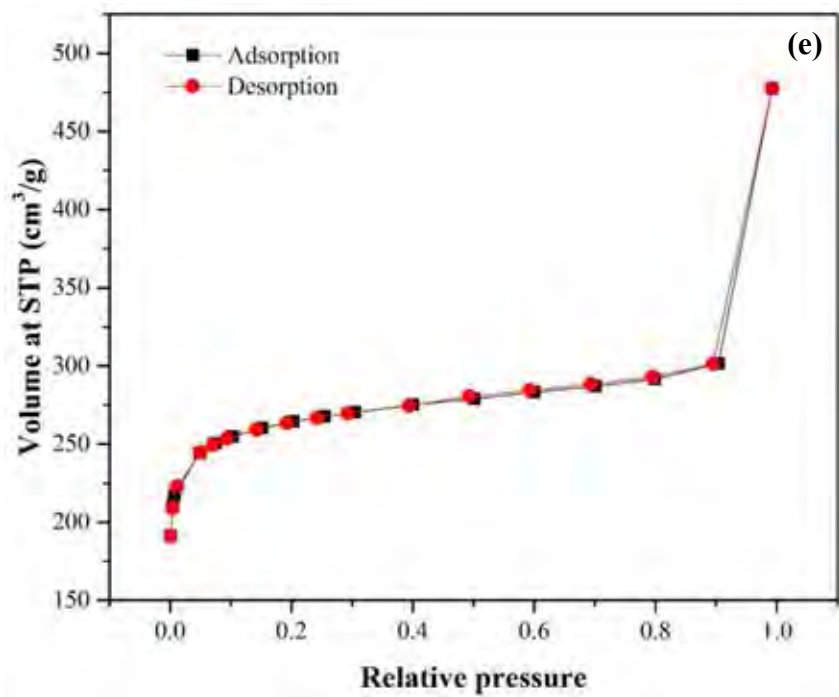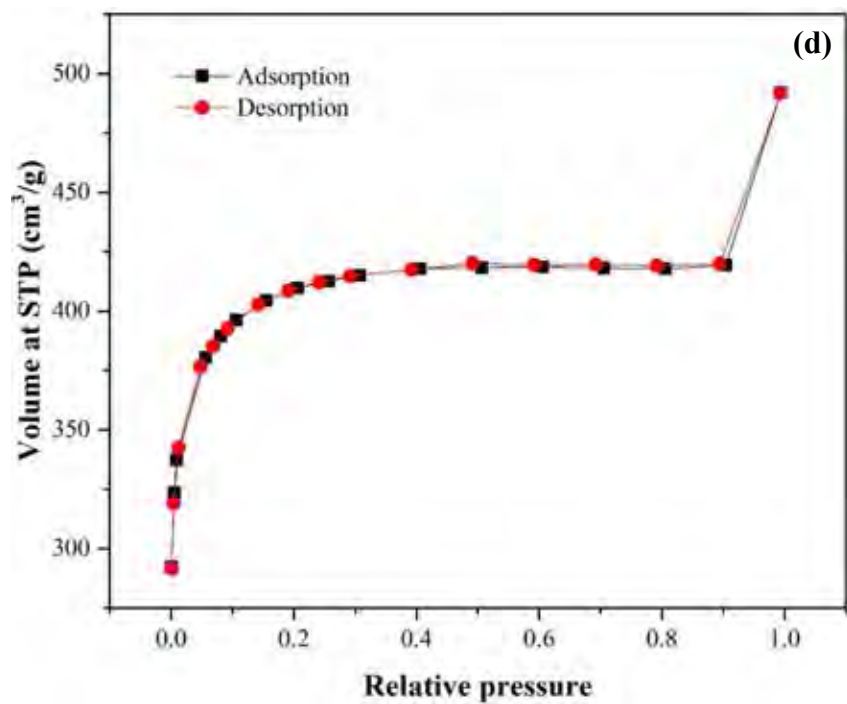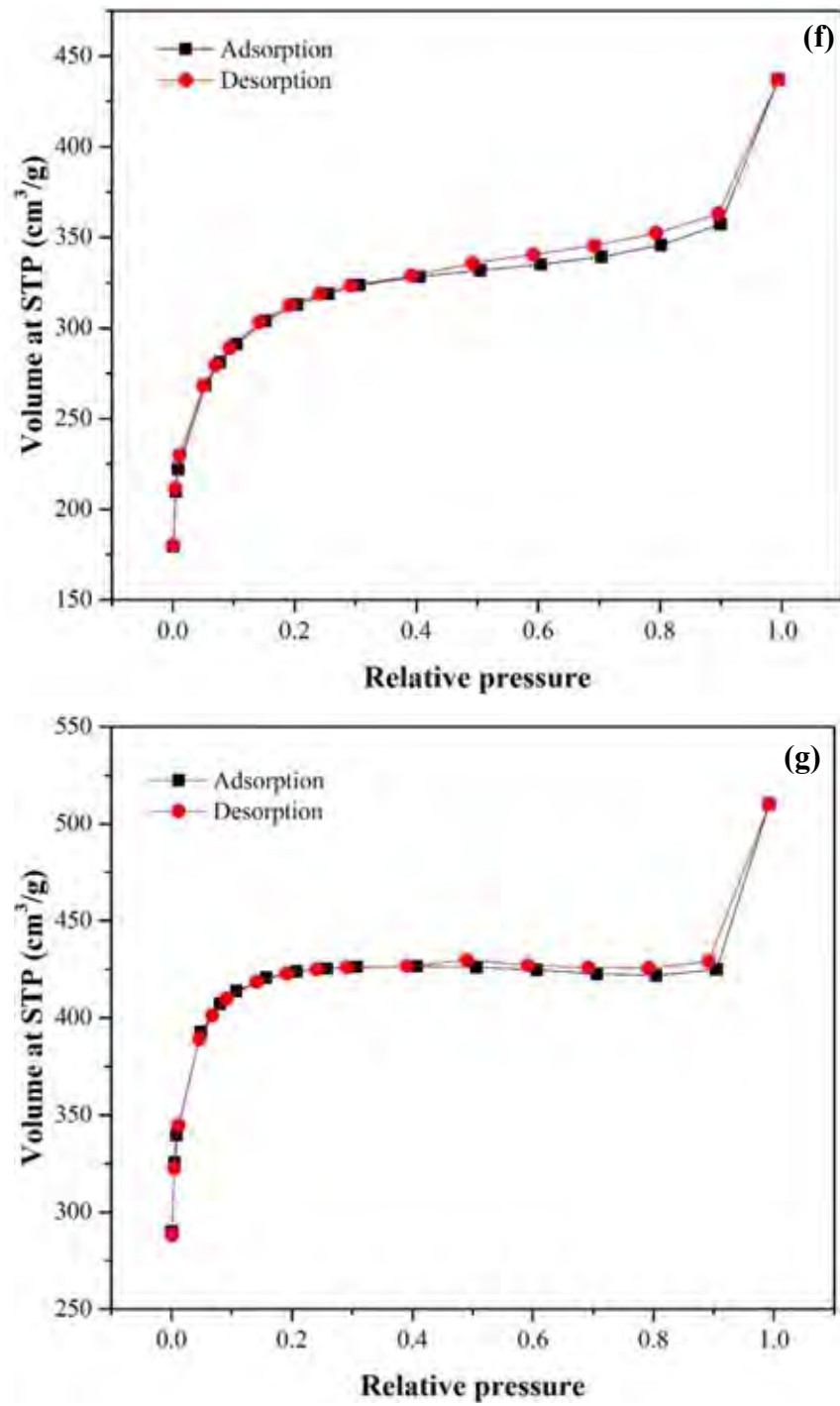
Figure 4.10 Isotherms of (a) CA-6SP20, (b) CA-6SP30, (c) CA-6SP40, (d) CA-6SC20, (e) CA-6SC20, (f) CA-7SC20, and (g) CA-8SC20.
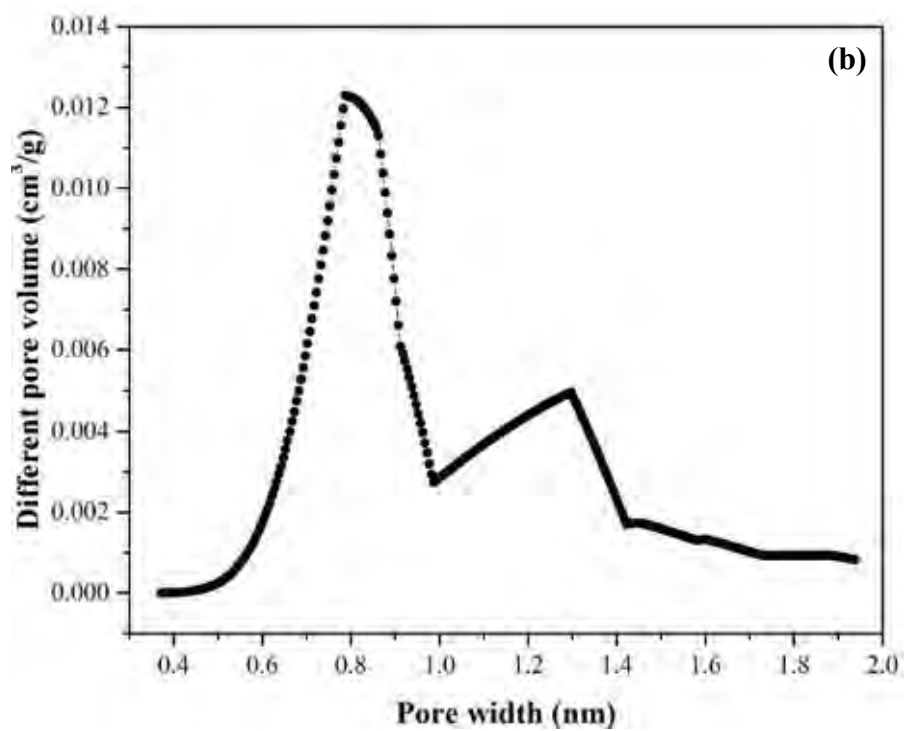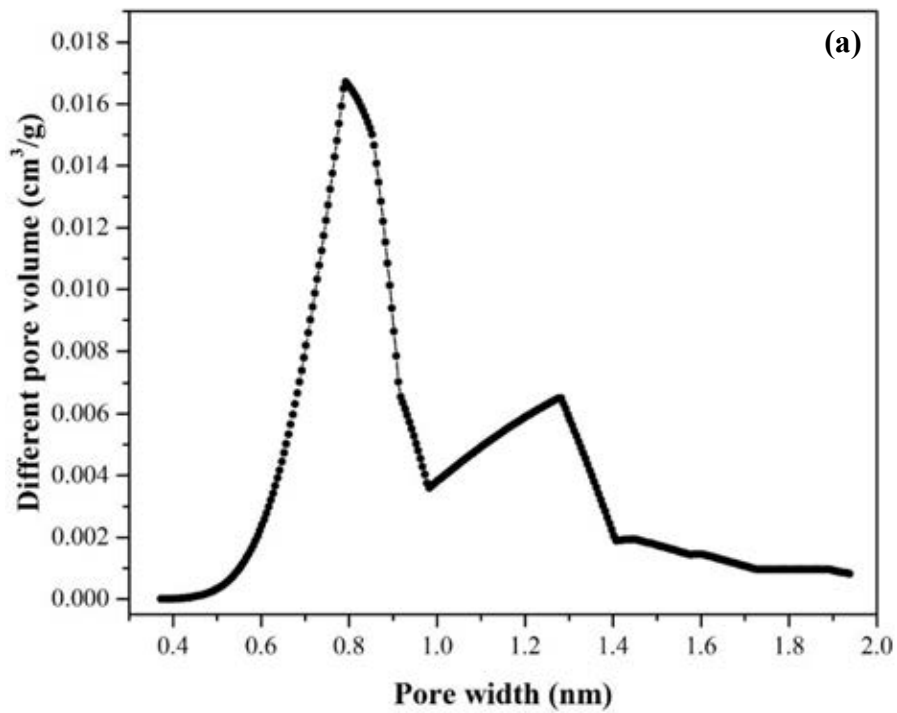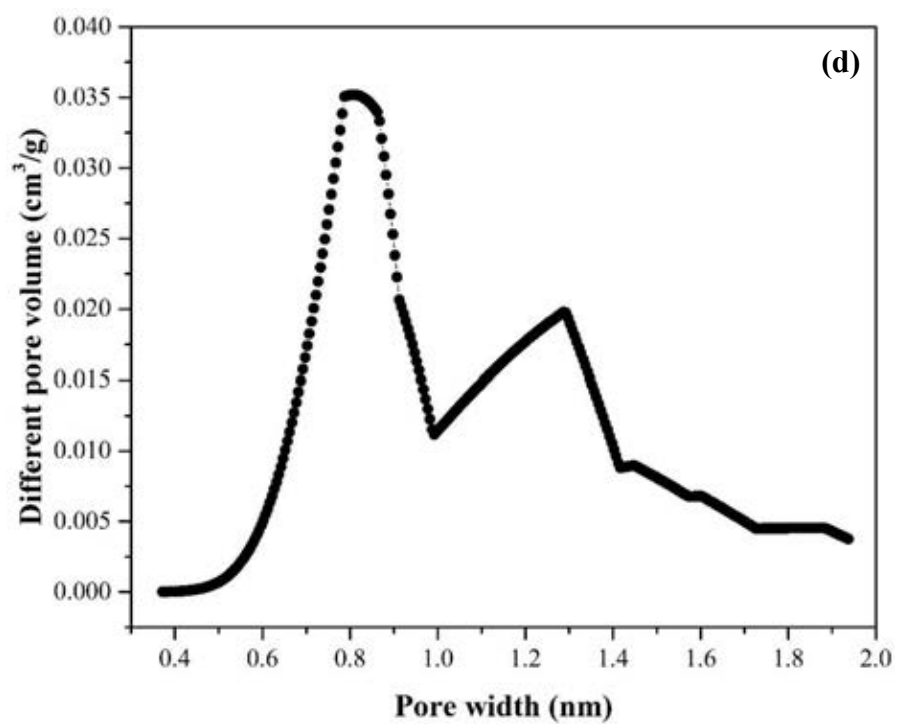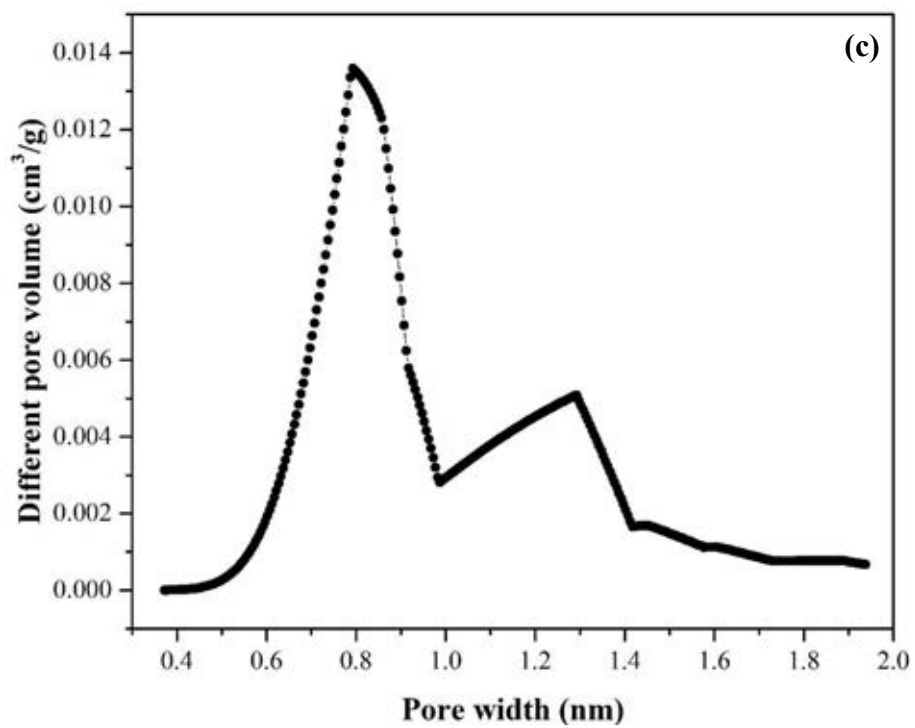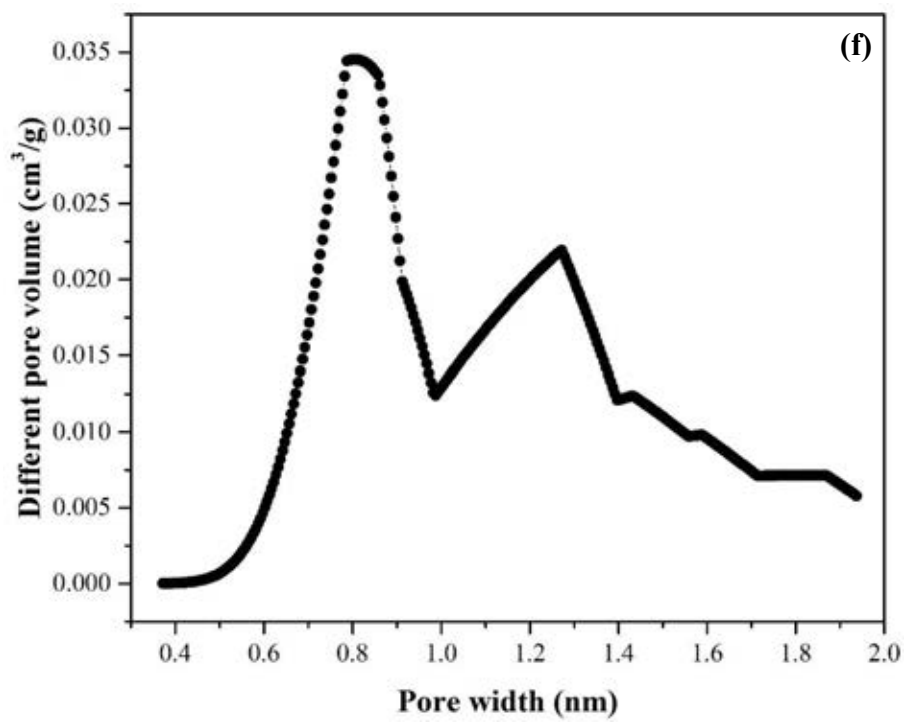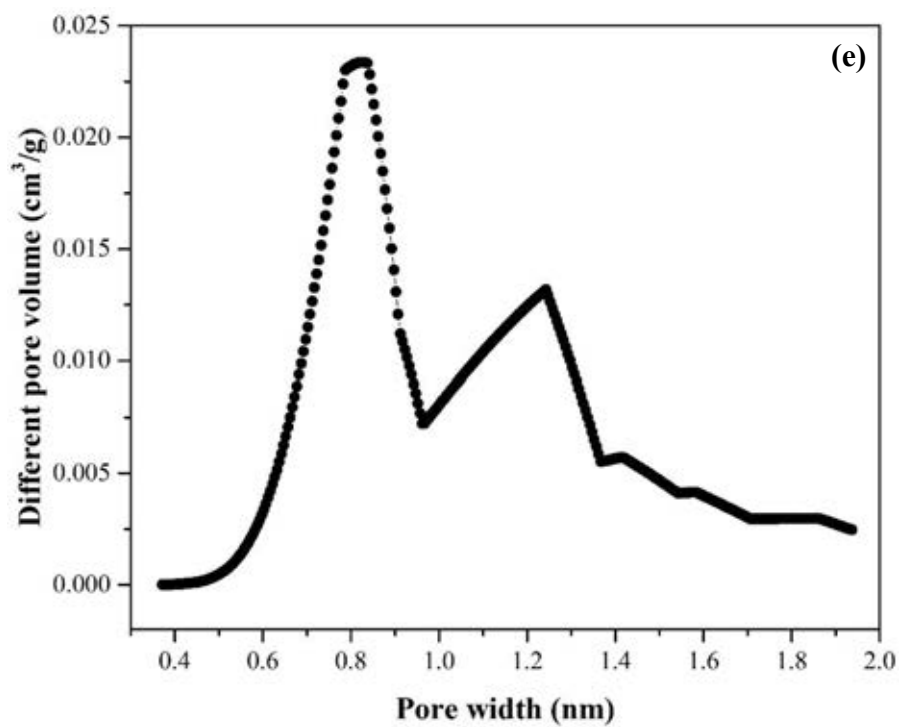
(e)

(f)
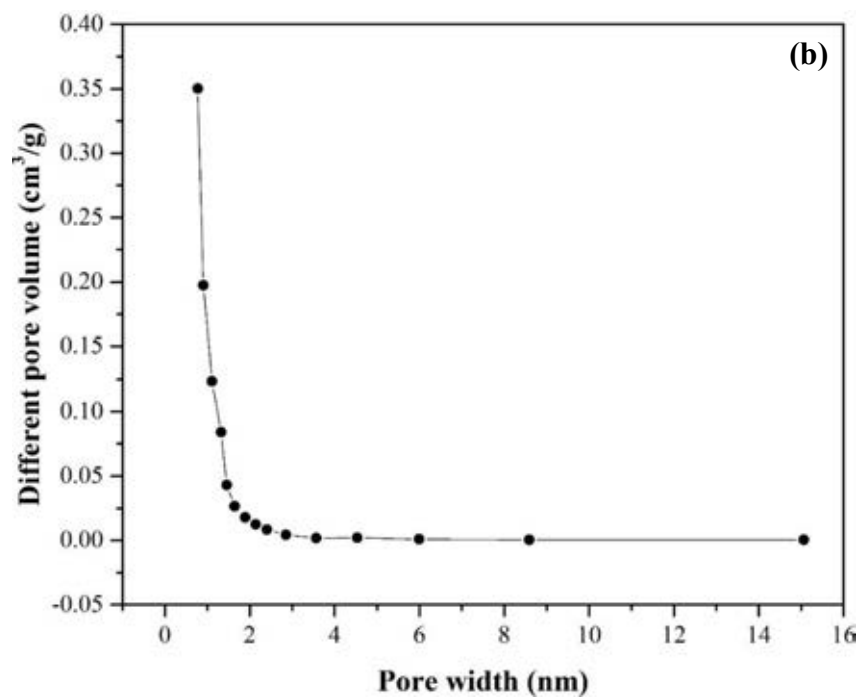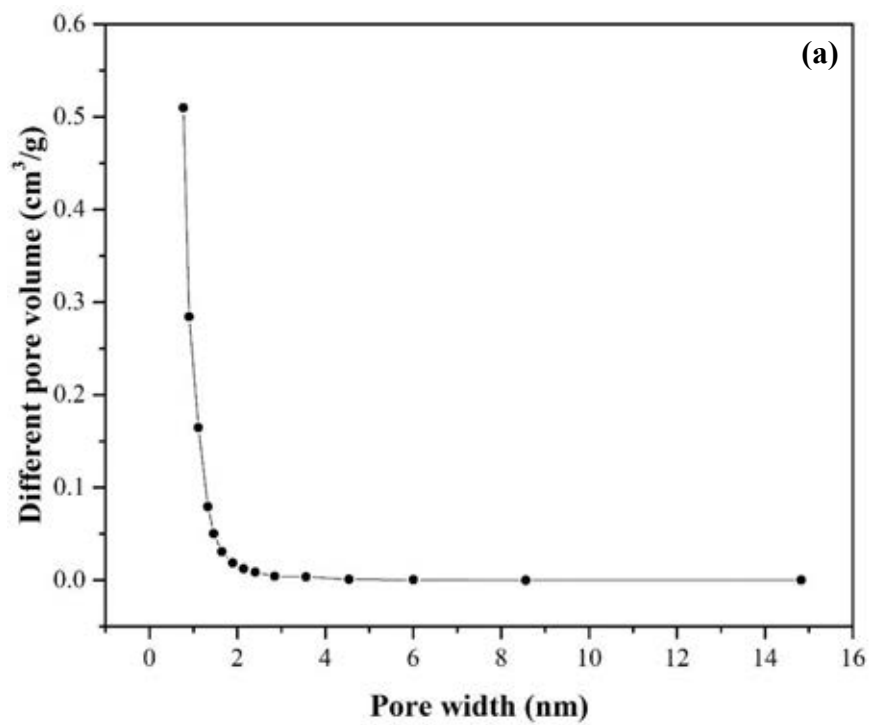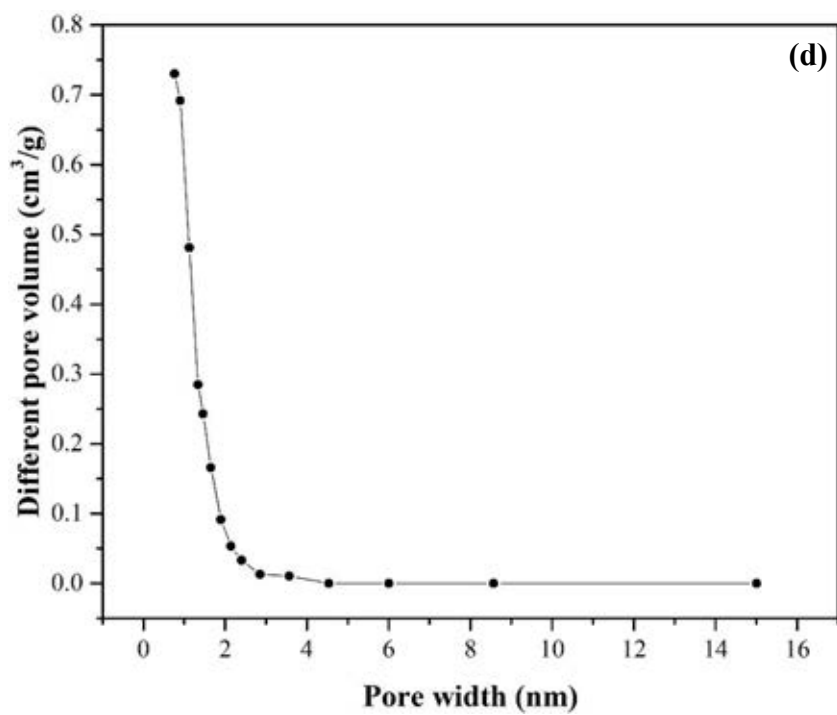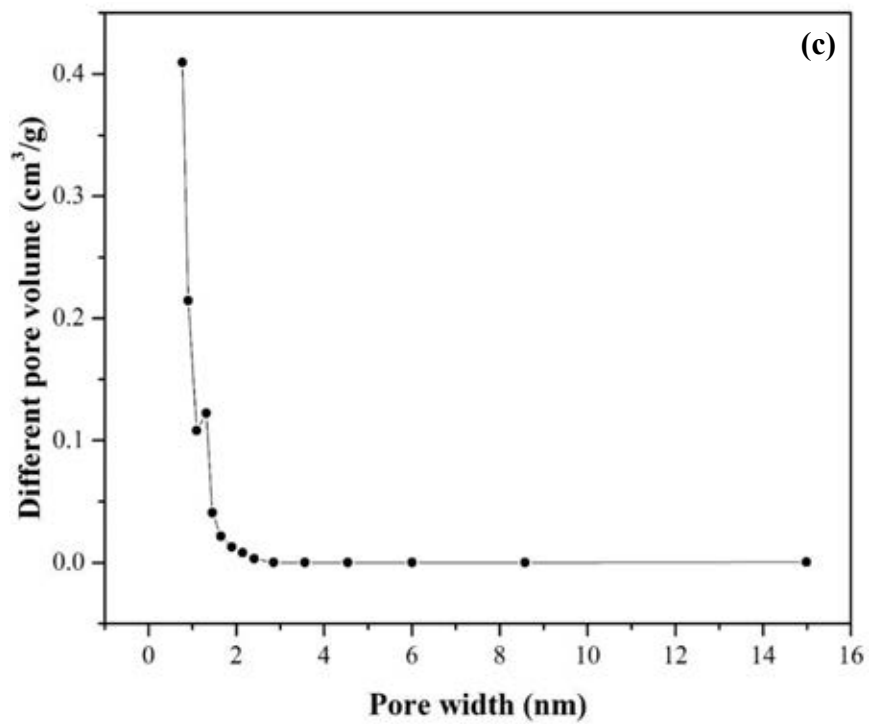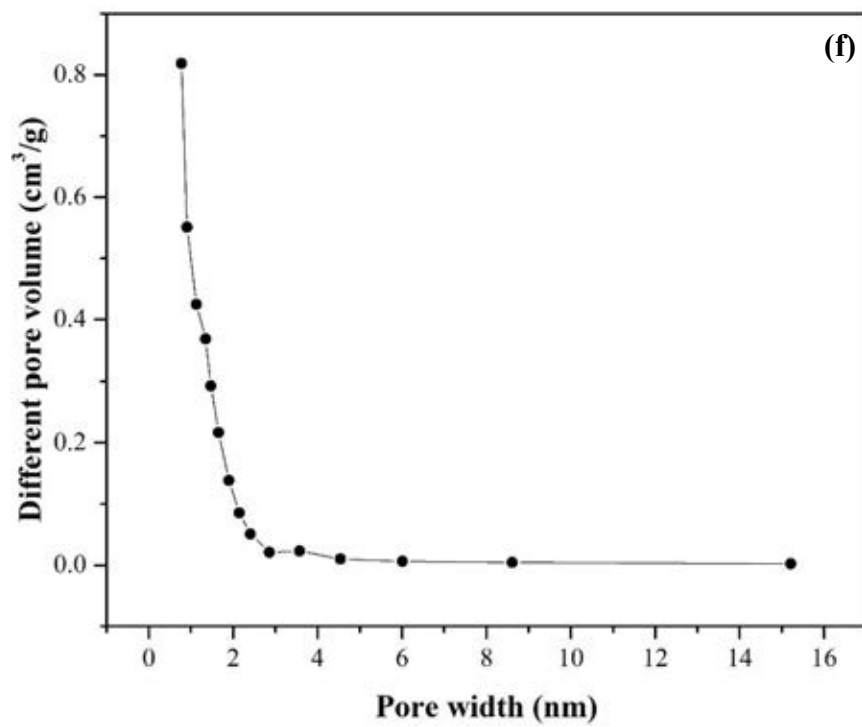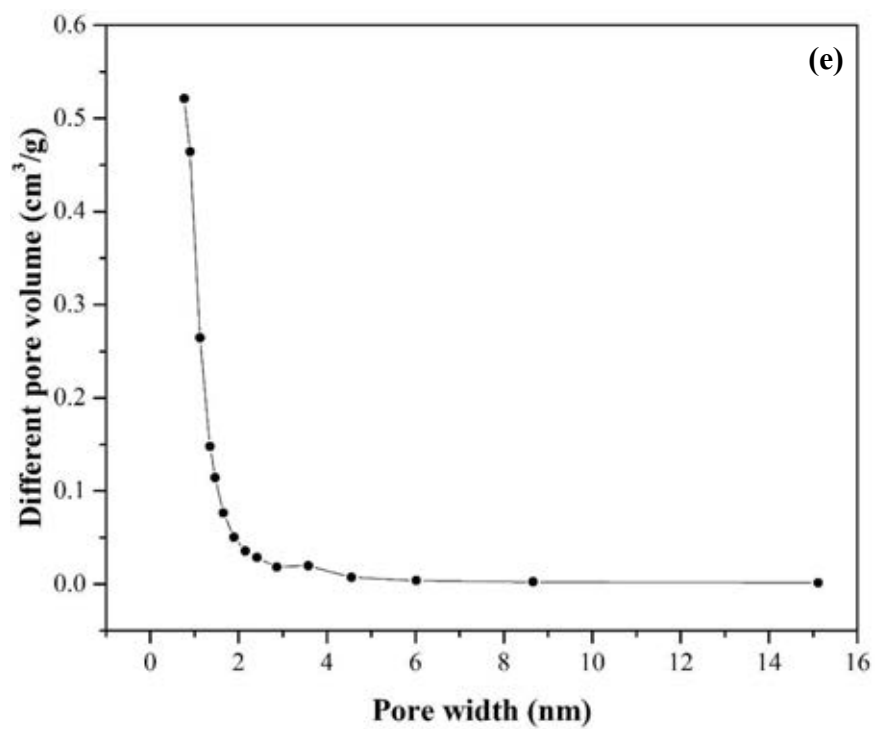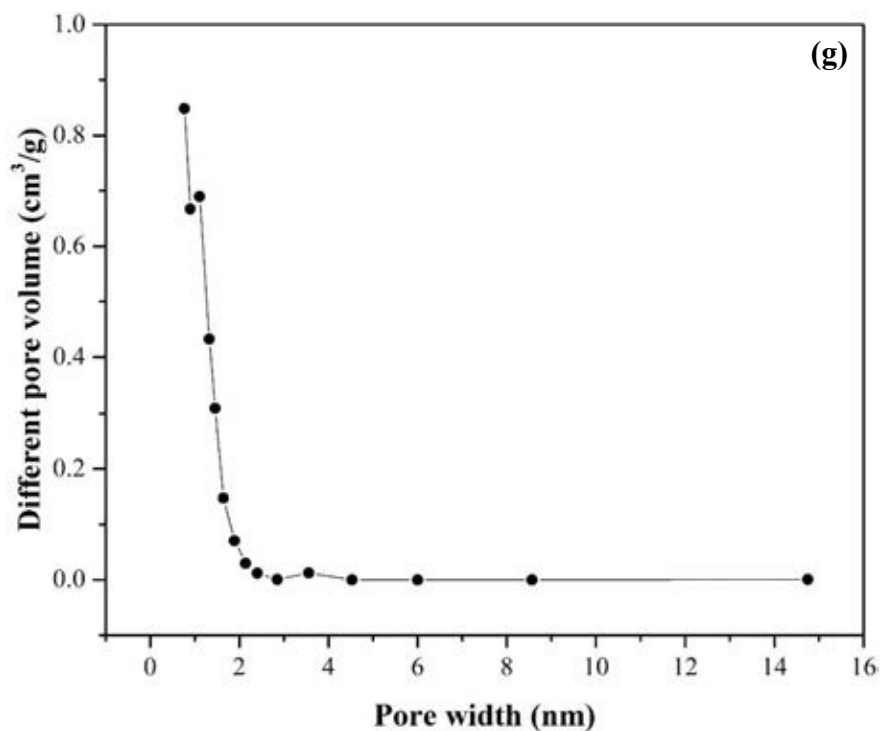
Figure 4.11 Pore size distribution with BJH method of (a) CA-6SP20, (b) CA-6SP30, (c) CA-6SP40, (d) CA-6SC20, (e) CA-6SC20, (f) CA-7SC20, and (g) CA-8SC20.

Figure 4.11 shows the pore size distribution calculated with Barret-Joyner-Halenda (BJH) equation of various adsorbents: (a) CA-6SP20, (b) CA-6SP30, (c) CA-6SP40, (d) CA-6SC20, (e) CA-6SC20, (f) CA-7SC20, and (g) CA-8SC20. The BJH equation was used to calculate the pore size distribution of mesopore. From the observation, pore size of mesoporous structure of all adsorbents is similar to each other and is around 0.7725 nm.
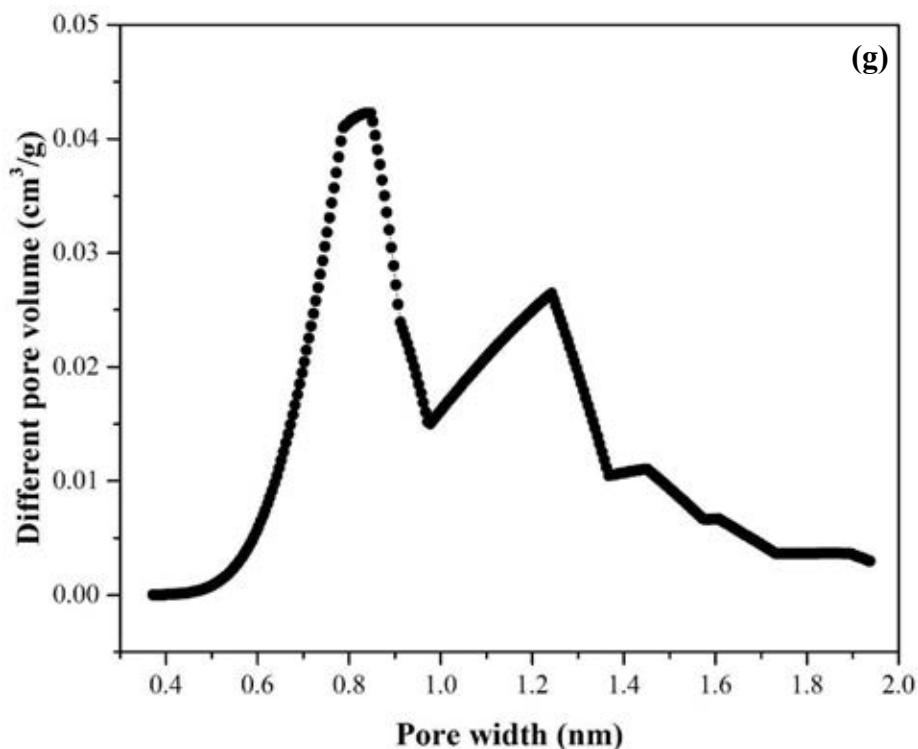
(c)

(d)

(e)

(f)

Figure 4.12 Pore size distribution with HK method of (a) CA-6SP20, (b) CA-6SP30, (c) CA-6SP40, (d) CA-6SC20, (e) CA-6SC20, (f) CA-7SC20, and (g) CA-8SC20.

Figure 4.12 shows the pore size distribution calculated with Horváth-Kawazoe (HK) method of various adsorbents: (a) CA-6SP20, (b) CA-6SP30, (c) CA-6SP40, (d) CA-6SC20, (e) CA-6SC20, (f) CA-7SC20, and (g) CA-8SC20. The result shows that the pore size of microporous structure of all adsorbents was in range of 0.6 – 1.4 nm.

4.4 Effect of Carbonization Temperatures on The Structure of Adsorbents

For bulk polymerization, this method gave the highly dense structure of the bulk adsorbent which is durable to the high temperature; therefore, carbonization could not help bulk adsorbent to generate the porous structure before activation. Furthermore, when the carbonization could not create more porosity, the activation could not increase pores of bulk adsorbents.

In sol-gel polymerization, the sol-gel method could generate pores in the adsorbents with the aid of solvent penetrated in the polymer skeleton. Therefore, the carbonization could helped adsorbents to create more porosity: increasing BET surface area and total pore volume as shown in the Table 4.2. Furthermore, the carbonization temperatures at 600 and 700 gave similar values of BET surface area and total pore volume, but the carbonization temperature was increased to 800 °C that affected the BET surface area and total pore volume to increase. It means that increasing carbonization temperature could increase porosity of sol-gel adsorbents.

4.5 Effect of Different Activations on The Structure of Adsorbents

In bulk polymerization, CA-6BP or bulk adsorbent activated with physical activation gave better textural properties (i.e. BET surface area, total pore volume, and micropore volume) than CA-6BC or bulk adsorbent activated with chemical activation since the structure of the furfurylamine-based polybenzoxazine is very dense. KOH could not penetrate in the adsorbent structure to generate the micropores.

Considering sol-gel technique, the sol-gel process could generate interconnected pores, providing space for gas to expand during carbonization. These pores generated during the sol-gel process also aided the penetration of KOH into the polymer skeleton and provided good contact between the activating agent and the polymer, resulting in the generation of micropores. Comparing the activation technique, chemical activation gave adsorbents with better textural properties than those adsorbents activated with physical activation in terms of BET surface area, total pore volume and micropore volume. Therefore, this study confirmed that the chemical activation was better than physical activation to generate high porous adsorbent (Hu *et al.*, 2011).
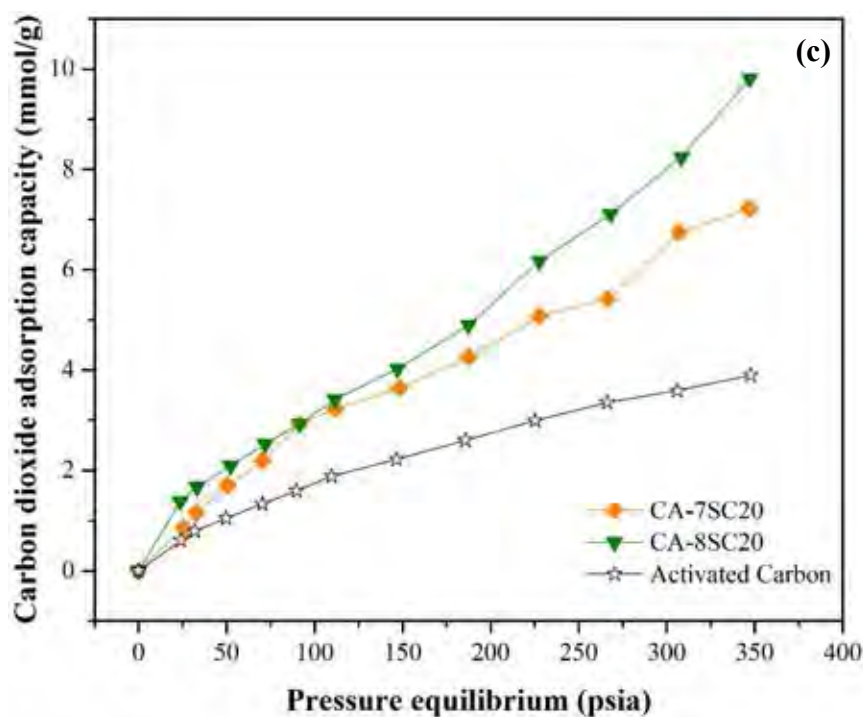
4.6 Carbon Dioxide Adsorption Performance
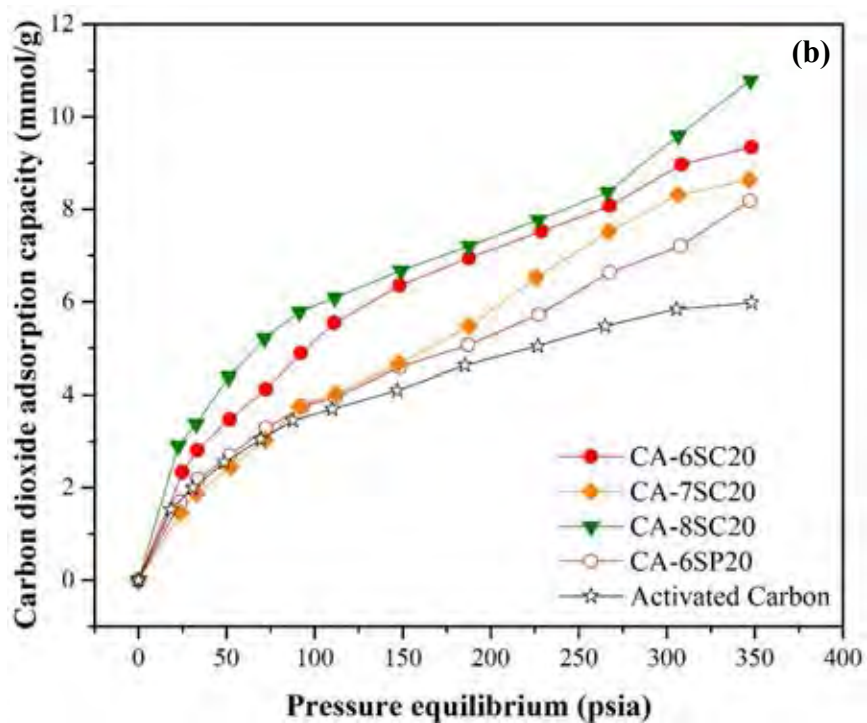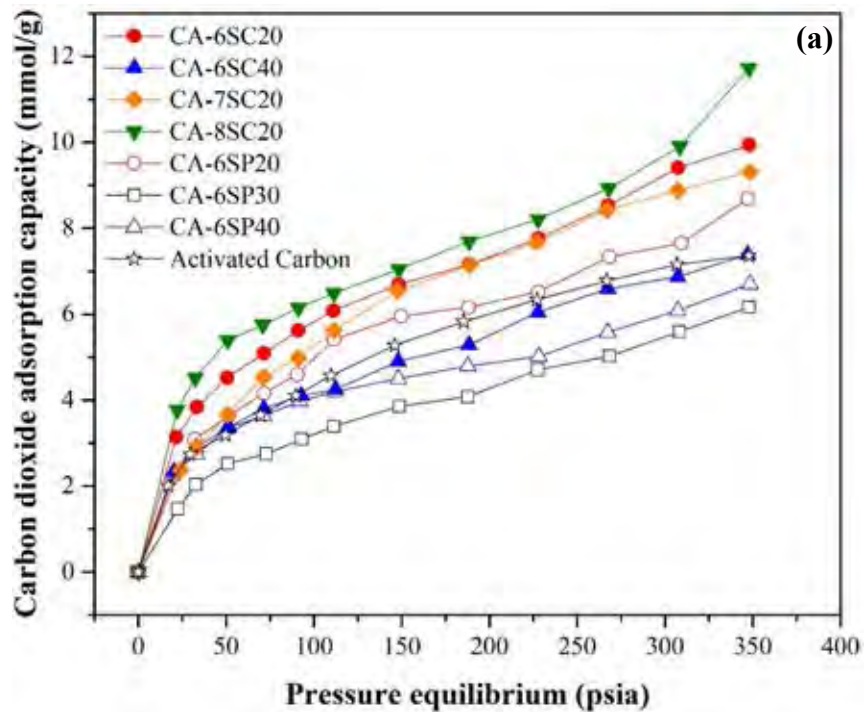
Figure 4.13 CO_2 adsorption isotherms of carbon adsorbent synthesized by sol-gel method: (a) at 40 °C, (b) at 70 °C, and (c) at 110 °C.

Table 4.6 The CO_2 adsorption performance of all adsorbents at 40 °C, 70 °C and 110 °C and 350 psia

Adsorbent	CO₂ Uptake at 40 °C (mmol/g)	CO₂ Uptake at 70 °C (mmol/g)	CO₂ Uptake at 110 °C (mmol/g)
CA-6SP20	8.69	8.18	N/A
CA-6SP30	6.16	N/A	N/A
CA-6SP40	6.71	N/A	N/A
CA-6SC20	9.94	9.34	N/A
CA-6SC40	7.40	N/A	N/A
CA-7SC20	9.32	8.64	7.22
CA-8SC20	11.73	10.79	9.81
Activated Carbon	7.36	5.98	3.90

Figure 4.13 shows the CO_2 adsorption isotherms at 40, 70 °C, and 110 °C of carbon adsorbents synthesized by a sol-gel technique and activated with physical and chemical activation. CA-8SC20 gave the highest adsorption capacity in the range of pressure up to 350 psia. The maximum capacity at 40 °C of CA-6SP20, CA-6SP30, CA-6SP40, CA-6SC20, CA-6SC40, CA-7SC20, CA-8SC20, and activated carbon is 8.69 mmol/g, 6.16 mmol/g, 6.71 mmol/g, 9.94 mmol/g, 7.40 mmol/g, 9.32 mmol/g, 11.73 mmol/g, and 7.36 mmol/g at 348 psia, respectively as shown in Table 4.2. Comparing samples with the same physical activation, since these samples derived from the same materials and undergone the same polymer preparation, carbonization temperature, they have the same surface chemistry. The only differences are the adsorbent skeleton and surface morphology as they were derived based on different monomer content and the surface functionalities in each component are not different as shown in the Table 4.4. As the surface area increased, the CO2 adsorption capacity increased. Similar result was observed in the adsorbents from chemical activation, but the surface chemistry between physical activation and chemical activation was different. Therefore, surface morphology plays an important role in the adsorption performance. Hence, the monomer content of 20% by weight seems to be the optimum value for furfuryl-based polybenzoxazine carbon adsorbent to generate carbon with high surface area and high micropore volume with appropriate mesopore volume. From the XPS results in the Tables 4.2 to 4.4, the surface functionality component between physical adsorbents and chemical adsorbents were different in term of the N functionalities. The imine group was not found in the physical adsorbents and the oxized-N group was not detected in the chemical adsorbents. However, both of adsorbents contained the amine, pyridinic, and pyrrolic or pyridonic groups. These functional groups are the strong basic (Nanthiya *et al.*, 2016). Furthermore, it might help the carbon adsorbents derived from furfurylamine-based polybenzoxazine to generate the chemical adsorption and increase the CO_2 adsorption capacity.

At high adsorption temperature of 70 °C and 350 psia, the CO_2 adsorption capacity by CA-6SP20, CA-6SC20, CA-7SC20, and CA-8SC20 was 8.18 mmol/g, 9.34 mmol/g, 8.64 mmol/g, and 10.79 mmol/g, respectively, which are slightly

decreased from the CO_2 adsorption capacity at 40 °C. The decrease of CO_2 adsorption capacity was resulted from the effect of temperature in adsorption because the adsorption was the exothermic process meaning that the CO_2 uptake decreased when the adsorption temperature increased (Zulfiqar *et al.*, 2015). Typically the CO_2 adsorption capacity is tremendously decreased at higher temperature. The results from CA-6SP20, CA-6SC20, CA-7SC20, and CA-8SC20 show a mild decrease in CO2 uptake at 70 ° as compared to that at 40 °C. This suggested that both chemical and physical adsorption processes occurred during the CO_2 adsorption of some polybenzoxazine-derived adsorbents.

Considering adsorption at 110 °C and 350 psia, CA-7SC20 and CA-8SC20 could capture CO_2 around 7.22 mmol/g and 9.81 mmol/g, respectively. When compared the CO_2 adsorption capacity at 110 °C with at 40 °C and 70 °C, the CO_2 uptake at 110 °C was decreased from at 40 °C and 70 °C, but the decreased CO_2 capacity of chemical adsorbent was still lower than activated carbon which mainly adsorbed with physical adsorption. It might be said that both chemical and physical adsorption occurred in the furfurylamine-based polybenzoxazine adsorbents.

4.6.1 Effect of Different Polymerizations

The adsorbent synthesized with bulk polymerization was very dense as evidenced in the Table 4.5 by the lower BET surface area and the total pore volume when compared with the adsorbent synthesized by sol-gel process, meaning that the carbonization and activation could not increase porosity of bulk adsorbent. On the other hands, sol-gel process could help the adsorbents to generate more porosity than bulk method by reducing the crosslink density. Therefore, the sol-gel adsorbent could obtain higher CO_2 adsorption capacity than the bulk adsorbent.

4.6.2 Effect of Different Monomer Contents in Sol-gel Process

In the sol-gel polymerization, the benzoxazine monomer was varied at 20, 30, and 40 wt%. From the results of textural properties and surface morphology, the adsorbent that contained with 20 wt% benzoxazine monomer gave the highest BET surface area and micropore volume according to its FE-SEM image showing the structure which was porous more than the adsorbent contained 30 and 40 wt% benzoxazine monomer. Besides, the adsorbent contained 30 and 40 wt% monomer

might be high which affected the amount of crosslink density to be high. Therefore, the adsorbent that contained the lowest monomer content gave the highest CO_2 adsorption capacity as shown in Table 4.6.

4.6.3 Effect of Various Carbonization Temperatures

To enhance CO_2 adsorption performance, adsorbents were carbonized at various temperatures: 600, 700, and 800 °C. From the results, the adsorbent carbonized at 800 °C gave higher porosity than the adsorbent carbonized at 600 and 700 °C since the higher temperature could remove high amount of microgel particles as compared with the lower temperature which is according to textural properties. However, the adsorbent carbonized at 700 °C obtained similar textural properties to the adsorbent which was carbonized at 600 °C. Therefore, it might assume that the increase of carbonization temperature might increase the porosity which affected the CO_2 adsorption capacity to increase.

4.6.4 Effect of Physical and Chemical Activations

After carbonization, adsorbents were activated with different activation methods: physical and chemical activation. Chemical activation using KOH as an activating agent gave better textural properties in terms of BET surface area, total pore volume, and micropore volume than physical activation with CO_2 because KOH can penetrate and generate more pores. Therefore, chemical activation help the adsorbent's structure to be porous more than physical activation. Furthermore, the adsorbent activated with chemical activation could adsorb CO_2 higher than the adsorbent activated with physical activation.

From many studied effects in this study, the adsorbent was synthesized by sol-gel method, contained 20 wt% monomer, carbonized at 800 °C, and activated with chemical activation gave the best textural properties (BET surface area, total pore volume, and micropore volume). Therefore, CA-8SC20 could adsorb CO_2 more than other adsorbents.

CHAPTER V
CONCLUSIONS AND RECOMMENDATIONS

5.1 Conclusions

This study developed the carbon adsorbent to be suitable for CO_2 adsorption which focused on the effect of different polymerizations, carbonizations, and activations. Carbon adsorbents were prepared by bulk or sol-gel polymerizations and using furfurylamine-based polybenzoxazine as a precursor. In the sol-gel method, percentage of benzoxazine monomer was varied at 20, 30, and 40 wt%. Adsorbents were carbonized at various temperatures (600, 700, and 800 °C) under N_2 atmosphere and were activated at 900 °C with physical or chemical activations. The nitrogen content of carbon adsorbents decreased with increasing carbonization temperature and adsorbent with chemical activation gave lower nitrogen content than that of with physical activation. Besides, increasing carbonization temperature yielded adsorbent with higher porosity. Furthermore, activation enhanced the textural properties of adsorbents such as surface area and micropore volume; therefore, these effects affected adsorbents to adsorb high amount of carbon dioxide. Carbon adsorbents adsorb CO_2 with the physical adsorption more than chemical adsorption because physical adsorption is an exothermic process since the CO_2 adsorption capacity decreased when the adsorption temperature increased. However, it still occurred both physical and chemical adsorption. From the results, the adsorbent activated with chemical activation gave higher CO_2 adsorption capacity than adsorbents activated with physical activation since chemical activation could penetrate and generate high amount of micropores. For CO_2 adsorption performance, CA-8SC20 performed the highest CO_2 adsorption capacity of 11.73 mmol/g at 40 °C, 10.79 mmol/g at 70 °C, and 9.81 mmol/g at 110 °C and 350 psia

5.2 Recommendations

Based on what has been discovered in this study, the following recommendations were suggested:

- Other solvents should be employed in the sol-gel process to study the effect of the solvent on the furfurlamine-based polybenzoxazine adsorbent's structure.

- Other weight ratios of an activating agent in the chemical activation should be varied with different values. If it is a suitable ratio, it might help carbon adsorbents to generate more porosity.

- The adsorbents should be activated at different temperatures to study the effect of activation temperatures on the porous structure of adsorbents.

- Regeneration study of the carbon adsorbent derived from furfurylamine-based polybenzoxazine should be conducted to study the effect of chemical adsorption and regenability of the adsorbents.

REFERENCES

Alhassan, S., Schiraldi, D., Qutubuddin, S., Agag, T. and Ishida, H. (2011). Various Approaches for Main-Chain Type Benzoxazine Polymers. 309-318.

Banisheykholeslami, F., Ghoreyshi, A.A., Mohammadi, M. and Pirzadeh, K. (2015). Synthesis of a Carbon Molecular Sieve from Broom Corn Stalk via Carbon Deposition of Methane for the Selective Separation of a CO_2/CH_4 Mixture. CLEAN - Soil, Air, Water 43(7), 1084-1092.

Bello, G., García, R., Arriagada, R., Sepúlveda-Escribano, A. and Rodríguez-Reinoso, F. (2002). Carbon molecular sieves from Eucalyptus globulus charcoal. Microporous and Mesoporous Materials 56(2), 139-145.

Blackman, J.M., Patrick, J.W. and Snape, C.E. (2006). An accurate volumetric differential pressure method for the determination of hydrogen storage capacity at high pressures in carbon materials. Carbon 44(5), 918-927.

Bolotov, V.A., Kovalenko, K.A., Samsonenko, D.G., Han, X., Zhang, X., Smith, G.L., McCormick, L.J., Teat, S.J., Yang, S., Lennox, M.J., Henley, A., Besley, E., Fedin, V.P., Dybtsev, D.N. and Schröder, M. (2018). Enhancement of CO_2 Uptake and Selectivity in a Metal–Organic Framework by the Incorporation of Thiophene Functionality. Inorganic Chemistry 57(9), 5074-5082.

Burg, P., Fydrych, P., Cagniant, D., Nanse, G., Bimer, J. and Jankowska, A. (2002). The characterization of nitrogen-enriched activated carbons by IR, XPS and LSER methods. Carbon 40(9), 1521-1531.

Chai, S.W., Kothare, M.V. and Sircar, S. (2011). Rapid Pressure Swing Adsorption for Reduction of Bed Size Factor of a Medical Oxygen Concentrator. Industrial & Engineering Chemistry Research 50(14), 8703-8710.

Chaisuwan, T., Komalwanich, T., Luangsukrerk, S. and Wongkasemjit, S. (2010). Removal of heavy metals from model wastewater by using polybenzoxazine aerogel. Desalination 256(1–3), 108-114.

Chen, Z., Deng, S., Wei, H., Wang, B., Huang, J. and Yu, G. (2013). Activated carbons and amine-modified materials for carbon dioxide capture — a review. Frontiers of Environmental Science & Engineering 7(3), 326-340.

Fayemiwo, K.A., Vladisavljević, G.T., Nabavi, S.A., Benyahia, B., Hanak, D.P., Loponov, K.N. and Manović, V. (2018). Nitrogen-rich hyper-crosslinked polymers for low-pressure CO2 capture. Chemical Engineering Journal 334, 2004-2013.

Ghoshal, A.K. and Manjare, S.D. (2002). Selection of appropriate adsorption technique for recovery of VOCs: an analysis. Journal of Loss Prevention in the Process Industries 15(6), 413-421.

Grande, C.A., Ribeiro, R.P.P.L. and Rodrigues, A.E. (2009). CO2 Capture from NGCC Power Stations using Electric Swing Adsorption (ESA). Energy & Fuels 23(5), 2797-2803.

Hu, X., Radosz, M., Cychosz, K.A. and Thommes, M. (2011). CO2-filling capacity and selectivity of carbon nanopores: synthesis, texture, and pore-size distribution from quenched-solid density functional theory (QSDFT). Environ Sci Technol 45(16), 7068-7074.

Huang, H.Y., Yang, R.T., Chinn, D. and Munson, C.L. (2003). Amine-Grafted MCM-48 and Silica Xerogel as Superior Sorbents for Acidic Gas Removal from Natural Gas. Industrial & Engineering Chemistry Research 42(12), 2427-2433.

Ishida, H. (2011). Chapter 1 - Overview and Historical Background of Polybenzoxazine Research. Handbook of Benzoxazine Resins. Amsterdam, Elsevier: 3-81.

Jones, C.W. and Koros, W.J. (1994). Carbon molecular sieve gas separation membranes-I. Preparation and characterization based on polyimide precursors. Carbon 32(8), 1419-1425.

Leung, D.Y.C., Caramanna, G. and Maroto-Valer, M.M. (2014). An overview of current status of carbon dioxide capture and storage technologies. Renewable and Sustainable Energy Reviews 39, 426-443.

Liu, Y.-L., Chang, C.-Y., Hsu, C.-Y., Tseng, M.-C. and Chou, C.-I. (2010). Preparation, characterization, and properties of fluorene-containing benzoxazine and its corresponding cross-linked polymer. Journal of Polymer Science Part A: Polymer Chemistry 48(18), 4020-4026.

Liu, Y.-L. and Chou, C.-I. (2005). High performance benzoxazine monomers and polymers containing furan groups. Journal of Polymer Science Part A: Polymer Chemistry 43(21), 5267-5282.

Liu, Z., Yang, Y., Du, Z., Xing, W., Komarneni, S., Zhang, Z., Gao, X. and Yan, Z. (2015). Furfuralcohol Co-Polymerized Urea Formaldehyde Resin-derived N-Doped Microporous Carbon for CO_2 Capture. Nanoscale Research Letters 10(1), 333.

Lorjai, P., Chaisuwan, T. and Wongkasemjit, S. (2009). Porous structure of polybenzoxazine-based organic aerogel prepared by sol–gel process and their carbon aerogels. Journal of Sol-Gel Science and Technology 52(1), 56-64.

Nanthiya, T., Oi Lun Helena, L., Wattanachai, Y., Nagahiro, S. and Uthaiporn, S. (2016). Adsorption of carbon dioxide by solution-plasma-synthesized heteroatom-doped carbon nanospheres. Japanese Journal of Applied Physics 55(1S), 01AE10.

Pietrzak, R. (2009). XPS study and physico-chemical properties of nitrogen-enriched microporous activated carbon from high volatile bituminous coal. Fuel 88(10), 1871-1877.

Plaza, M.G., Thurecht, K.J., Pevida, C., Rubiera, F., Pis, J.J., Snape, C.E. and Drage, T.C. (2013). Influence of oxidation upon the CO_2 capture performance of a phenolic-resin-derived carbon. Fuel Processing Technology 110, 53-60.

Regufe, M.J., Ferreira, A.F.P., Loureiro, J.M., Shi, Y., Rodrigues, A. and Ribeiro, A.M. (2018). New hybrid composite honeycomb monolith with 13X zeolite and activated carbon for CO_2 capture. Adsorption 24(3), 249-265.

Rouquerol, F., Rouquerol, J., Sing, K.S.W., Maurin, G. and Llewellyn, P. (2014). 1 - Introduction. Adsorption by Powders and Porous Solids (Second Edition). Oxford, Academic Press: 1-24.

Roy, P. and Dias, G. (2017). Prospects for pyrolysis technologies in the bioenergy sector: A review. Renewable and Sustainable Energy Reviews 77, 59-69.

Rungta, M., Xu, L. and Koros, W.J. (2015). Structure–performance characterization for carbon molecular sieve membranes using molecular scale gas probes. Carbon 85, 429-442.

Sethia, G. and Sayari, A. (2014). Nitrogen-Doped Carbons: Remarkably Stable Materials for CO2Capture. Energy & Fuels 28(4), 2727-2731.

Shen, C., Grande, C.A., Li, P., Yu, J. and Rodrigues, A.E. (2010). Adsorption equilibria and kinetics of CO2 and N2 on activated carbon beads. Chemical Engineering Journal 160(2), 398-407.

Sing, K.S.W., Rouquerol, F. and Rouquerol, J. (2014). 5 - Classical Interpretation of Physisorption Isotherms at the Gas–Solid Interface. Adsorption by Powders and Porous Solids (Second Edition). Oxford, Academic Press: 159-189.

Steel, K.M. and Koros, W.J. (2005). An investigation of the effects of pyrolysis parameters on gas separation properties of carbon materials. Carbon 43(9), 1843-1856.

Tan, J.S. and Ani, F.N. (2004). Carbon molecular sieves produced from oil palm shell for air separation. Separation and Purification Technology 35(1), 47-54.

Thongwichit, N., Li, O., Yaowarat, W., Saito, N. and Suriyapraphadilok, U. (2015). Adsorption of carbon dioxide by solution-plasma-synthesized heteroatom-doped carbon nanospheres. Jpn. J. Appl. Phys. 55(1), 01AE10.

Wang, C., Sun, J., Liu, X., Sudo, A. and Endo, T. (2012). Synthesis and copolymerization of fully bio-based benzoxazines from guaiacol, furfurylamine and stearylamine. Green Chemistry 14(10), 2799.

Wang, C., Zhao, C., Sun, J., Huang, S., Liu, X. and Endo, T. (2013). Synthesis and thermal properties of a bio-based polybenzoxazine with curing promoter. Journal of Polymer Science Part A: Polymer Chemistry 51(9), 2016-2023.

Xu, S., He, J., Jin, S. and Tan, B. (2018). Heteroatom-rich porous organic polymers constructed by benzoxazine linkage with high carbon dioxide adsorption affinity. J Colloid Interface Sci 509, 457-462.

Yu, C.H., Huang, C.H. and Tan, C.S. (2012). A review of CO2 capture by absorption and adsorption. Aerosol and Air Quality Research 12(5), 745-769.

Zulfiqar, S. and Sarwar, M.I. (2015). Aramid as potential solid Sorbent for CO2 capture. Polymer Science Series B 57(6), 702-709.

APPENDICES

Appendix A   Calculations for Benzoxazine Synthesis Ratio and Bezoxazine Solution

To synthesize monomer, Benzoxazine monomer was prepared by using three main precursors including paraformaldehyde, furfurylamine, and phenol. The molar ratio of this preparation was 2:1:1 for paraformaldehyde, furfurylamine, and phenol respectively. The monomer was synthesized via a solvent-less method.

Molecular weight of paraformaldehyde   =   30.03 g/mol

Molecular weight of furfurylamine   =   97.12 g/mol

Molecular weight of phenol   =   94.11 g/mol

Table A1 Benzoxazine monomer calculation

Precursor	Molecular weight (g/mol)	Molar Ratio	Concentration (g)	Batch Scale (0.2:0.1:0.1)	Weight (g)
Paraformaldehyde (95% wt)	30.03	2	60.06	6.01	6.32
Furfurylamine (99%)	97.12	1	97.12	9.71	9.81
Phenol	94.11	1	94.11	9.41	9.41

Note: True weight calculation of paraformaldehyde (95% wt) = $\dfrac{100 \times 6.01}{95} = 6.32$ g

Table A2 Benzoxazine solution calculation

Concentration	Benzoxazine monomer (g)	Xylene solvent (g)	Total weight (g)
20% wt benzoxazine	$\dfrac{20 \times 5}{100} = 1.00$	$5.00 - 1.00 = 4.00$	5.00
30% wt benzoxazine	$\dfrac{30 \times 5}{100} = 1.50$	$5.00 - 1.50 = 3.50$	5.00
40% wt benzoxazine	$\dfrac{40 \times 5}{100} = 2.00$	$5.00 - 2.00 = 3.00$	5.00

Appendix B FT-IR Spectras of Benzoxazine Monomer and Polybenzoxazine
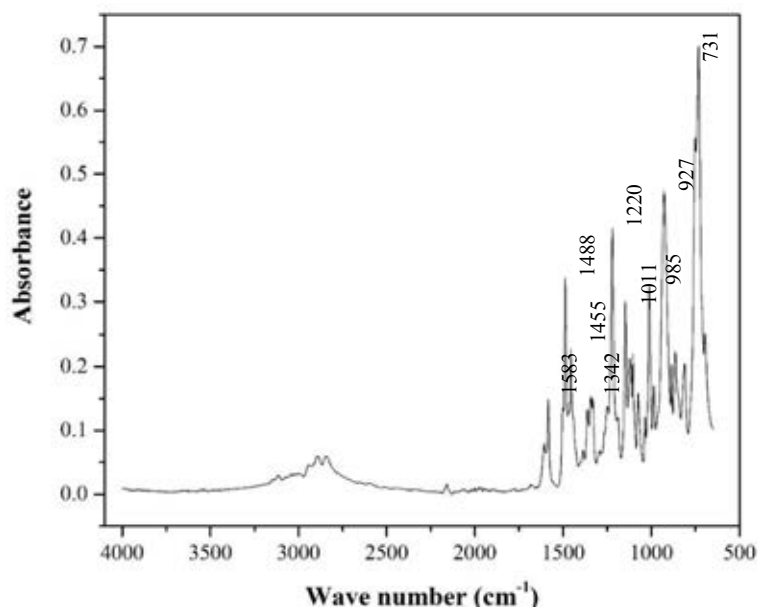
Figure B1 FT-IR spectra of furfurylamine-derived benzoxazine monomer.
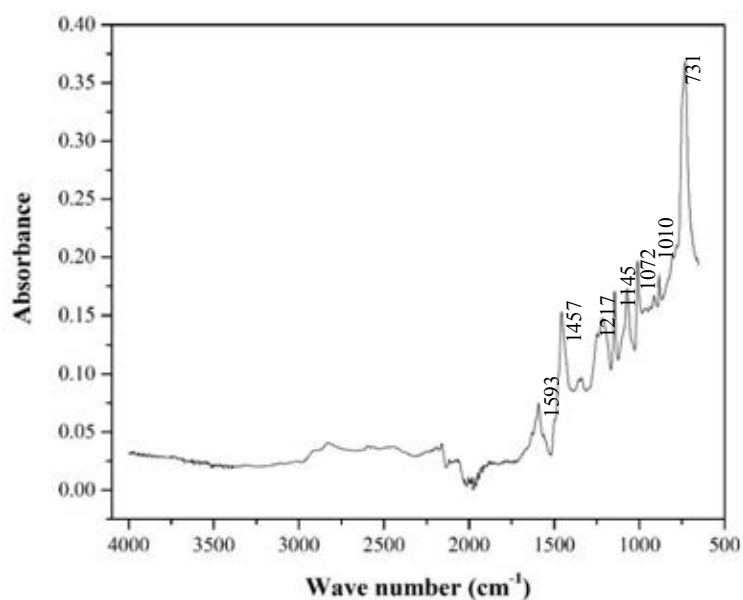
Figure B2 FT-IR spectra of furfurylamine-derived polybenzoxazine.

Appendix C DSC Thermograms of Benzoxazine Monomer.
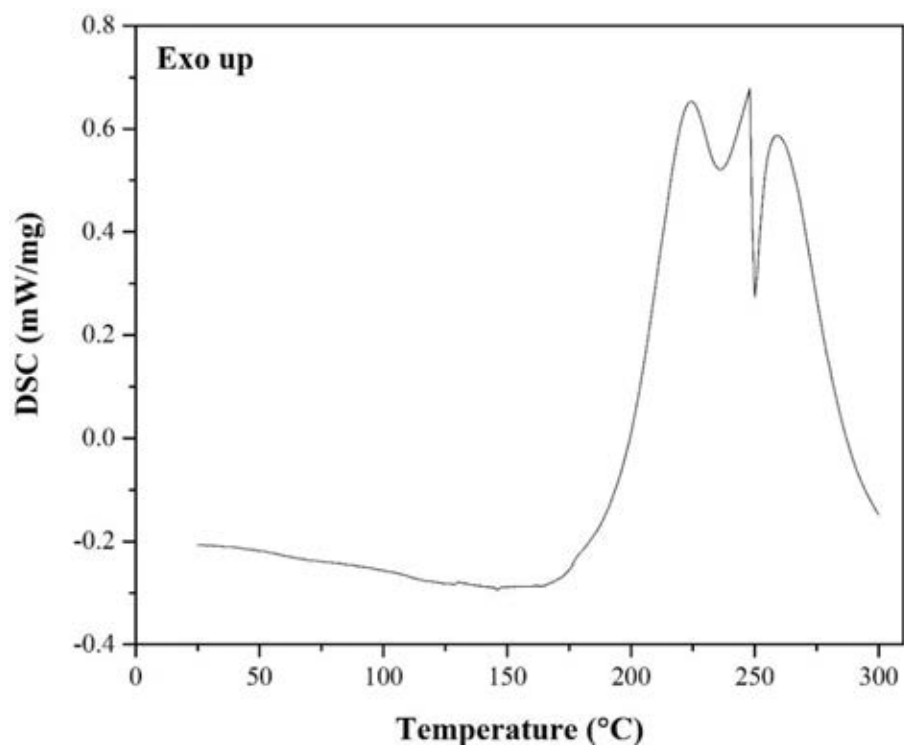
Figure C1 DSC thermograms of furfurylamine-derived benzoxazine monomer..

Appendix D TGA Thermograms of Polybenzoxazine
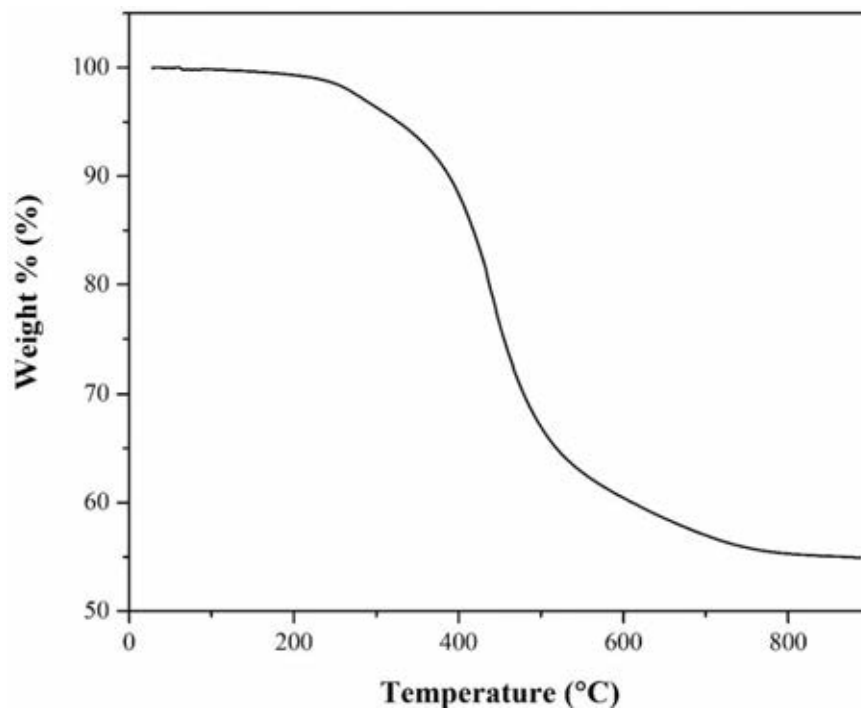
Figure D1 TGA thermograms of furfurylamine-derived polybenzoxazine.

Appendix E Composition of Carbon Adosrbents

Table E1 Element content of carbon adsorbents

Sample	% C	% H	% N	% O (by difference)
Activated carbon	88.98 ± 0.05	1.18 ± 0.13	0.26 ± 0.04	9.58
PO-S20	68.87 ± 0.42	5.11 ± 0.01	5.17 ± 0.06	20.85
PO-S30	67.86 ± 0.16	5.00 ± 0.05	5.16 ± 0.04	21.98
PO-S40	68.03 ± 1.34	4.94 ± 0.11	5.21 ± 0.05	21.82
CA-6N20	87.60 ± 4.96	2.27 ± 0.14	3.96 ± 0.06	6.17
CA-6N40	86.02 ± 4.80	2.16 ± 0.41	4.77 ± 0.65	7.05
CA-7N20	85.57 ± 0.47	1.42 ± 0.09	3.52 ± 0.04	9.49
CA-8N20	87.75 ± 1.01	1.01 ± 0.01	3.28 ± 0.07	7.96
CA-6SP20	81.24 ± 3.44	1.48 ± 0.30	2.34 ± 0.12	14.94
CA-6SP30	85.30 ± 2.69	0.99 ± 0.20	2.22 ± 0.12	11.49
CA-6SP40	86.66 ± 0.94	0.80 ± 0.02	2.41 ± 0.00	10.13
CA-6SC20	60.25 ± 6.87	1.32 ± 0.18	1.42 ± 0.42	37.01
CA-6SC40	64.96 ± 6.48	1.10 ± 0.52	1.70 ± 0.84	32.24
CA-7SC20	65.08 ± 1.48	1.80 ± 0.04	1.28 ± 0.28	31.84
CA-8SC20	78.72 ± 0.71	1.24 ± 0.24	0.37 ± 0.03	19.67

Note: CA is carbon adsorbent; numbers 6, 7, and 8 are the carbonization temperature at 600, 700, and 800 °C, respectively; B stands for bulk polymerization; S means the sol-gel polymerization; P stands for physical activation; C is chemical activation; N means sample without activation; and PO stands for polymer.

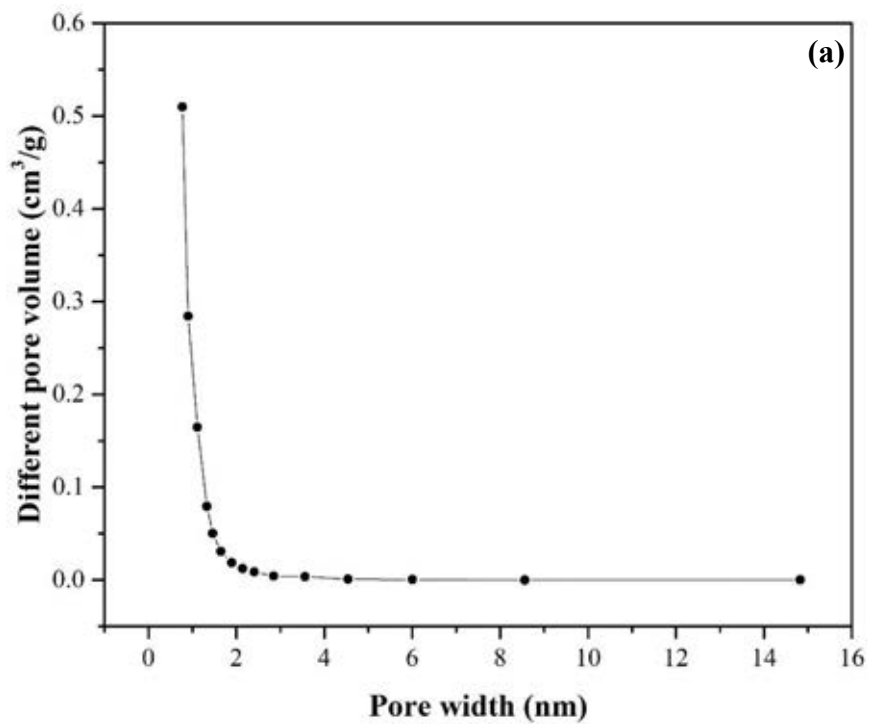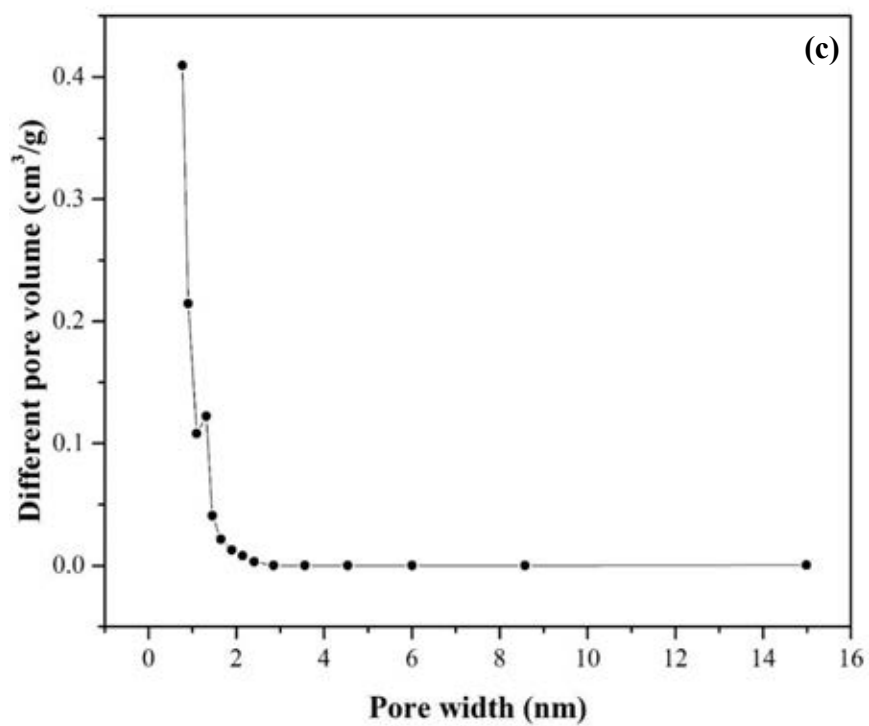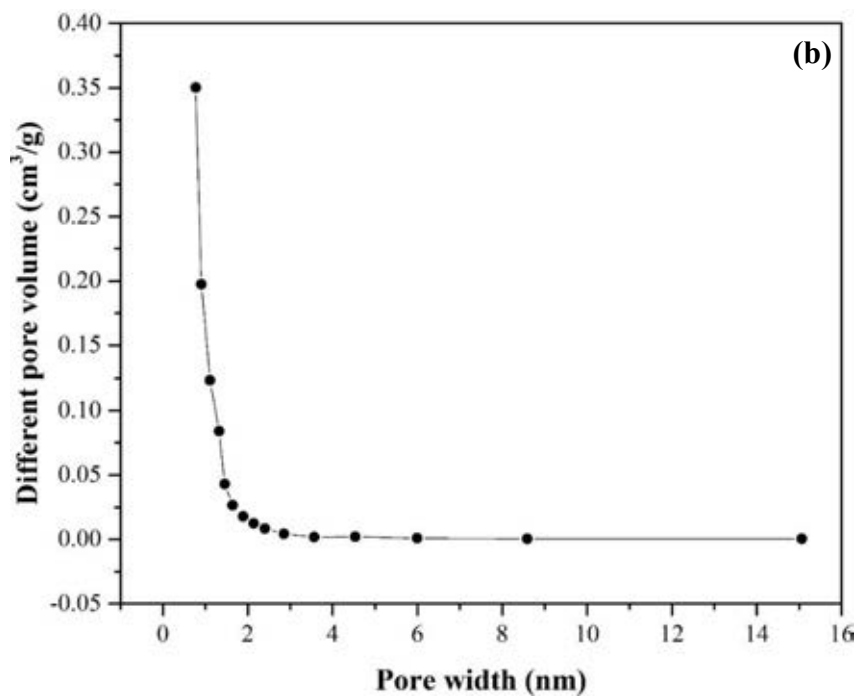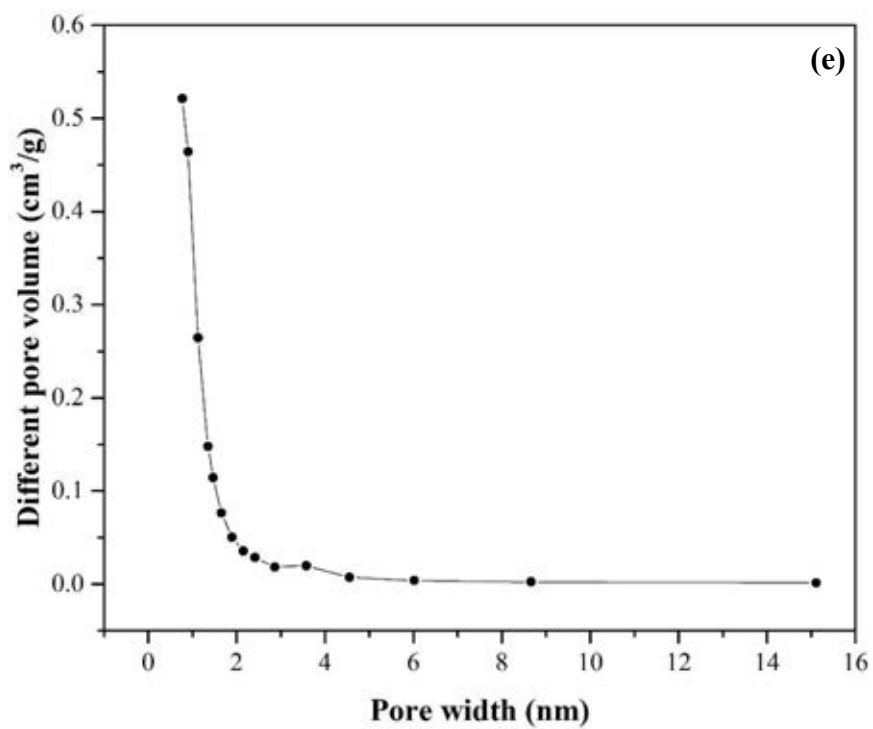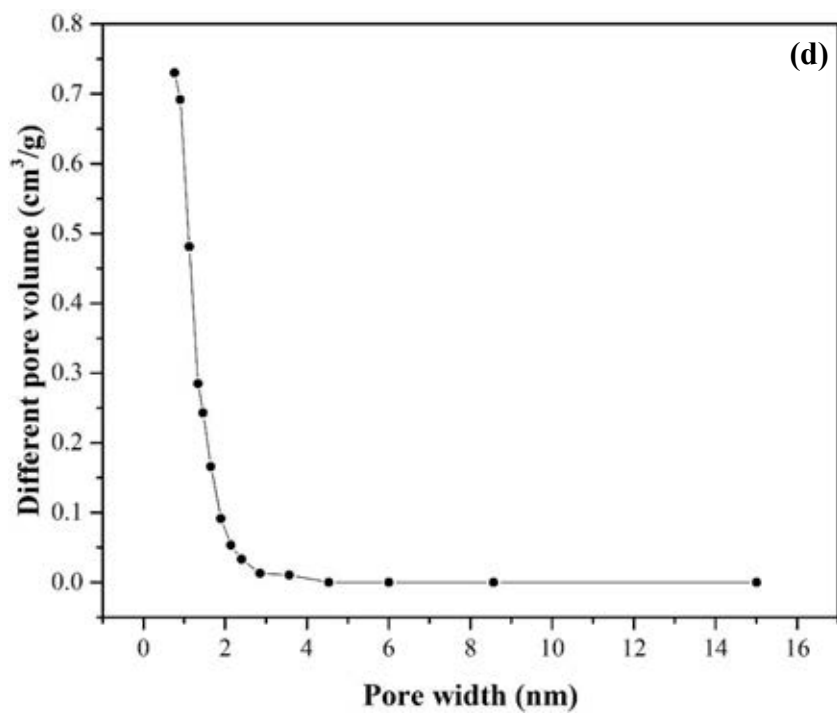**Appendix F Textural Properties of All Adsorbents**
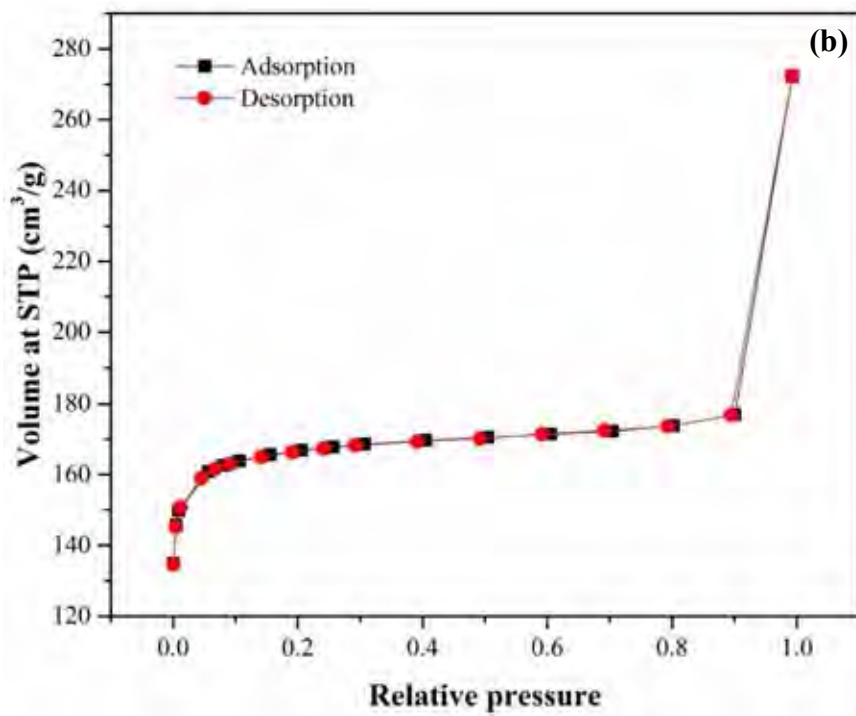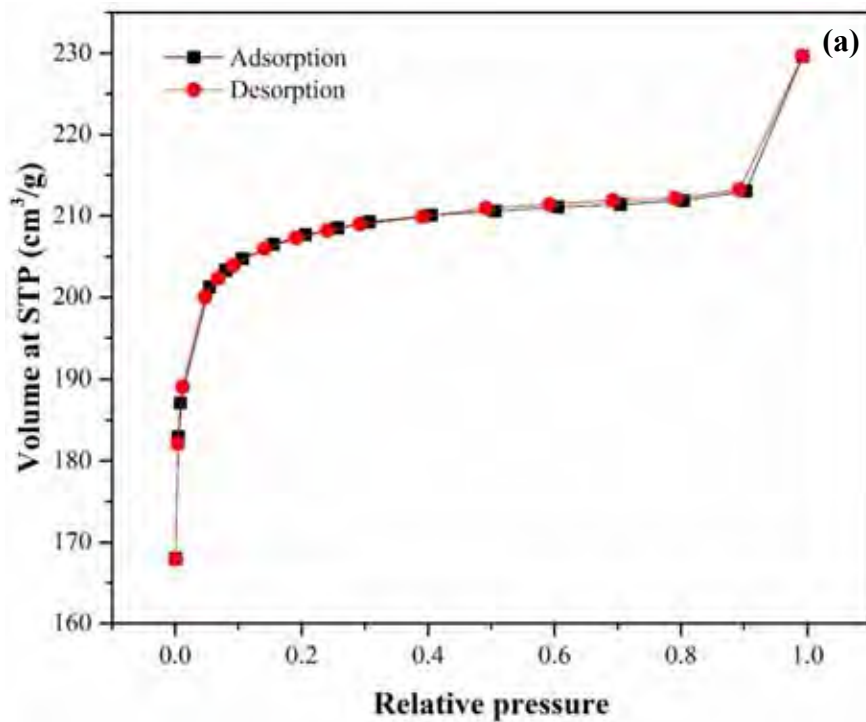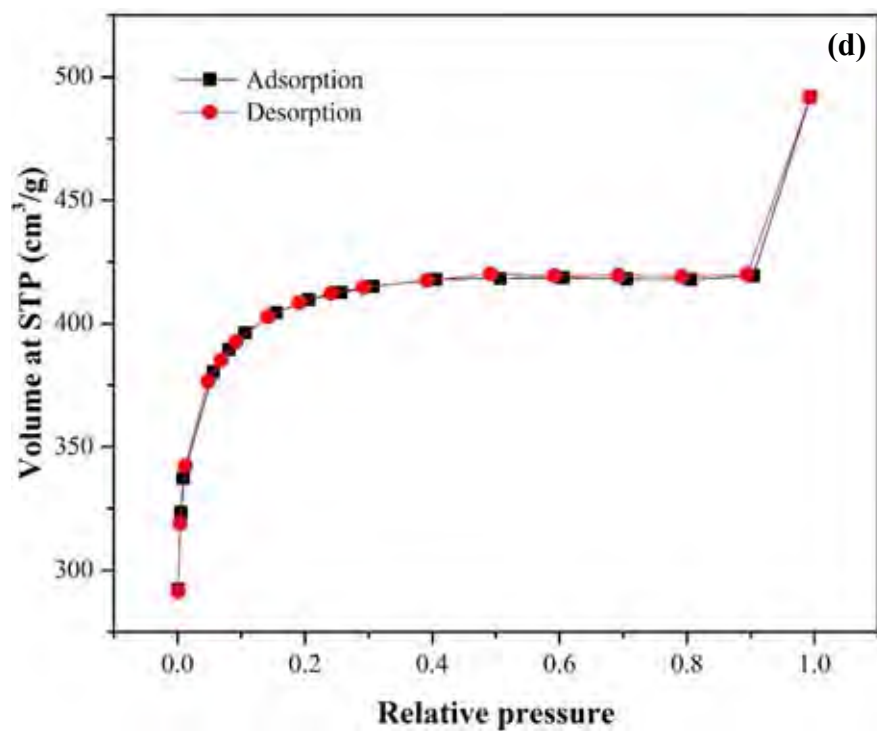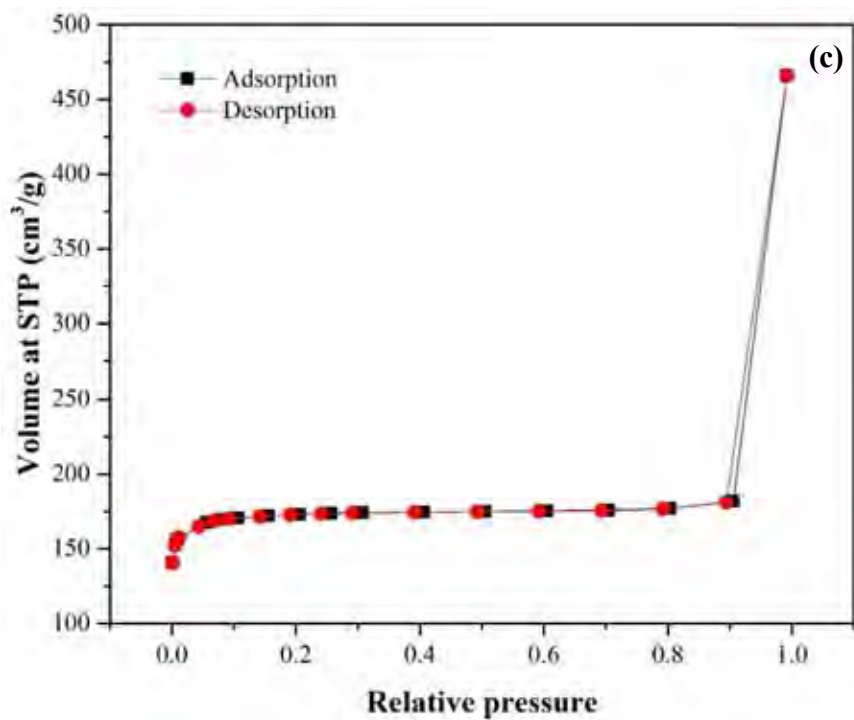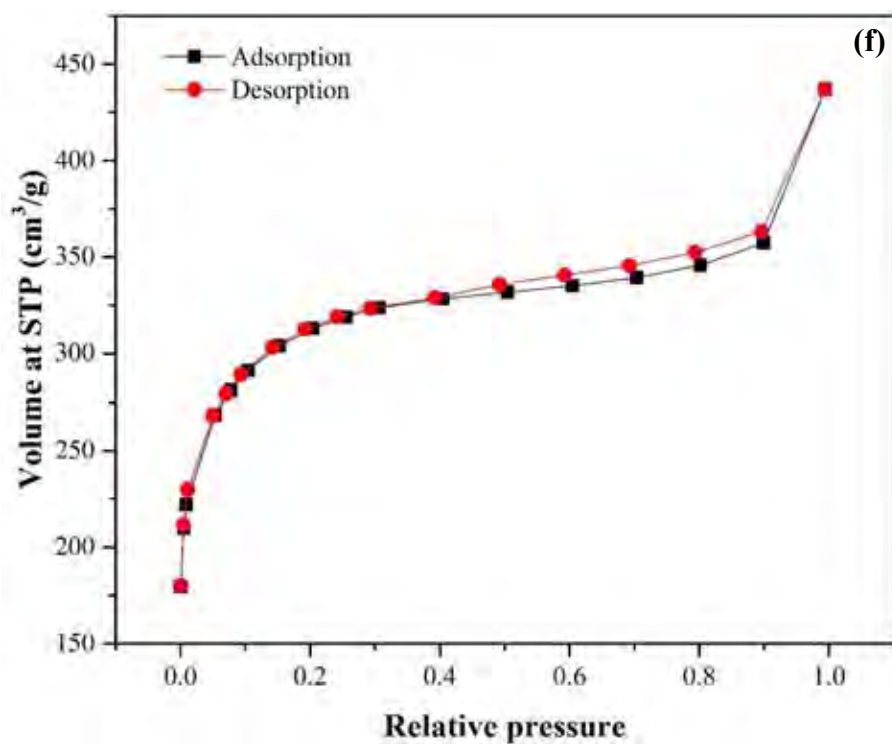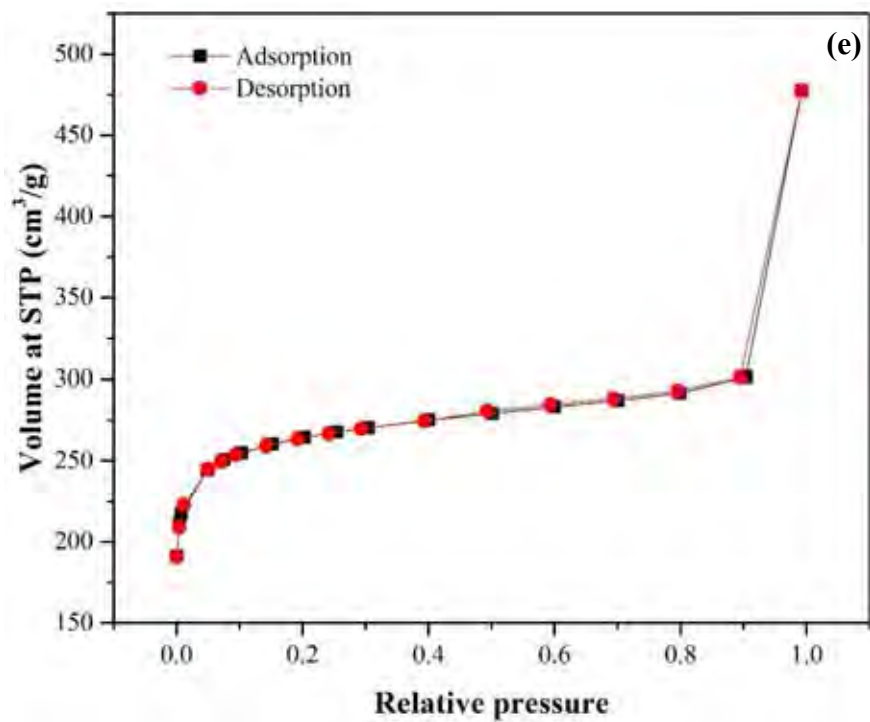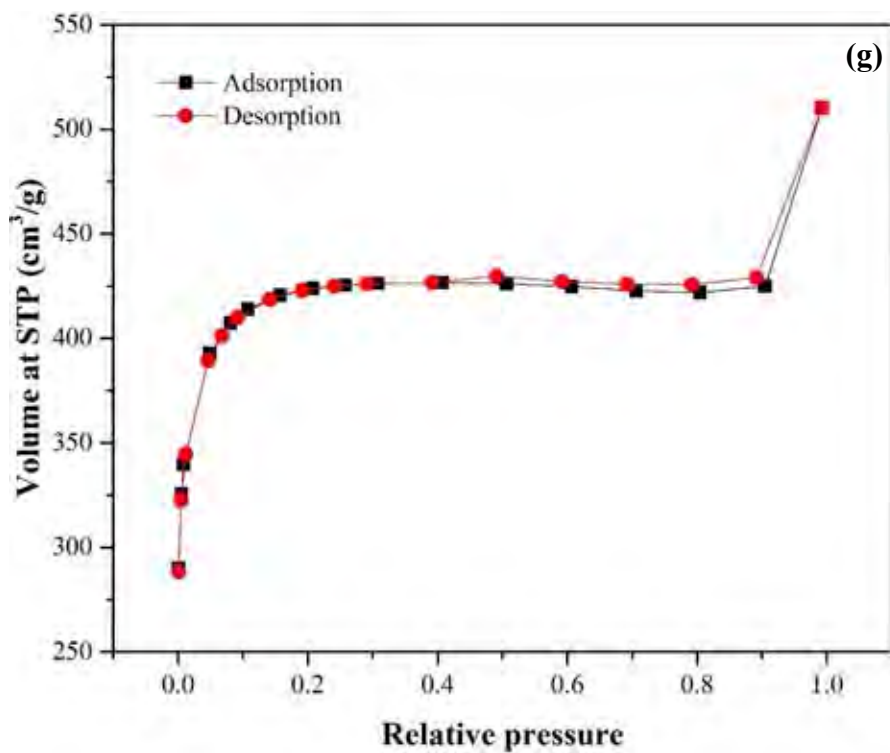
Figure F1 Isotherms of (a) CA-6SP20, (b) CA-6SP30, (c) CA-6SP40, (d) CA-6SC20, (e) CA-6SC20, (f) CA-7SC20, and (g) CA-8SC20.

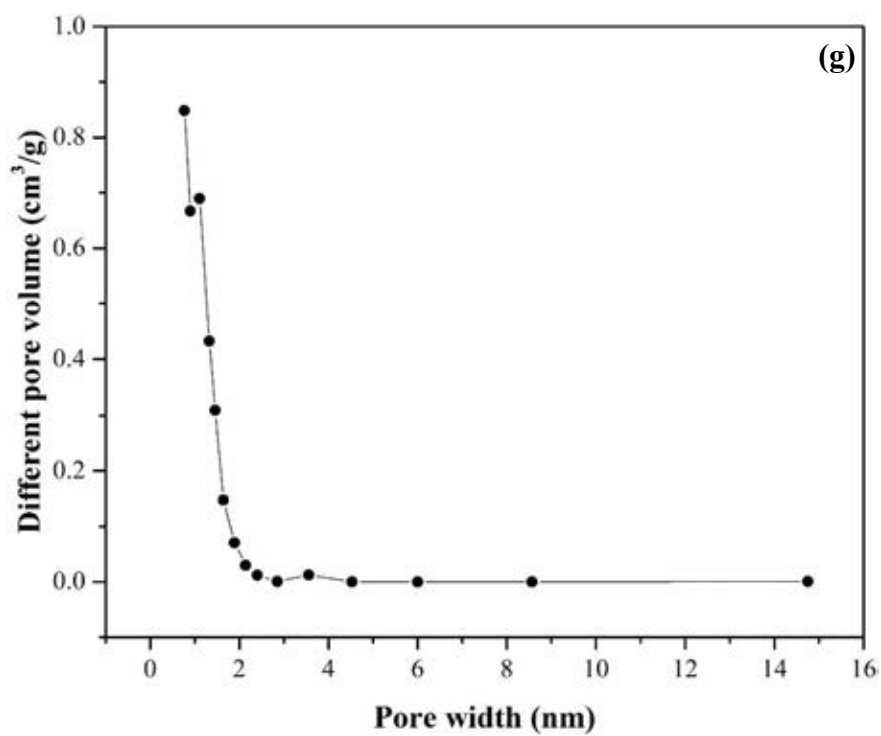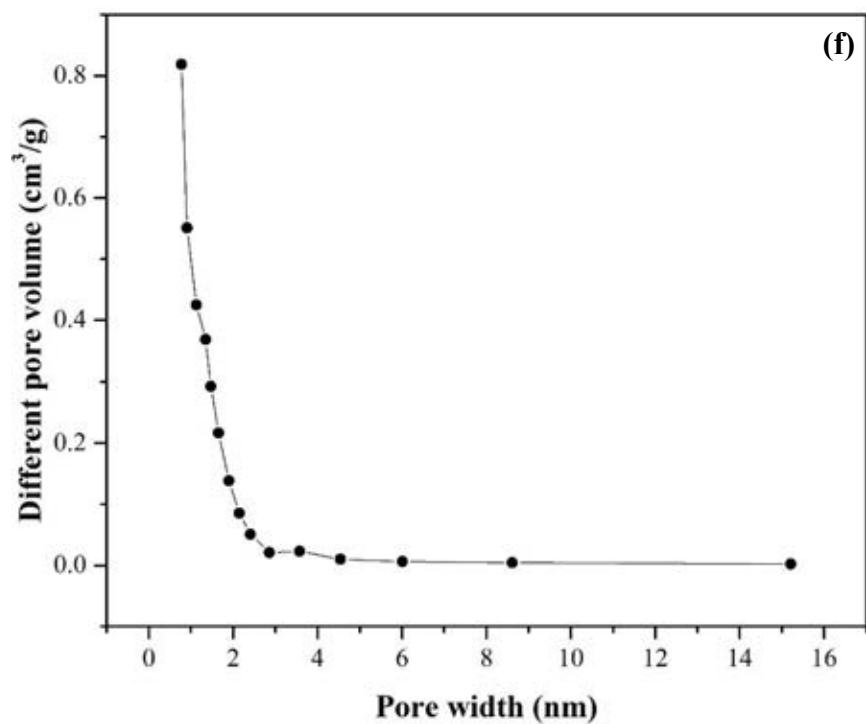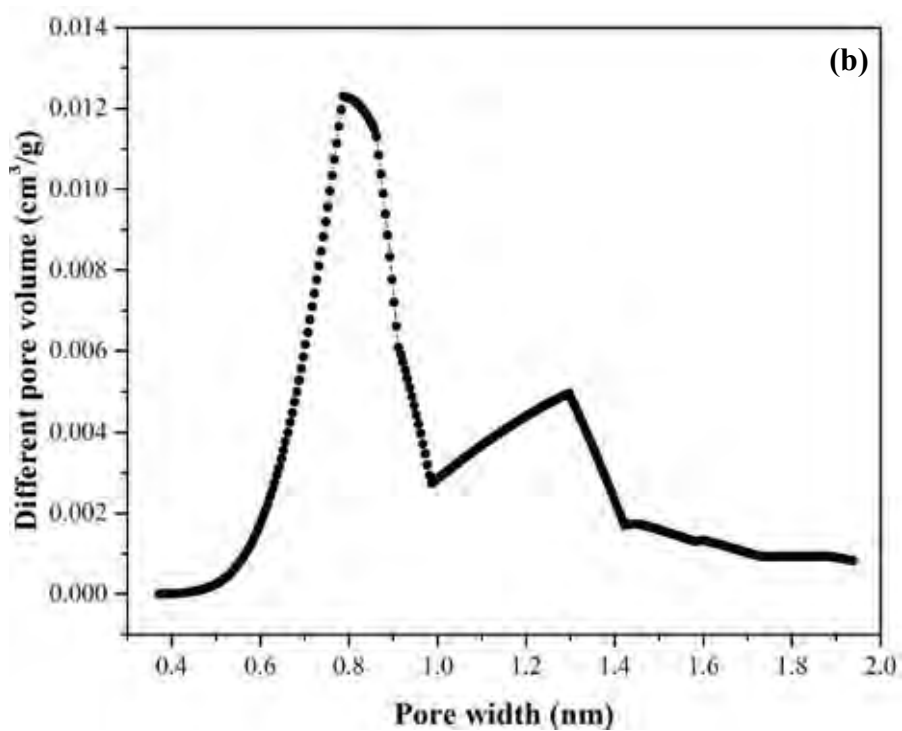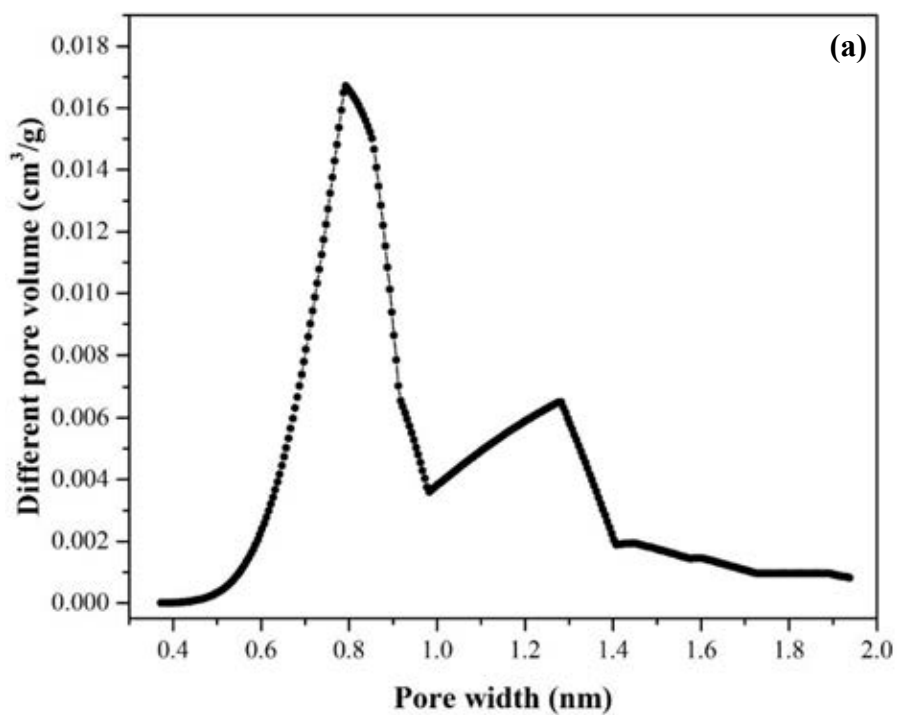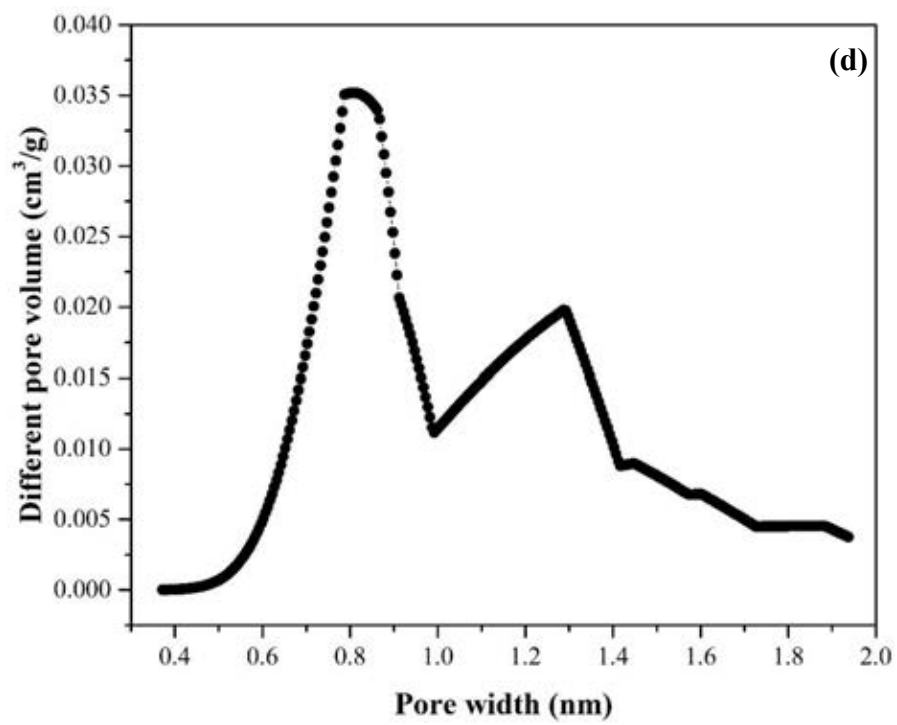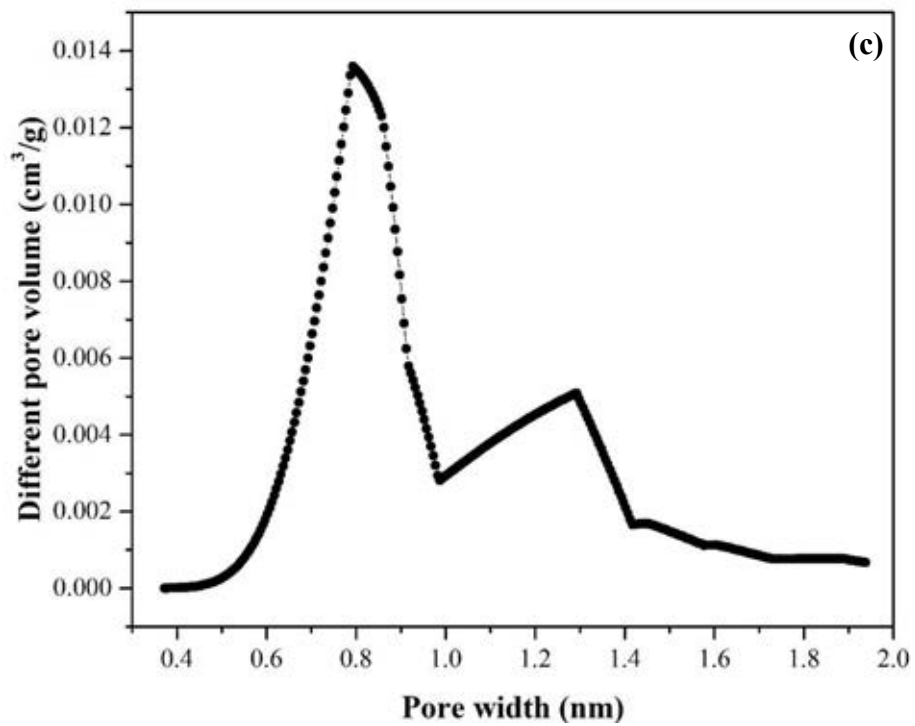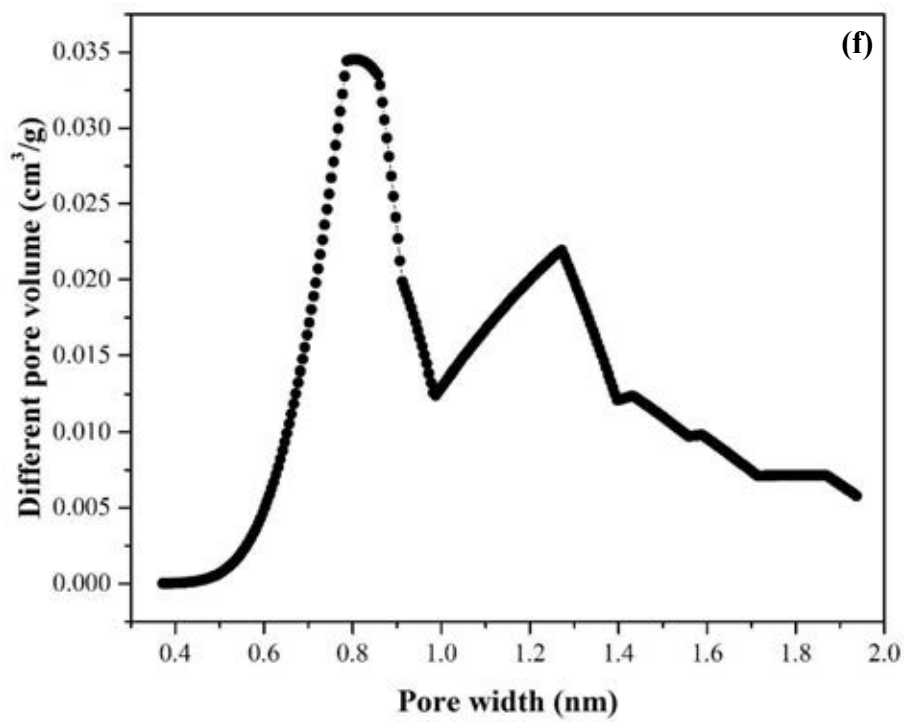**Figure F2** Pore size distribution with BJH method of (a) CA-6SP20, (b) CA-6SP30, (c) CA-6SP40, (d) CA-6SC20, (e) CA-6SC20, (f) CA-7SC20, and (g) CA-8SC20.
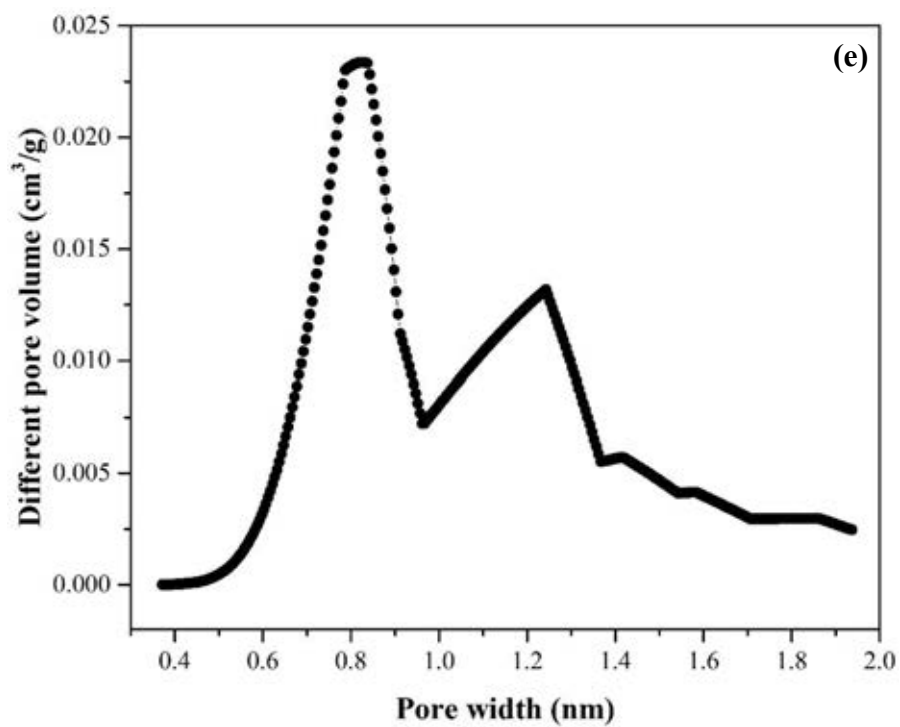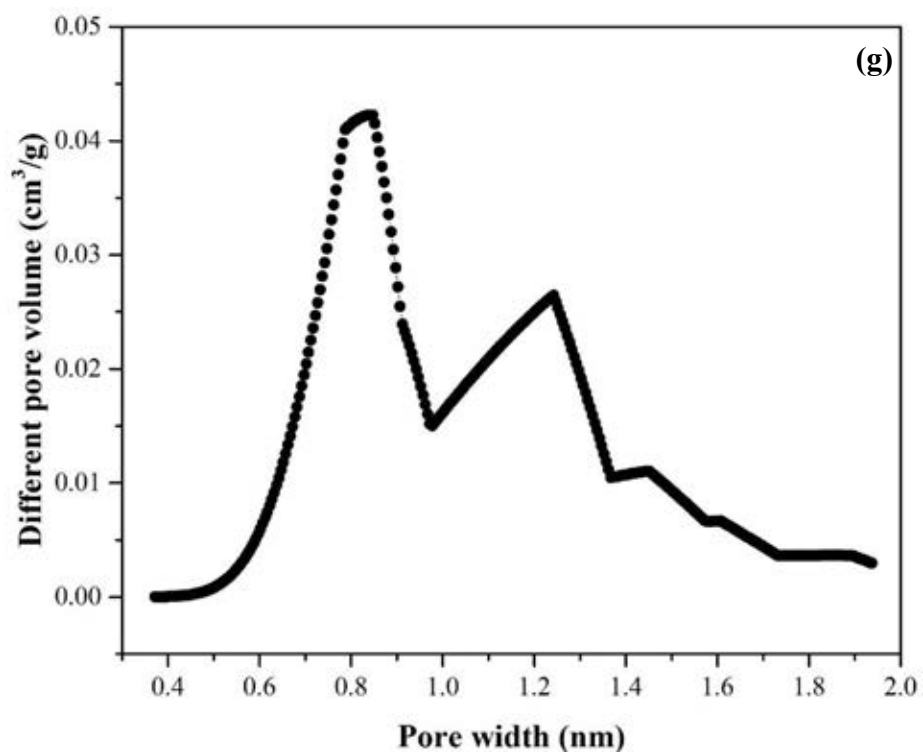
Figure F3 Pore size distribution with HK method of (a) CA-6SP20, (b) CA-6SP30, (c) CA-6SP40, (d) CA-6SC20, (e) CA-6SC20, (f) CA-7SC20, and (g) CA-8SC20.

**Table F1** BET surface area, total pore volume, micropore volume, and average pore diameter of all adsorbents

Sample	S_{BET} (m^2/g)	V_{Total} (cm^3/g)	V_{Micro} (cm^3/g)	D_{Avg} (nm)
Bulk polymerization				
• Physical activation (CA-6BP)	49.40	0.0434	0.022063	3.51979
• Chemical activation (CA-6BC)	10.83	0.0059	0.000830	2.20043
Sol-gel polymerization				
• No carbonization				
- PO-S20	3.671	0.2046	0.000	222.9
- PO-S30	8.195	0.3594	0.000	175.4
- PO-S40	12.883	0.4141	0.000	128.6
• No activation				
- CA-6N20	326.712	0.2413	0.145	2.954
- CA-6N40	437.754	0.5291	0.183	4.834
- CA-7N20	325.344	0.2303	0.143	2.832
- CA-8N20	393.420	0.2677	0.165	2.712
• Physical activation				
- CA-6SP20	621.033	0.3552	0.291	2.288
- CA-6SP30	499.808	0.4211	0.228	3.370
- CA-6SP40	516.248	0.7207	0.243	5.584

Table F1 BET surface area, total pore volume, micropore volume, and average pore diameter of all adsorbents (continuous)

Sample	S_{BET} (m²/g)	V_{Total} (cm³/g)	V_{Micro} (cm³/g)	D_{Avg} (nm)
Sol-gel polymerization				
• Chemical activation				
- CA-6SC20	1237.144	0.7609	0.499	2.460
- CA-6SC40	812.228	0.7387	0.312	3.638
- CA-7SC20	979.131	0.6761	0.270	2.762
- CA-8SC20	1273.321	0.7891	0.537	2.479
Activated Carbon	892.967	0.4920	0.379	2.204

Note: CA is carbon adsorbent**,** 6, 7, and 8 is the carbonization temperature (600, 700, and 800 °C), B is bulk polymerization, S is sol-gel polymerization, P is physical activation, C chemical activation, N is no activation, and PO is polymer. S_{BET} : specific surface area calculated using Brunauer–Emmett Teller equation, V_{total} : total pore volume, V_{micro} : micropore volume determined from the t-plot method, D_p : average pore diameter.

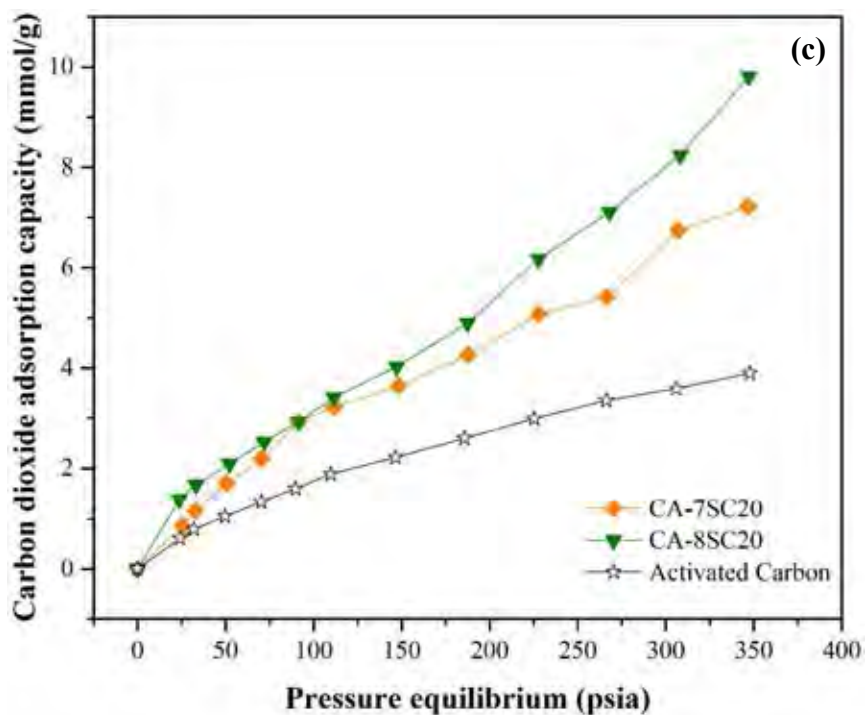**Appendix G Carbon Dioxide Adsorption Performance of All Adsorbents**
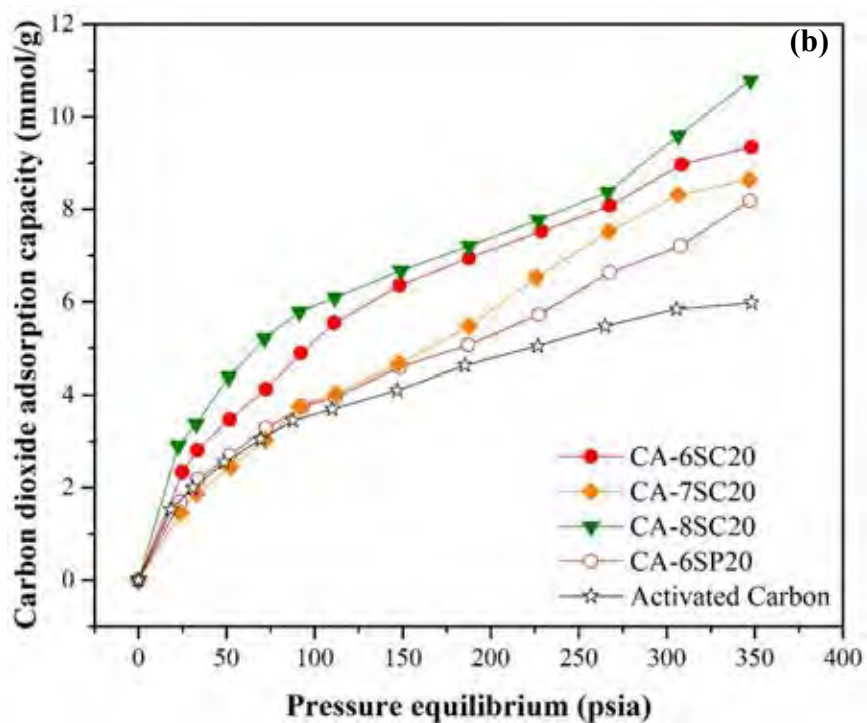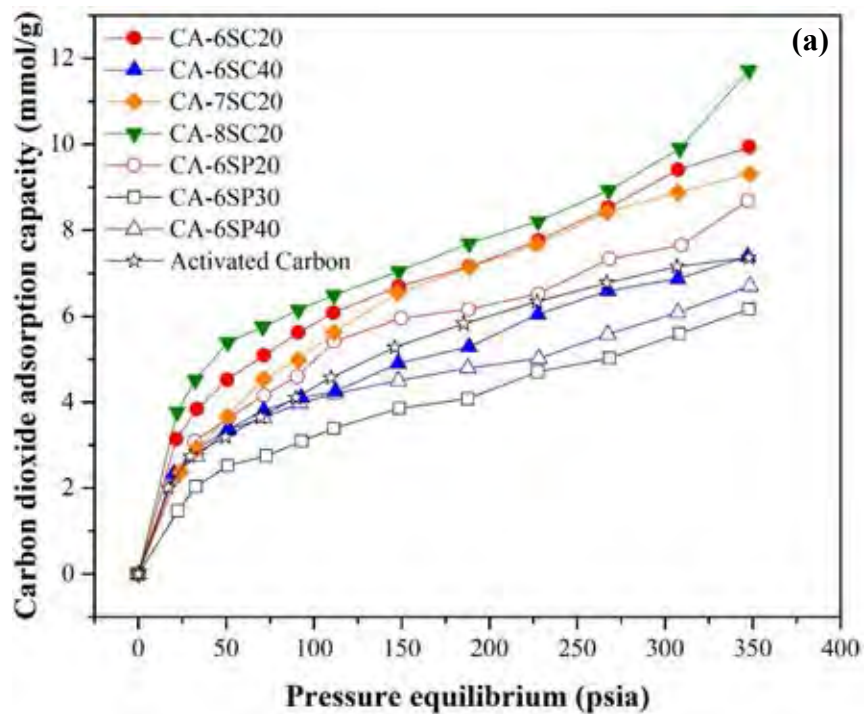
Figure G1 CO$_2$ adsorption isotherms of carbon adsorbent synthesized by sol-gel method: (a) at 40 °C, (b) at 70 °C, and (c) at 110 °C.

Table G1 The CO$_2$ adsorption performance of all adsorbents at 40 °C

Adsorbent	CO$_2$ Uptake (mmol/g)
CA-6SP20	8.69
CA-6SP30	6.16
CA-6SP40	6.71
CA-6SC20	9.94
CA-6SC40	7.40
CA-7SC20	9.32
CA-8SC20	11.73
Activated Carbon	7.36

Table G2 CO_2 adsorption performance of 20 wt% benzoxazine activated with physical and chemical activation.at 70 °C

Adsorbent	CO₂ Uptake (mmol/g)
CA-6SP20	8.18
CA-6SC20	9.34
CA-7SC20	8.64
CA-8SC20	10.79
Activated Carbon	5.98

Table G3 CO_2 adsorption capacity of adsorbents carbonized at 700 and 800 °C at 110 °C

Adsorbent	CO₂ Uptake (mmol/g)
CA-7SC20	7.22
CA-8SC20	9.81
Activated Carbon	3.90

CURRICULUM VITAE

Name: Mr. Thanabhumi Vongtiang

Date of Birth: October 29, 1993

Nationality: Thai

University Education:

2016-2018   Master Degree of Petroleum Technology, The Petroleum and Petrochemical College, Chulalongkorn University, Bangkok, Thailand

2012-2015   Bachelor Degree of Petrochemicals and Polymeric Materials, Faculty of Engineering, Silpakorn University, Nakorn Pathom, Thailand

Proceedings:

1. Vongtiang, T., Chaisuwan, T., and Suriyapraphadilok, U. (2018, June 5) Furfurylamine-based Polybenzoxazine Adsorbent for CO_2 Capture: Effect of Carbonization Temperature and Activation Methods. <u>Proceedings of The 24rd PPC Symposium on Petroleum, Petrochemicals, and Polymers, and The 9th Research Symposium on Petrochemical and Materials Technology, Bangkok, Thailand</u>.

2. Vongtiang, T., Chaisuwan, T., and Suriyapraphadilok, U. (2017, Oct 19) Effect of Activation Methods on Carbon Adsorbent from Polybenzoxazine for Carbon Dioxide Adsorption. <u>Proceedings of The 7th International Thai Institute of Chemical Engineering and Applied Chemistry Conference 2017 (ITChE 2017)</u>, Bangkok, Thailand.